

**University of Crete, Department of Biology
Institute of Molecular Biology and Biotechnology, FORTH**

Molecular Biology – Biomedicine MSc program



**Evaluation of NSC-based implants
for a spinal cord injury mouse model**

Efstathia Bampoula

Supervisors

Prof. Achilleas Gravanis

Prof. Ioannis Charalampopoulos

Dr. Dimitrios Tzeranis

October 2020

Acknowledgements

I would like to thank my supervisor Professors Achilleas Gravanis and Ioannis Charalampopoulos, who gave me the opportunity to work in their laboratories, for the inspiration and their guidance.

I should also acknowledge my supervisor Dr. Dimitrios Tzeranis for his unlimited help, guidance and of course patience, which were valuable for the fulfilment of this thesis.

I am also grateful to Dr. Kanelina Karali, Dr. Konstantina Chanoumidou and Constantina Georgelou for their support, guidance and our great cooperation.

Finally, I would like to thank all the other members of the laboratory for our cooperation and also for the beautiful and friendly working environment.

Abstract

Spinal Cord Injury (SCI) refers to a damage to the spinal cord or specific nerves located at the spinal canal's end, which temporarily or permanently causes functional problems. SCI is recognized as a global health issue due to its complex and multifactorial pathophysiology and its significant impact on patient quality of life. In combination with failure of CNS neurons, to maintain their intrinsic growth capacity and the great inability to regenerate their axons following injury, SCI treatment strategies still remain controversial.

NSPC-seeded scaffolds engrafted after the SCI are a promising SCI treatment, since they seem to be able to impact the lesion site and improve functional recovery.

This study builds upon previous work of the IMBB Neural Tissue Engineering Lab on SCI grafts based on NSPCs-seeded porous collagen-based scaffolds (PCS). According to a recent study by Kouriantaki et al., NSPC-seeded PCS engrafted in a dorsal column crush SCI mouse model lead to significant improvement in locomotion recovery 10-12 weeks post injury. The objective of this thesis is to characterize the utilized NSPC-seeded grafts in more detail and evaluate the ability to modulate NSPCs fate once seeded in PCSs.

NSPC fate characterization inside scaffolds utilized immunocytochemistry. Fluorescence microscopy images were utilized to quantify the percentage of cells that stain positive for markers of specific cell developmental stages and thereby discriminate different NSPCs subpopulations. Results demonstrate that in NSPC-seeded grafts the largest percentage of cells are NSPCs, characterized by the expression of Sox2, Nestin and GLAST, with the highest percentage being RGCs. However, results demonstrate that the cell population of such implants consisted also of GRPs and astrocytes (based on GFAP expression) and OPCs (based on PDGFRa expression). The lower percentage of Tuj1 positive cells, in comparison with the glial markers, indicates a preference of cell differentiation towards glial cells in PCSs. In comparison with 2D culture, where cells remain in the median stage of NSPCs, cells grown inside scaffolds culture seem to follow a stricter pattern, being either at the stage of NECs or even of more mature progenitors-GRPs. Inducing NSPCs towards a neural fate by RA treatment did not work in this system both in 3D culture (inside scaffolds) and in ordinary 2D monolayer culture. Even when treated with differentiation mediums, PCSs favor NSPC differentiation towards OPCs and enhanced the expression of NSPC markers over a longer time compared to ordinary 2D culture.

Keywords: Spinal Cord Injury, Neural Stem Cells, Porous Collagen Scaffolds, Neuroimplants

Περίληψη

Ο τραυματισμός του νωτιαίου μυελού (TNM) αναφέρεται σε βλάβη του νωτιαίου μυελού ή σε συγκεκριμένα νεύρα που βρίσκονται στο άκρο του νωτιαίου σωλήνα, η οποία προκαλεί προσωρινά ή μόνιμα λειτουργικά προβλήματα. Ο TNM είναι ένα παγκόσμιο πρόβλημα υγείας λόγω της πολύπλοκης και πολυπαραγοντικής παθοφυσιολογίας του και του σημαντικού αντίκτυπου που έχει στην ποιότητα ζωής των ασθενών. Σε συνδυασμό με την αδυναμία των νευρώνων του ΚΝΣ να διατηρήσουν την ικανότητα ανάπτυξης και αναγέννησης των αξόνων τους μετά από τραυματισμό, οι στρατηγικές θεραπείας για τον TNM παραμένουν αμφιλεγόμενες.

Ικρίωματα με νευρικά βλαστικά-προγονικά κύτταρα (NSPCs) που εμφυτεύονται μετά το TNM αποτελούν ένα τρόπο θεραπείας με πολλά υποσχόμενα θετικά αποτελέσματα, καθώς φαίνεται να έχουν τεράστιες επιπτώσεις στο σημείο της βλάβης, αλλά μπορούν ακόμη και να οδηγήσουν σε λειτουργική ανάκαμψη.

Η μελέτη αυτή βασίζεται σε προηγούμενες μελέτες του Εργαστηρίου Μηχανικής Νευρικού Ιστού στο IMBB, οι οποίες αφορούν εμφυτεύματα για τη θεραπεία TNM που αποτελούνται από πορώδη ικρίωματα κολλαγόνου μέσα στα οποία και καλλιεργούνται NSPCs. Σε μια πρόσφατη μελέτη (Kouriantaki et al. 2020) τα εμφυτεύματα αυτά οδήγησαν σε σημαντική βελτίωση και ανάκαμψη της κίνησης τραυματισμένων ποντικών με τραύμα στη ραχιαία στήλη του νωτιαίου μυελού. Στόχος της παρούσης εργασίας είναι ο περαιτέρω χαρακτηρισμός αυτών των εμφυτευμάτων και η αξιολόγηση της ικανότητας ελέγχου και επαγωγής της κυτταρικής διαφοροποίησης των NSPCs μέσα στα ικρίωματα κολλαγόνου.

Ο χαρακτηρισμός βασίστηκε στη μέθοδο της ανοσοκυτταροχημείας και η αξιολόγηση πραγματοποιήθηκε ποσοτικοποιώντας το ποσοστό των κυττάρων που ήταν θετικά για δείκτες που εκφράζονται σε συγκεκριμένα στάδια της ανάπτυξης κυττάρων και μπορούν να διακρίνουν τους διαφορετικούς υποπληθυσμούς NSPCs. Τα αποτελέσματα δείχνουν ότι στα εμφυτεύματα που χρησιμοποιήθηκαν από τους Kouriantaki et al., το μεγαλύτερο ποσοστό κυττάρων παραμένει στο στάδιο των NSPCs που εκφράζουν τους δείκτες Sox2, Nestin και GLAST, με το υψηλότερο ποσοστό να είναι ακτινικά γλοιακά κύτταρα (RGCs). Ωστόσο, τα αποτελέσματα δείχνουν ότι ο κυτταρικός πληθυσμός αποτελείται επίσης από προγονικά κύτταρα περιορισμένα προς τη γλοιακή κυτταρική μοίρα ή και αστροκύτταρα (με βάση την έκφραση του GFAP) και πρώιμα ολιγοδενδροκύτταρα (με βάση την έκφραση του PDGFRα). Το χαμηλότερο ποσοστό κυττάρων θετικών σε Tuj1, σε σύγκριση με τους γλοιακούς δείκτες, δείχνει τη προτίμηση της κυτταρικής διαφοροποίησης προς τα γλοιακά κύτταρα. Σε σύγκριση με καλλιέργεια NSPCs σε κλασική δισδιάστατη (2D) καλλιέργεια, όπου τα περισσότερα κύτταρα παραμένουν στο ενδιάμεσο στάδιο των νευρικών βλαστικών-προγονικών κυττάρων, τα περισσότερα NSPCs που καλλιιεργήθηκαν μέσα σε ικρίωματα κολλαγόνου φαίνεται να

ακολουθούν ένα πιο αυστηρό μοτίβο και να βρίσκονται είτε στο στάδιο των νευροεπιθλιακών κυττάρων είτε στο στάδιο των πιο ώριμων προγονικών κυττάρων (GRPs). Η επαγωγή της νευρικής κυτταρικής διαφοροποίησης, μέσω ρετινοϊκού οξέος, των βλαστικών-προγονικών κυττάρων στα ικρίωματα κολλαγόνου δεν λειτούργησε σε αυτό το σύστημα καλλιέργειας. Ωστόσο, ακόμη και στα θρεπτικά κυτταρικής διαφοροποίησης που χρησιμοποιήθηκαν, τα ικρίωματα κολλαγόνου φαίνεται να ευνοούν την ανάπτυξη των πρώιμων ολιγοδενδροκυττάρων, ενώ η παρουσία δεικτών NSPCs διήρκησε για μεγαλύτερο χρονικό διάστημα.

Λέξεις-κλειδιά: Τραύμα Νωτιαίου Μυελού, Νευρικά Βλαστικά Κύτταρα, Πορώδη Ικρίωματα Κολλαγόνου, Νευροεμφυτεύματα

Table of Contents

1	Introduction	11
1.1	Spinal Cord Injury (SCI)	11
1.1.1	Traumatic SCI	11
1.1.2	Epidemiology of Traumatic SCI	11
1.1.3	SCI Pathophysiology	12
1.1.4	Failure of Axon Regeneration after SCI	14
1.1.5	Therapeutic Approaches	16
1.1.5.1	Neuroprotective therapies	16
1.1.5.2	Neuroregenerative therapies	17
1.1.5.3	Cell transplantation	18
1.1.6	Biomaterials in SCI	20
1.2	Central Nervous System Development	22
1.2.1	Cortex Development	23
1.2.2	Terminology of Neural Stem Cells	29
1.2.3	<i>In Vitro</i> Characterization of Stem Cells	30
1.2.3.1	Sox2	30
1.2.3.2	Nestin	31
1.2.3.3	GLAST	32
1.2.3.4	GFAP	32
1.2.3.5	Tubulin beta 3	32
1.2.3.6	Tbr2	32
1.2.3.7	PDGFRa	32
1.2.4	Neurosphere assay	33
1.3	NSPC-based Grafts in SCI	35
1.4	Thesis Objectives and Outline	38
2	Methods	39

2.1	Primary Neural Stem Cell Isolation	39
2.2	Cell Culture	39
2.2.1	2D Culture	39
2.2.2	3D Culture	40
2.2.3	Neural Differentiation	40
2.3	Image Acquisition	40
2.3.1	2D culture	40
2.3.2	3D culture	40
2.4	Image Processing	41
2.4.1	Processing images from 2D cell culture	41
2.4.2	Processing images from 3D cell culture	42
2.5	Antibody Staining and Image Processing Optimization	43
2.5.1	Sox2	43
2.5.2	Nestin	44
2.5.3	GLAST	45
2.5.4	GFAP	46
2.5.5	Tubulin β 3	46
2.5.6	Tbr2	48
2.5.7	PDGFRa	49
2.6	Quantification	51
2.6.1	Cell Counting	51
2.6.1.1	2D culture	51
2.6.1.2	3D culture	52
2.6.2	Analysis	52
3	Results	53
3.1	Immunocytochemical Characterization of NSPCs and NSPC-Derived Progeny	53
3.1.1	NSPCs	53
3.1.2	RGCs	55
3.1.3	IPCs	55

3.1.4	Neurons	57
3.1.5	Astrocytes	58
3.1.6	OPCs and Preoligodendrocytes	59
3.1.7	Nestin-Sox2, Nestin-GLAST double stainings	60
3.2	Characterization of NSPC-seeded Porous Collagen Scaffolds	62
3.2.1	3D Culture	62
3.2.2	2D Culture	65
3.2.3	Comparison of NSPC Differentiation in 3D & 2D Culture	68
3.2.3.1	Detailed characterization of NSPCs	69
3.2.4	NSPC Differentiation Capacity as a Function of NSPC Passage	70
3.2.4.1	3D Culture	71
3.2.4.2	2D Culture	71
3.3	Neural fate manipulation of NSPCs in PCSs	73
3.3.1	3D culture	73
3.3.2	2D Culture	76
3.3.3	Comparison of NSPC Differentiation between 3D & 2D Culture	79
3.3.3.1	Detailed characterization of NSPC fates	80
3.3.4	NSPC Differentiation Capacity as a Function of NSPC Passage	81
3.3.4.1	3D Culture	81
3.3.4.2	2D Culture	81
3.3.5	Comparison between 3DIV and 8DIV in NSC full medium	83
4	Discussion	85
5	References	88
6	Protocols	98
6.1	Cortical E13.5 Neural Stem Cell Culture	98
6.1.1	Tissue Dissection	98
6.1.2	Tissue processing for NSC	98
6.1.3	Cell Culture Media	99
6.1.4	Passage	100

6.1.5	Cell seeding	100
6.1.5.1	2D culture	100
6.1.5.2	3D culture	101
6.1.6	Differentiation	101
6.1.7	NSC Freezing Protocol	101
6.1.8	Thawing Cells	102
6.2	Immunocytochemistry (ICC) Fluorescence Staining	103
6.2.1	Preparation	103
6.2.2	Procedure	103
6.2.2.1	Fixation, Permeabilization and Blocking	103
6.2.2.2	Primary Antibody Incubation	104
6.2.2.3	Secondary Antibody Incubation	104
6.2.2.4	Counterstain	105

1 Introduction

1.1 Spinal Cord Injury (SCI)

Spinal cord injury (SCI) is defined as damage to the spinal cord, which temporarily or permanently causes functional problems. SCI can be stratified according to the spinal cord level affected. Higher cervical lesions can lead to partial or full tetraplegia (paralysis of the four limbs), while lower lesions can lead to paraplegia (paralysis of the lower limbs). SCI could be divided into traumatic and non-traumatic etiologies. Traumatic SCI results from an external physical impact sufficient to acutely damage the spinal cord, for example due to motor vehicle accident, fall, sports-related injury or violence. Non-traumatic SCI occurs when an acute or chronic disease process, such as a tumor, infection or degenerative disc disease, generates the primary injury. (Ahuja et al., 2017; Pereira et al., 2019).

Field Code Changed

1.1.1 Traumatic SCI

Traumatic injury to the spinal cord can be caused by compressions, lacerations, and contusions, which lead to a spectrum of neurological symptoms depending on the level and the severity of the injury such as motor/sensory dysfunction, autonomic deficits, neuropathic pain, autonomic dysreflexia, and bowel/bladder dysfunction (Katoh et al., 2019).

Field Code Changed

1.1.2 Epidemiology of Traumatic SCI

SCI is recognized as a global health issue due to its complex and multifactorial pathophysiology and its significant impact on patient quality of life. According to the World Health Organization, the estimated annual incidence of SCI ranges from 250,000–500,000 individuals worldwide. Although global incidence is similar between genders, men have higher incidence compared to women at ages 20–40 years. The age profile of individuals with a traumatic SCI has a bimodal distribution; the first peak lies between 15 and 29 years old. The second, smaller but growing peak covers people older than 50 years old (Ahuja et al., 2017; Pereira et al., 2019).

Up to 90% of SCI cases are due to traumatic causes, though the proportion of non-traumatic spinal cord injury appears to be growing. Among the main causes of SCI are motor vehicle accidents, falls, sports-related injuries and violent acts. The profile of elderly SCI patients changes due to low-energy impacts, such as falls or spinal degenerative changes (e.g. degenerative cervical myelopathy). In the general population, traumatic SCI occurs most frequently at the level of the cervical spine (~60%), followed by thoracic (32%) and lumbosacral (9%)(Ahuja et al., 2017; Katoh et al., 2019).

Field Code Changed

SCI has a tremendous impact on the personal, professional, and social life of patients, imposing enormous psychological and financial burdens on the patients and their caregivers. Thus, the loss of independence and persistently increased lifelong mortality rates are the hallmarks of SCI. In addition, the medical care of SCI patients is very expensive: the overall lifetime economic cost is staggering at US\$1.1–4.6 million per patient (Ahuja et al., 2017).

1.1.3 SCI Pathophysiology

The processes occurring within the injured spinal cord can be divided according to the elapsed time from the precipitating injury into acute (<48h), subacute (48h to 14 days), intermediate (14 days to 3 months), and chronic phases (>3 months). Also, the initial acute phase could be further divided into the “primary injury”, which corresponds to the time when the spinal cord is actually lesioned, and the “secondary injury” events that occur over the time course of minutes to weeks, relying on the complexity of each situation (Kato et al., 2019; Pereira et al., 2019).

The initial traumatic event leads to the primary injury through mechanical compression, contusion, stretching, or kinking of the spinal cord, which often accompany fractures and/or vertebral column dislocation. This physically insults cellular components essential for neuronal transmission (including neurons, oligodendrocytes) and disrupts vascular components, including the blood-spinal cord barrier (BSCB), inducing infiltration of inflammatory cells (Kato et al., 2019).

The subsequent secondary injury cascade leads to further chemical and physical damage to the spinal cord and results in severe neurological deficits. Increased glutamate at the site of lesion results in neuronal excitotoxicity due to the accumulation of intracellular calcium (Ca^{2+}), leading to an increase in reactive oxygen species (ROS) that damage cellular components (nucleic acids, proteins, and phospholipids) and cause cellular loss and subsequent neurological dysfunction. Increased permeabilization of cells, pro-apoptotic signaling, ischemia and breakdown of the BSCB further exacerbates insult to the injured spinal cord. Disrupted blood vessels cause severe hemorrhage and allow infiltration of inflammatory cells including neutrophils, monocytes/macrophages, T cells, and B cells into the spinal cord tissue. These inflammatory cells release inflammatory cytokines such as tumor necrosis factor (TNF)- α , interleukin (IL)-1 α , IL-1 β and IL-6. These cytokines, which often reach their peak 6–12 h after injury, further induce an overwhelming inflammatory response during the acute to subacute phase that expands the lesion in the rostral and caudal direction. Activated microglia and infiltrated macrophages have been shown to be responsible for the necrosis and apoptosis of neurons, astrocytes and oligodendrocytes residing in the lesion, finally resulting in anterograde (Wallerian degeneration) and

retrograde (axonal dieback) axonal degeneration. Furthermore, reactive astrocytes and other glial cells secrete chondroitin sulfate proteoglycans (CSPGs), which act as a physical and chemical barrier that impedes endogenous tissue repair processes such as axonal sprouting and synaptic reorganization (Figure 1.A) (Kato et al., 2019).

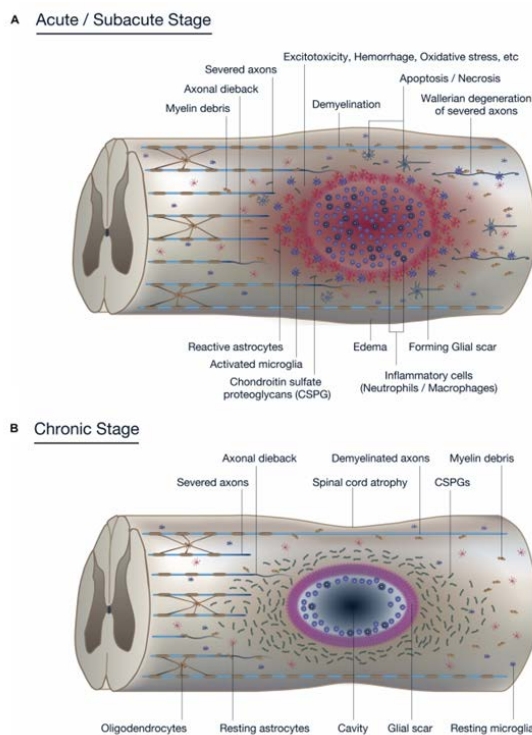


Figure 1 – Pathophysiology of spinal cord injury. A. During the acute to subacute phase of SCI, primary and secondary injury mechanisms lead to inflammation, haemorrhage, apoptosis, and necrosis. Resident neurons, oligodendrocytes, and astrocytes near the lesion are forced into apoptosis or necrosis, resulting in anterograde (Wallerian degeneration) and retrograde (axonal dieback) axonal degeneration. Reactive astrocytes and other glial cells secrete chondroitin sulfate proteoglycans (CSPGs). **B.** During the chronic phase of SCI, the epicenter of the lesion contain cavitations that are surrounded by connective scar tissue and contain cerebrospinal fluid (CSF). Scar-forming astrocytes impede regenerating axons from crossing the lesion. Inflammatory immune cells remain around the lesion. (Kato et al., 2019)

Finally, the onset of the chronic phase can occur days to months after primary injury and continues throughout the patient’s life. During the chronic phase there is grey matter dissolution, white matter demyelination, deposition of connective tissue, and the formation of

the glial scar. The phenotype of reactive astrocytes has changed into scar-forming astrocytes that impede regenerating axons from crossing the lesion. Microglia/macrophages, pericytes, and extracellular matrix molecules, act as a physical barrier that limits axonal growth, whereas myelin-associated proteins and proteoglycans are among the most inhibitory molecules in the central nervous system. Cavitation takes place in the epicenter of the lesion, where cysts containing cerebrospinal fluid (CSF) are surrounded by connective scar tissue. Many SCI patients also develop pain syndromes and mood disorders, like depression (Figure 1.B) (Katoh et al., 2019; Pereira et al., 2019).

The above-mentioned event cascade, leads to severe changes in the organization and structural architecture of the spinal cord, including the formation of a glial scar and cystic cavities. Combined with poor endogenous remyelination and axonal regrowth, these result in the poor intrinsic recovery potential of the spinal cord and finally permanent neurological deficits (Ahuja et al., 2017).

1.1.4 Failure of Axon Regeneration after SCI

During adulthood, CNS neurons, in contrast to PNS neurons, do not maintain their intrinsic growth capacity and demonstrate great inability to regenerate their axons following injury (van Niekerk et al., 2016). Limited axonal regeneration in the CNS is partially attributed to a non-permissive environment for axon outgrowth, especially the extracellular milieu surrounding CNS injury, where there is abundance of inhibitory proteins and glycoproteins, deficient trophic support, and finally the formation of cystic or trabeculated cavities at the lesion site (Figure 2) (van Niekerk et al., 2016).

In the acute phase, signaling from activated microglia, astrocytes and macrophages causes the secretion of ECM proteins that are inhibitory to axonal growth, such as CSPGs, tenascin and NG2 proteoglycan, which condense with astrocytes to form the glial scar. Specifically, naive astrocytes change their phenotype to reactive astrocytes and then to scar-forming astrocytes. In the subacute phase, reactive astrocytes proliferate, get organized around the lesion edges and eventually migrate into the lesion epicenter where they remove inflammatory cells, leading to tissue repair and functional improvement. However, at later stages, elongated reactive astrocytes along with pericytes form the glial scar. While glial scar prevents the spread of injury to the surrounding healthy tissue, it restricts axon regeneration and anatomical plasticity by inhibiting neurite outgrowth (Ahuja et al., 2017; Katoh et al., 2019).

CSPGs are growth-inhibitory extracellular matrix glycoproteins that include neurocan, versican, brevican, phosphacan, and NG2. CSPGs normally serve as guiding molecules during development and modulate synaptic connections in the adult CNS. After trauma,

CSPGs have been shown to repel regenerating axons and prevent oligodendrocyte maturation and remyelination. CSPGs are secreted after the inflammatory response and act as a chemophysical barrier to axonal regrowth. Therefore, CSPGs are regarded as a major cause of failed regeneration in the CNS (Ahuja et al., 2017; Katoh et al., 2019).

Oligodendrocyte progenitor cells (OPC) that express the NG2 proteoglycan migrate to the lesion site and associate with dystrophic axons. Pericytes also proliferate after SCI, giving rise to stromal cells that can deposit numerous ECM proteins. Furthermore, fibroblasts can infiltrate into the perilesional region in order to replace the ECM with fibrous connective tissue and dense collagen deposits (Ahuja et al., 2017; Katoh et al., 2019).

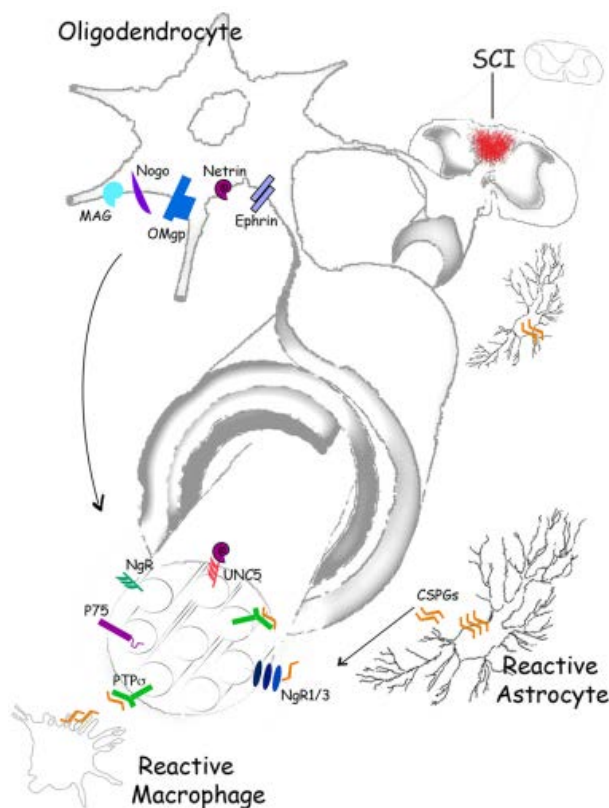


Figure 2 - Non-permissive environment for axon outgrowth after SCI. Limited axonal regeneration in the CNS by the formation of a non-permissive environment, where inhibitory molecules act as barriers of axon outgrowth. Two classes of these inhibitors: inhibitory molecules of the extracellular matrix such as the CSPGs; and inhibitory proteins associated with adult myelin - Nogo, oligodendrocyte-myelin glycoprotein (OMgp), myelin-associated glycoprotein (MAG), Netrin-1, Ephrins.
(van Niekerk et al., 2016)

Myelin-associated inhibitors (MAIs) include Nogo, oligodendrocyte-myelin glycoprotein (OMgp), myelin-associated glycoprotein (MAG), Netrin-1 and Ephrins. MAIs bind to their receptors (Nogo receptor and p75 neurotrophin receptor (p75NTR)) on the surface of injured axons, activating downstream effectors, such as RHOA and Rho-associated protein kinase (ROCK), which cause growth cone collapse, neurite retraction and lead to neuronal apoptosis (van Niekerk et al., 2016; Ahuja et al., 2017).

Apart from MAIs, axon regeneration in CNS is further blocked by microtubule stabilization. Following injury, most mammalian CNS axons retract and only a few axons sprout for short distances. Being exposed to the inhibitory environment in a CNS lesion site, axons exhibit dystrophic and swollen endings and fail to initiate growth cones, whereas a disorganized microtubule network is formed, finally leading to regeneration failure (van Niekerk et al., 2016; Ahuja et al., 2017).

Lack of localization of ribosomes and mRNAs in CNS axons could also correlate with their poor regeneration ability, since local protein synthesis and mRNA localization have been closely associated with successful peripheral nerve regeneration (Ahuja et al., 2017; van Niekerk et al., 2016).

1.1.5 Therapeutic Approaches

Based on the knowledge of the underlying mechanisms of SCI pathophysiology, several neuroprotective and regenerative approaches have been evaluated as treatments for SCI. Neuroprotective therapy works by limiting secondary damage, while neuroregenerative strategies aim to replace damaged cells, axons and circuits in the spinal cord. Major efforts are currently underway in order to develop new therapies for SCI, with numerous studies having reported some positive results in preclinical SCI models. However, their clinical translation still remains questionable and controversial.

1.1.5.1 Neuroprotective therapies

According to the current clinical practice, a SCI patient is initially immobilized and is constantly monitored to prevent possible complications, such as respiratory dysfunctions, cardiovascular aberrations, and hypoxia. After patient stabilization, clinicians surgically decompress the spinal cord and control the lesion site (Pereira et al., 2019).

The first-line of drug treatment for SCI includes the anti-inflammatory compound methylprednisolone sodium succinate (MPSS) (Bartholdi & Schwab, 1995). Despite its neuroprotective effects and neurological improvements, MPSS side effects prevent it from becoming a viable long-term therapeutic choice (Caruso et al., 2017).

Other pharmacological alternatives are minocycline and riluzole, which are already under clinical trials. Both compounds target secondary events such as inflammation and excitotoxicity. Minocycline, a semisynthetic tetracycline antibiotic, is classified as a neuroprotective agent by improving the exacerbated inflammatory microenvironment observed during secondary SCI (Zhong & Shultz, 2017). Riluzole is a benzothiazole anticonvulsant that can block the abnormal glutamatergic transmission in neuronal synapses (Nagoshi et al., 2015).

Also, Fibroblast growth factor-2 (FGF-2; basic fibroblast growth factor), due to its function in cell proliferation and survival, has been implied in different studies that provide evidence on its role in spinal cord neural stem and progenitor cells proliferation, angiogenesis and glial cavitation reduction (Zhou et al., 2018).

Morphological and functional recovery of the spinal cord after trauma has also been demonstrated after cytokines administration. The most widely studied cytokine for SCI treatment is Granulocyte Colony-Stimulating Factor (G-CSF), a glycoprotein that can reduce inflammatory cytokine expression and promote the survival of ischemic cells (Kamiya et al., 2015). Another promising cytokine for SCI treatment is interleukin-4 (IL-4), which can activate macrophages to a phenotype associated with repair (Francos-Quijorna et al., 2016).

1.1.5.2 Neuroregenerative therapies

Neuroregenerative therapies aim to repair disrupted neural networks by supporting and enhancing the endogenous potential of sprouting axons and remyelination, which would hopefully lead to the reconnection of descending neural fibers with their original targets such as spinal interneurons and motor neurons in the caudal spinal cord.

Recent evidence proved that mammalian CNS finally maintains the capacity for neural tissue remodeling and axonal plasticity (i.e. sprouting). Damaged axons are able to regenerate to some degree, but within a certain time window, depending on the level of their intrinsic capacity to activate a regeneration-associated gene (RAG) expression program. Such strategies of neural regeneration include neutralization of myelin-derived inhibitors (e.g., anti-Nogo-antibodies), downstream inhibition of the related intracellular signaling pathways (Rho-GTPase signaling), and degradation of inhibitory components of the glial scar (e.g. degradation of CSPG by chondroitinase-ABC). It has also been proved that neurotrophic factor action or manipulation of pro-regenerative or inhibitory neuronal signaling pathways (mTOR/PTEN) can stimulate axon growth through the traumatic lesion site (Soares et al., 2020).

1.1.5.3 Cell transplantation

Cell transplantation in a CNS lesion site is one of the most promising treatments regarding neuroprotective effects and neuroregeneration potential. Engrafted cells repopulate the lesion cavity and modulate the transplantation site into a more hospitable environment that prevents demyelination and apoptosis of neural cells (Kato et al., 2019).

The most widely studied cell types are Schwann cells, neural stem and progenitor cells (NSPCs), oligodendrocyte precursor cells (OPCs), olfactory ensheathing cells (OECs) and mesenchymal stem cells (MSCs) (Figure 3). Following transplantation in a SCI lesion, cells are hypothesized to mediate functional improvements through a variety of mechanisms, including neuroprotection, immunomodulation, axon sprouting and/or regeneration and myelin regeneration (Assinck et al., 2017).

Stem cells, retaining their multipotency, have their own differentiation capacity and could replace degenerative necrotic cells. In addition, stem cells secrete anti-inflammatory factors that inhibit the inflammatory reaction in the lesion site. Finally, stem cells produce many cytokines, growth factors, and cell adhesion factors that play important roles in improving the microenvironment and promoting tissue regeneration (Figure 4) (Shao et al., 2019).

Neural Stem/Progenitor Cells (NSPCs) are the most well-studied cell source for the treatment of SCI, due to their multipotency and capacity to differentiate into all neural lineage types - neurons, astrocytes and oligodendrocytes. The modulation of the astrocytes contribution to the glial scar is considered as the main mechanism of therapeutic effect of NSPCs. NSPCs function as a scaffold within the scar to restrict the secondary enlargement of the lesion and prevent the lesion from expanding after the initial insult. NSPCs transplantation also promotes functional recovery, since NSPC-derived neurons provide a neuronal substrate for electrical signals to bridge the lesion area. Injured axons after SCI can form connections with the transplanted NSPCs, creating a relay circuit that may potentially bridge the disrupted tracts. Furthermore, secretion of growth-promoting factors (BDNF, CNTF, GDNF, NGF, IGF-1) by NSPCs promotes the survival and growth of damaged neurons. Finally, the capacity of NSPCs to differentiate into oligodendrocytes leads to the myelination and consequently to motor and sensory function improvement (Assinck et al., 2017; Shao et al., 2019).

Table 1 Cell sources and proposed mechanisms of cited transplantation work

Schwann cells: peripheral myelinating glia required for the regeneration of axons following nerve injury.	
Source \ Species \ Age \ Cotransplant agent	Proposed mechanism
Sciatic nerve \ rat \ adult \ none ^{101,104,132} , embedded in Matrigel ^{61,65,67,73} , intraspinal cAMP ²⁵ , embedded in Matrigel with OEC cotransplant and systematic chondroitinase ABC ⁶⁵	Neuroprotection ^{61,101} , axon regeneration and sprouting ^{25,65,67,73,101,104,132} , myelination ^{25,65,67,101}
Back skin \ rat ¹⁰² or mouse ²⁶ \ neonatal \ none ^{26,102}	Neuroprotection ^{26,102} , axon regeneration and sprouting ^{26,102} , myelination ^{26,102}
Olfactory ensheathing cells (OEC): glia that support the axonal growth of olfactory receptor neurons into the olfactory bulb.	
Source \ Species \ Age \ Cotransplant agent	Proposed mechanism
Olfactory bulb \ rat ^{27,42,62,65,101,132} or mouse ⁴³ \ adult \ none ^{27,42,43,62,101,132} embedded in Matrigel with Schwann cell cotransplant and systematic chondroitinase ABC ⁶⁵	Neuroprotection ^{27,42,62,101} , axon regeneration and sprouting ^{27,43,62,65,101,132}
Lamina propria \ mice \ neonatal \ none ^{43,44}	axon regeneration and sprouting ^{43,44}
MSCs and multipotent adult progenitor cells (MAPCs): multipotent progenitors found in tissues such as adult bone marrow isolated by virtue of their adherence during tissue culturing and/or distinct cell surface markers.	
Source \ Species \ Age \ Cotransplant agent	Proposed mechanism
Tibia or femur bone marrow \ rat \ adult \ none ^{30,33,56} , cells overexpressing BDNF ³⁵ , cAMP injected into DRG to precondition neurons with intraspinal NT-3 ⁶⁴ , or intraspinal BDNF along with BDNF overexpression in transplanted cells ⁷¹	Neuroprotection ^{33,35,56} , immunomodulation ^{30,56} , axon regeneration and sprouting ^{64,71}
Iliac crest (pelvic) bone marrow ⁹⁵ or MAPCs ⁵⁷ \ human \ adult \ none ^{95,57}	Neuroprotection ^{55,57} , immunomodulation ^{55,57}
NSPCs: multipotent progenitors isolated from the CNS and often grown as neurospheres with the capacity to differentiate into neurons and glia.	
Source \ Species \ Age \ Cotransplant agent	Proposed mechanism
Spinal cord \ rat \ adult ^{30,110,115} or embryonic ^{39-41,63,86,87,89,113} \ none ³⁰ , cells infected with neurogenin-2 overexpressing retrovirus ¹¹⁵ , transplanted as a graft ^{39-41,86,87} , cells infected with D15A retrovirus which secretes a bioactive growth factor with BDNF and NT3 activities ¹¹³ or overexpressing CNTF ¹¹⁰ , dissociated cells suspended in fibrin gel with growth factor cocktail ^{63,89}	Neuroprotection ¹¹³ , immunomodulation ³⁰ , axon regeneration and sprouting ^{63,87,89,115} , relay formation ⁶³ , myelinogenesis ^{110,113}
Brain \ mouse \ embryonic ^{112,117} or adult ^{54,111,116,139} \ none ⁵⁴ , cells from a shiverer mouse ^{116,117} , exogenous FGF and/or PDGF ¹¹² , exogenous PDGF, FGF, EGF for 1 week ¹¹¹ and 1 week of chondroitinase ABC ¹³⁹	Neuroprotection ^{54,116,117} , myelinogenesis ^{111,112,139} , axon regeneration and sprouting ^{116,117}
Brain \ human \ fetal ^{14,90} \ none ^{14,90} , retroviral overexpression of Olig2 ¹¹⁴	Neuroprotection ¹¹⁴ , myelinogenesis ¹¹⁴
Spinal cord \ human \ fetal \ transplanted in fibrin matrix with trophic factor cocktail ⁶³	Axon regenerating and sprouting ⁶³ , relay formation ⁶³
Embryonic stem cell-derived or inducible pluripotent stem cell (iPSC)-derived neural precursor cells: cells derived from immortalized cell lines or from adult tissues and induced into pluripotent stem cells. Cells are then differentiated into desirable cell type prior to transplantation.	
Source \ Species \ Age \ Cotransplant agent	Proposed mechanism
Stem cells \ human \ embryonic \ predifferentiated into OPCs ^{32,108} , sorted for NSPCs and transplanted in fibrin matrix with growth factor cocktail ⁶³	Neuroprotection ³² , immunomodulation ³² , axon regeneration and sprouting ⁶³ , relay formation ⁶³ , myelinogenesis ¹⁰⁸
Fibroblasts \ human \ adult \ iPSCs differentiated into NSPCs ^{121,128} , with fibrin matrix and growth factor cocktail ^{12,68}	Neuroprotection ¹²⁸ , axon regeneration and sprouting ^{12,68,121,128} , relay formation ^{12,68}
Peripheral blood monocytes, fetal lung fibroblasts or BMSCs predifferentiated into OPCs \ mouse \ adult or fetal \ none ¹⁰⁹	Neuroprotection ¹⁰⁹ , myelinogenesis ¹⁰⁹

Figure 3 - Table of cell types used for SCI transplantation and proposed mechanism of anatomical and functional improvement after SCI.

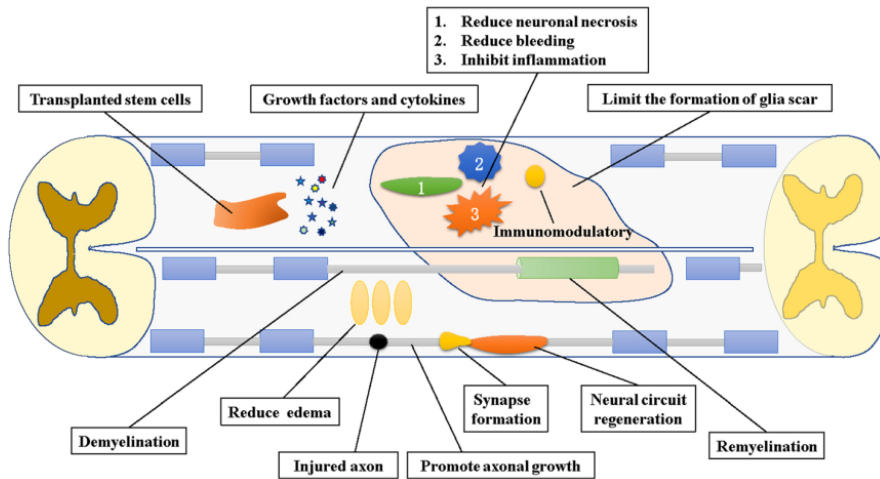


Figure 4 – Possible mechanisms of stem cells to mediate functional improvement following SCI. Multipotent stem cells retain their differentiation capacity and could replace degenerative necrotic cells. They secrete anti-inflammatory factors and inhibit the inflammatory reaction in the damaged microenvironment. They produce cytokines, growth factors, and cell adhesion factors that play important roles in improving the microenvironment and promoting tissue regeneration. (Shao et al., 2019)

1.1.6 Biomaterials in SCI

Biomaterials have been widely used in SCI as implant constructs. Biomaterials can be placed into the cavity and function as substrates where cells can grow, or even be seeded with different cell types in order to enhance tissue continuity across the trauma (Figure 5).

Many biomaterial substrates have been studied as candidate scaffolds for the treatment of SCI, such as collagen, laminin, fibrin matrices, fibronectin, hyaluronan-methylcellulose, chitosan, agarose, alginate, methylcellulose, poly(2-hydroxyethyl methacrylate) or PHEMA, poly(N-(2-hydroxypropyl) methacrylamide) or PHPMA, and poly(lactic-co-glycolic) acid or PLGA (Kato et al., 2019).

A scaffold should have specific characteristics in order to be suitable as an SCI graft. Since scaffolds permit the 3D culture of cells, they should exhibit features that emulate complex *in vivo* conditions and provide a biologically relevant environment (Ravi et al., 2015). Scaffolds allow cells to grow in three dimensions and act as substrates for growing axons. Scaffolds provide a structural support for the regrowth and migration of damaged axons and newly-generated neurons into the lesion site. They also improve revascularization and should not generate a frontier at the host tissue-scaffold interface. Scaffolds can be also modified in order to secrete factors or deliver drugs into the lesion site in order to enhance tissue growth and vascularization. Scaffolds should have a simple design that allows smooth

manufacturing and easy placement into the lesion site. Finally, they should have good biocompatibility with low immunogenicity and be biodegradable (Kato et al., 2019; Li et al., 2019, Soares et al., 2020).

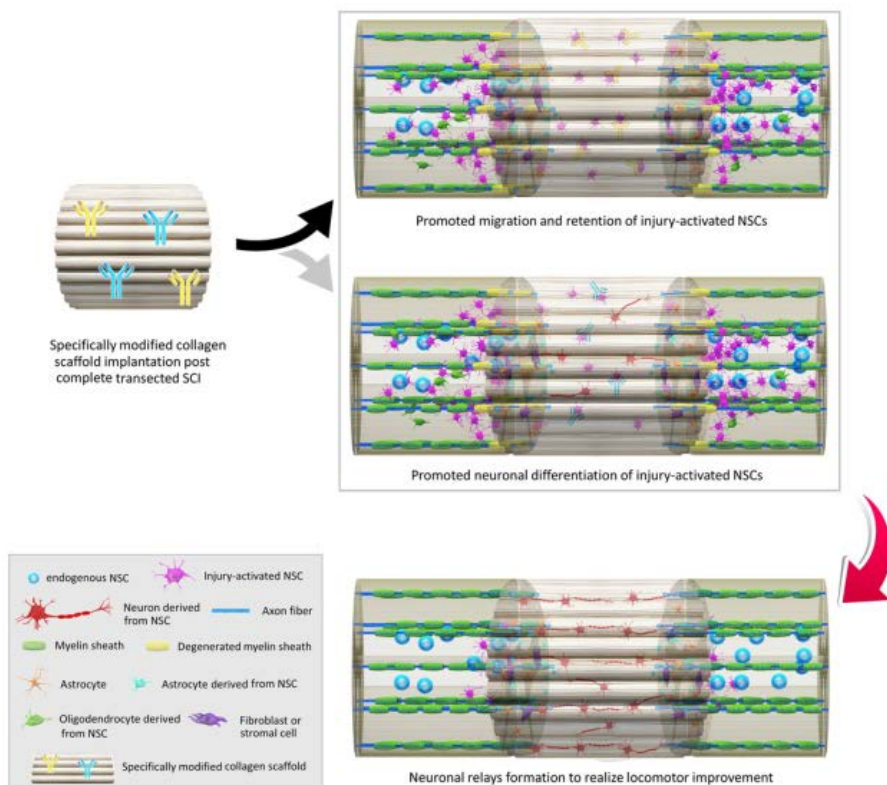


Figure 5 – Biomaterial scaffolds in SCI. NSCs-seeded scaffolds can be placed at the lesion site in order to function as substrates for cell growth. Scaffolds could modulate the directed migration and neuronal differentiation of NSCs, or even be specifically modified for drug delivery. Finally, scaffolds seem restore tissue continuity across the trauma and promote locomotor outcome after SCI. (Li et al., 2019)

1.2 Central Nervous System Development

The mammalian nervous system is the most complex organ of any living organism. A great diversity of neural cell types forms the mature central nervous system (CNS). All these cell types derive from the neuroepithelial cells (NECs) of the neural tube. The adult vertebrate CNS consists of four major cell types: neurons, oligodendrocytes, astrocytes and ependymal cells (Kintner, 2002). This cellular diversity originates to a large extent from the specification of progenitor populations during development, where both cell proliferation and withdrawal from the cell cycle are regulated in spatiotemporal manner.

In mice, during patterning of the neural plate and neural tube, floor plate and roof plate cells secrete morphogens such as fibroblast growth factors (FGFs), retinoic acid (RA), Sonic hedgehog (Shh) and bone morphogenetic proteins (BMPs) in distinct spatial patterns, sequentially leading to regional expression of homeodomain and bHLH transcription factors. These transcription factors are responsible for patterning the dorsal–ventral, anterior–posterior and medial–lateral axes of the developing neural tube, thus driving the initial specification of the main CNS regions (forebrain, midbrain, hindbrain, spinal cord) and guiding progenitor cells to follow specific cell lineages during neurogenesis (Guérout et al., 2014).

The primordium of the CNS, the neural plate, originates from the ectoderm of gastrulating vertebrate embryos. It is formed by a single sheet of NECs, which undergo rapid symmetric divisions that result in planar expansion of the neural plate and neurulation ending to the generation of the neural tube (E5.5-E8.0) (Martynoga et al., 2012). At this stage NECs, a relatively homogenous cell population, undergo massive proliferation to expand their population prior to cell fate specification and also transit from leukemia inhibitory factor (LIF)-dependency to fibroblast growth factor (FGF)-dependency (Ramasamy et al., 2013). Finally, NECs, which form a polarised pseudostratified neuroepithelium, possess a basal side attached to the pial surface and an apical side that contacts the lumen of the neural tube (Barry et al., 2014).

NECs mature into regionally-specified neural progenitor cells (NPCs) and form the CNS germinal zones, the ventricle zone (VZ) (E13) and subventricular zone (SVZ) (E14.5). Subsequently NECs lose some of their epithelial properties changing their proliferation mode from symmetric to asymmetric divisions. This process is highly regulated by Notch signaling. Notch is unequally distributed to daughter cells and low Notch signaling in the second daughter cell allows neuronal differentiation.

At mid-gestation, between E9 and E10, the first neurons of the CNS are born (Martynoga et al., 2012). As neurogenesis proceeds, at E13 cells begin to respond to epidermal growth factor (EGF) in addition to FGF. Then, between E13.0 and E18.0, the differentiation process

of neurogenesis is followed by astrogenesis and oligodendrogenesis. At these later differentiation processes, the Platelet-derived growth factor (PDGF) is the major driver (Ramasamy et al., 2013).

Astrocytes in the CNS are responsible for structural support, maintenance of water balance and ion distribution, formation of the blood brain barrier, synaptic regulation and play crucial role in the repair and scarring process following traumatic injuries. Astrocytes are generated after neurogenesis has been completed, but also in a spatio-temporal manner, regulated by concentration gradients of transcription factors along the central canal. On the other hand, although oligodendrogenesis occurs concurrently to astrogenesis, the first mature oligodendrocytes appear after differentiated astrocytes, around birth, and their number increases dramatically for the following six postnatal weeks. The main function of oligodendrocytes is to provide support and insulation to CNS axons, wrapping each axon with a myelin sheath (Guérout et al., 2014).

Ependymal cells line the ventricular system, forming a continuous cellular barrier between the CSF and the adjacent parenchyma. Ependymal cells are specialized multi-ciliated cells, whose motile cilia beating is responsible for CSF flow, brain homeostasis, and normal function of adult stem cell niches. Three different subtypes of ependymal cells have been described based on morphological criteria and molecular markers (tanycytes, cuboidal and radial ependymal cells). Upon injury, ependymal cell progeny includes mostly astrocytes and a few oligodendrocytes (Guérout et al., 2014).

Neurogenesis ends soon after birth, when the vast majority of CNS neurons have already been generated. However, new neurons are also added throughout adulthood. Adult neurogenesis occurs only in two specific brain regions: the SVZ of the lateral ventricles and the subgranular zone (SGZ) of the hippocampal dentate gyrus. These two neurogenic niches contain slowly dividing, astrocyte-like adult neural stem cells, which give rise to rapidly amplifying intermediate progenitors, which produce committed neuroblasts that migrate and differentiate into olfactory bulb or hippocampal neurons, respectively (Guérout et al., 2014).

1.2.1 Cortex Development

The telencephalon, which includes the cerebral cortex and basal ganglia, is the seat of motor coordination, emotions, higher cognition and consciousness in humans. It is by far the most complex region of the adult mammalian brain. The two main subdivisions - the dorsal telencephalon (the pallium) and the ventral telencephalon (the subpallium) - generate very different types of neurons. The germinal zone of the dorsal telencephalon gives rise to the excitatory glutamatergic projection neurons of the cerebral cortex, which sequentially reach the different layers of the cortex by radial migration (pyramidal neurons). Progenitors of the

ventral telencephalon generate GABAergic inhibitory neurons, including basal ganglia neurons, as well as interneurons that migrate tangentially to contribute to the formation of the cortex. The mature cerebral cortex is comprised of six layers and contains both excitatory pyramidal neurons and inhibitory interneurons (Guillemot, 2005).

During embryogenesis (Figure 6), NECs in the dorsal telencephalon symmetrically divide until E9–E10. Then, soon after the beginning of neurogenesis (E11–E13), another progenitor population appears, apical radial glial cells (aRGCs), which give rise to most projection neurons of the cerebral cortex (NECs and aRGCs are noted as apical progenitors (AP)). aRGCs have glial cell features and radial processes extending from the pial (outer) surface to the lateral ventricle (inner surface) of the neural tube. Their basolateral plasma membrane is divided in two subcompartments: the apical and the basal process, where the basal process traverses the SVZ zone and all the forming neuronal layers and reaches the basal lamina. This conformation provides a scaffold for radial neuronal migration and guides the newborn excitatory cortical neurons from the place of birth to their final destination into cortical layers. aRGCs are the progenitors of most neurons and macroglia in the neocortex as just small populations of postmitotic cells are generated from NECs before they are differentiated into aRGCs.

NEC-to-aRGC transition is characterized by the loss of tight junctions, acquisition of glycogen storage granules and filaments, and the expression of astroglial genes such as brain lipid-binding protein (BLBP), astrocyte-specific glutamate transporter (GLAST), S100 β , glutamine synthase (GS), vimentin, and tenascin-C (TN-C) and in certain species GFAP (Franco & Müller, 2013). aRGC also express the intermediate filament Nestin and its post-translational modifications labeled by RC1 and RC2 antibodies. These astroglial characteristics of aRGCs are developed in a ventral to dorsal and lateral to medial gradient, with BLBP being amongst the earliest, followed by GLAST, vimentin, TN-C, and eventually S100 β and GS (Götz & Barde, 2005).

aRGCs divide at the ventricular surface and are connected to each other by adherence junctions forming the VZ (Guérout et al., 2014; Guillemot, 2005). aRGCs can divide both symmetrically to expand their population and asymmetrically to generate one daughter RGC and one non-RGC daughter cell. 10–20% of aRGCs directly generate neurons (Guérout et al., 2014; Paridaen & Huttner, 2014).

Non-aRGC daughter cells, known as intermediate progenitor cells (IPCs) (E13.5), are a more fate-restricted type of progenitors committed to the neuronal lineage (one of the types of basal progenitors (BP), see below). IPCs can undergo a few rounds of symmetric division in order to expand their population or can directly generate two neurons. Over the course of cortical neurogenesis, IPCs delaminate from the ventricular surface and lose their ventricular attachment. Dividing IPCs migrate away from the VZ and finally form a new germinal layer,

the subventricular zone (SVZ), where IPCs give rise to the majority of cortical projection neurons (Guérout et al., 2014; Paridaen & Huttner, 2014).

A key regulator of IPCs is Tbr2, a transcription factor expressed in IPCs when they start to appear at E11.5 in mice (Mihalas et al., 2016). Sox4 was also identified to be required for IPC specification, functioning as an upstream regulator of Tbr2, while it partners with the proneural gene Neurogenin 2 (Ngn2) to activate Tbr2 for maintenance of IPC fate (Dwyer et al., 2016). IPCs can be further distinguished from aRGCs by the downregulation of the RGC-specific Pax6 and GLAST (Englund et al., 2005; Götz & Barde, 2005).

As described above, all cortical excitatory pyramidal neurons are derived from aRGCs in the dorsal telencephalon VZ and from IPCs in the SVZ. Pyramidal neurons migrate to the preplate and form the nascent cortical plate, which further develops into layers II to VI. Early-born neurons occupy the deep layers (5–6) and are predominantly composed of corticofugal neurons that project away from the neocortex to subcortical targets, such as thalamus, brainstem, and spinal cord. Late-born neurons occupy the superficial layers (2–4) and are largely composed of intracortical neurons that project locally or to the contralateral cortical hemisphere (Guérout et al., 2014).

On the contrary, inhibitory cortical interneurons derive from aRGCs in the medial and caudal ganglionic eminences (GE) of the ventral telencephalon. These interneurons migrate first tangentially to reach the dorsal telencephalon and then radially within the different cortical layers starting around E15 (Guérout et al., 2014).

During neurogenesis the developing mammalian telencephalon consists of a large diversity of neural progenitor subtypes, which could be distinguished by their morphology, their mode of divisions and their progeny. Additional apical progenitors have been identified in the mouse neocortex, named short neural precursors (SNPs) and subapical RGCs (saRGCs) (Arai & Taverna, 2017). SNPs exhibit several features in common with aRGCs, such as the bipolar morphology and the integration into the AJ belt. SNPs also divide apically like aRGCs; however, SNPs have only short basal processes, which is confined only to the VZ, and undergo mainly neurogenic divisions and express markers of neurogenic fate (Dwyer et al., 2016). Based on their neurogenic properties, it has been proposed that SNPs may represent a subset of IPCs, having therefore some molecular differences, since SNPs express Pax6 but not Tbr2 (Franco & Müller, 2013). saRGCs are located in the developing ventral telencephalon of mice and therefore are proposed to add to cortical expansion through increased production of neurons. saRGCs are anchored to the ventricle with an apical process and they undergo mitosis at a subapical location (Paridaen & Huttner, 2014; Arai & Taverna, 2017).

The second class of neural BPs are basal radial glial cells (bRGCs), which appear to be born from divisions with oblique and horizontal cleavages of aRGCs. These recently

described cells keep radial glial characteristics, can divide repeatedly and are found at a very low abundance in the lissencephalic developing rodent dorsal telencephalon. bRGCs are monopolar cells lacking an apical attachment, but still maintain an attachment to the basal lamina via a basal process (Paridaen & Huttner, 2014; Arai & Taverna, 2017). bRGCs, which are intermediate progenitors, divide once in the subventricular zone (SVZ) into a pair of neurons (Paridaen & Huttner, 2014).

In conclusion, depending on the CNS region, different types of neural progenitors exist with a wide variety of morphologies, division modes, and lineages to generate diverse neuronal outputs. All these neural progenitor types and their lineages are by no means strictly separated and unidirectional, making their study even more complex.

Besides neurons, aRGCs also produce glial cells, including astrocytes and oligodendrocytes. Astrocytes are first detected around E16 and oligodendrocytes around birth; however, the vast majority of both cell types are produced during the first month of postnatal development.

In the cerebral cortex, astrocytes are produced by aRGCs within the cortical SVZ, whereas after birth astrocytes are generated locally in the cortex. During astrogenesis, most aRGCs release their apical attachment to the ventricle and move upward, away from the ventricular surface and gradually take on a multipolar, astrocytic morphology. The JAK-STAT signaling pathway is the best described gliogenic pathway regulating the neuron-to-astrocyte cell fate switch of progenitor cells. JAK signaling is activated by cytokines of the IL-6 family, such as ciliary neurotrophic factor (CNTF), leukemia inhibitory factor (LIF) or cardiotrophin 1 (CT-1) and results in the activation of STAT transcription factors. Notch signaling, previously described as a negative regulator of neurogenesis, can also actively promote astrogenesis. Finally, gliogenic cytokines are secreted in increasing amounts by newly generated neurons, inducing astrogenesis from remaining aRGCs (Martynoga et al., 2012; Guérout et al., 2014).

The glial specification is already induced at E11.5 by the expression of the nuclear factor I A/B (NFIA/B) and GLAST. These markers continue to be expressed in astrocytes during precursor migration and are down-regulated in oligodendrocyte precursor populations (E13.5–E16.5). Other reported markers of astrocytes and their precursors include S100-b, FGFR3, FABP7, BLBP and Sox9. However, these are not astrocyte-specific markers, since they are also expressed during neurogenic stages. Recent studies have also identified a new early stage marker of immature astrocytes, the folate metabolic enzyme Aldh1L1. On the other hand, GFAP expression is turned on relatively late in mice development. GFAP is a marker of terminally differentiated astrocytes, mature fibrous astrocytes and reactive astrocytes, and is poorly expressed in protoplasmic astrocytes (Molofsky et al., 2012).

The generation of cortical astrocytes after birth is mainly due to local division of mature astrocytes. Astrocytes born in the SVZ migrate within the cortex and generate the majority of

astrocytes by symmetric division giving two functional and differentiated daughter cells. Unlike neurons and oligodendrocytes, astrocytes remain capable of mitosis even in adulthood. They can divide to give rise to differentiated astrocytes. Astrocyte proliferation increases following CNS injury and results in the formation of the glial scar (Guérout et al., 2014).

Oligodendrocyte precursor cells (OPCs) are the progenitors of oligodendrocytes, the myelinating cell type of the CNS. OPCs appear in the developing brain with only a few days delay after the onset of neurogenesis. OPCs are detected in ventral regions of the developing CNS from where they spread throughout all brain regions by migration and proliferation (Leda Dimou & Götz, 2014).

Oligodendrocyte (OL) generation, in contrast to neurons and astrocytes that are produced from most, if not all, regions of the VZ/SVZ, takes place in a few restricted regions of the telencephalon, in a sequential appearance, first in the ventral region under the influence of Shh, and then in the dorsal region independent of Shh. OLs first appear in the VZ/SVZ of the ventral region from the medial ganglionic eminence (MGE) to the anterior entopeduncular area (AEP) that is defined by the expression of the Gbx2 homeobox gene, around E12. In these regions, OPC generation is regulated by the homeodomain transcription factor Nkx2.1 and subsequently induced by Shh signaling. Mash1 (Ascl1) is also required for the generation of the early population of OPCs in the ventral forebrain, but not at later stages. Then, at E16, Shh-independent OPCs appear from the dorsal telencephalon (Naruse et al., 2017).

Three waves of OPC generation have been described in the cerebral cortex. Around E12.5, the first OPCs, derived from Nkx2.1-lineage aRGCs, appear in the MGE and AEP in the ventral telencephalon. These progenitors migrate laterally and dorsally into all parts of the developing forebrain, including the cortex, where they mature and contribute to a subpopulation of myelinating OLs in the adult cortex. A few days later (E15.5), the second wave starts in the lateral ganglionic eminence (LGE), where the Gsx2 gene is specifically expressed, and OPCs migrate along the same route. At the third and final wave, around birth, OPCs are produced within the cortex itself. OPCs derived from dorsal neural precursors express the Emx1 gene and migrate, differentiate and populate all layers (Guérout et al., 2014; Naruse et al., 2017).

Oligodendrocytes generated by the first wave of OPCs are eliminated after birth in mammals. Thus most, if not all, of OLs in the adult cortex are derived from Emx1+ dorsal forebrain and Gsh2+ LGE. Recent studies, however, show that dorsal neural precursor cells never contribute to cortical OLs in the adult brain, but only produce neurons and astrocytes, and thus these Emx1- and Gsh2-lineage OLs found in the adult cortex are specifically derived from the lateral dorsoventral boundary (Guérout et al., 2014; Naruse et al., 2017).

OPC hallmarks are the expression of the platelet-derived growth factor receptor α (PDGFR α), the proteoglycan NG2 as well as transcription factors Olig1/2 and Sox10 (Leda Dimou & Götz, 2014).

Olig2, a basic helix–loop–helix transcription factor, is considered as a key factor for oligodendrocyte development. Olig2 is also expressed by motoneuron progenitors in the spinal cord. At later stages, Olig2 is specific for glial progenitors and mainly for OPCs. Long-term lineage tracing demonstrated a stage- and region-specific differentiation of embryonic Olig2+ cells. Olig2+ cells in the early fetal stage (E12.5 or earlier) primarily differentiated into GABAergic neurons in the adult telencephalon, while in later stages consisted of a mixed population of glial progenitor cells, which gave rise to both astrocytes and oligodendrocytes. In the late fetal telencephalon, the most common differentiation fate of Olig2+ cells seemed to be the astrocytes. Olig2+ progenitors in the diencephalon developed into oligodendrocytes, and a fraction developed into glutamatergic neurons. Therefore, during forebrain development Olig2+ cells form a dynamic, heterogeneous progenitor pool (Ono et al., 2008).

An additional OPC population, distinct from the previously-described PDGFR α + population, has been described. These OPCs are generated at very early stages (E9/E10), emerge from the ventral mouse forebrain and continuously express plp/dm-20 (the plp gene encodes the proteolipid protein and its alternatively spliced product DM-20, which are major proteins of CNS myelin). These OPCs are not sensitive to PDGF and seem to mature later. Genetic fate mapping experiments revealed that plp+ cells at early stages contribute to neuronal and glial lineages, while at later gestational stages (E13 and after) they generated only oligodendrocytes (Leda Dimou & Götz, 2014; Spassky et al., 1998).

Recently, another separate cell population has been described. Although it was widely accepted that the expression of Nerve/glia antigen 2 (NG2), a chondroitin sulfate proteoglycan, characterizes OPC progenitors, during the last years it has become obvious that these NG2-positive cells have further functions in the brain. So, now they are called NG2-glia cells and are distinct from neurons, astrocytes and oligodendrocytes. They represent an immature neural cell population that might give rise to distinct progenies depending on the brain region, the developmental stage and/or in pathological versus physiological conditions. NG2-glia cells can terminally differentiate into mature neural cell types, where the best described progeny are oligodendrocytes, or produce astrocytes or remain as self-renewing NG2-glia (L. Dimou & Gallo, 2015).

During their differentiation into myelin-forming cells, OPCs lose the above mentioned progenitor markers and could be characterized by the expression of O4, galactocerebrosides, and early myelin proteins like the 2',3'-cyclic nucleotide phosphodiesterase (CNPase) and myelin basic protein (MBP) (Leda Dimou & Götz, 2014).

Furthermore, among the main neural cells in the CNS exist also the ependymal cells. aRGCs, in most regions of the mammalian brain, undergo their last cell division during late embryogenesis (E14–18) and generate ependymal cells, which remain at the ventricle. However, ependymal cells acquire their mature features only during the first postnatal week (Guérout et al., 2014).

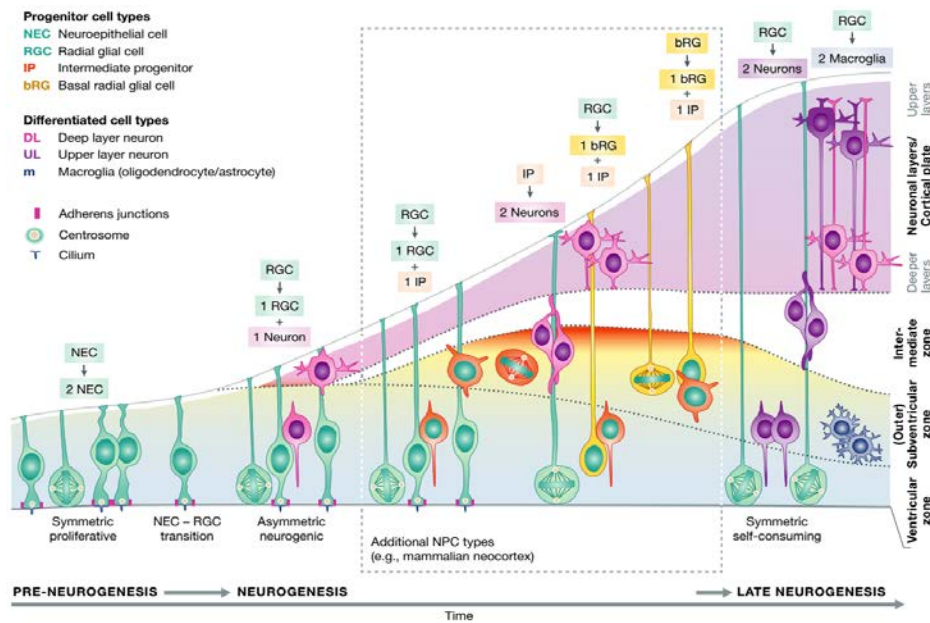


Figure 6 - Neurogenesis in the embryonic vertebrate CNS. Paridaen & Huttner, 2014

1.2.2 Terminology of Neural Stem Cells

The term neural stem cells (NSCs) generally refers to multipotent cells (able to produce multiple types of cells that are limited to one germ layer) that have the capacity for self-renewal and proliferation to identical cells, being capable to generate diverse neural lineages, including neurons, astrocytes and oligodendrocytes. NSCs are mainly present just after neural tube closure before the onset of neurogenesis and their number declines over subsequent stages of development. Specifically, neuroepithelial cells (NECs) of the neural tube represent the earliest multipotent NSCs. All neural cell types that form the mature CNS derive from NECs (Wu et al., 2008; Bonner et al., 2013).

The terms precursor and progenitor cells refer to a class of stem cells that are committed to a more restricted lineage profile than stem cells and therefore have a limited potency and

limited capacity for self-renewal (Bonner et al., 2013). In cerebral cortex, the earlier type of neural progenitor cells (NPCs) corresponds to the RGCs, which differ from their progenitors – NECs – due to their glial characteristics (Götz & Barde, 2005).

For further characterization of NPCs, the terms neuronal and glial restricted precursors (NRP and GRP, respectively) could be also used. NRPs that only differentiate into neurons (Bonner et al., 2013) could contain the populations of IPCs or bRGCs. On the other hand, GRPs only differentiate into glial cells - astrocytes and oligodendrocytes (Bonner et al., 2013). OPCs could be characterized as GRPs, since they are differentiated into oligodendrocytes. However, this discrimination is not feasible for astrocytes, since so far, no such intermediate progenitor (between aRGCs and astrocytes) has been described (Figure 7).

Neural lineage progenitors

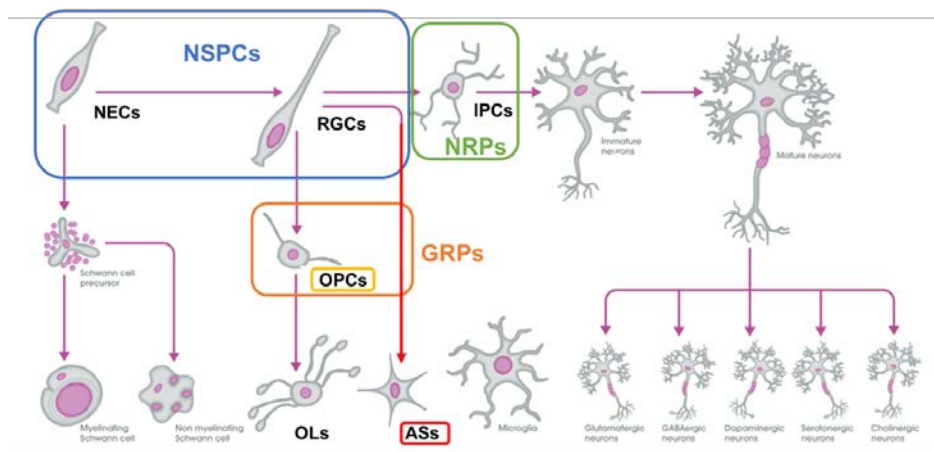


Figure 7 – Neural lineage progenitors. Colour code: blue – NSPCs, green – NRPs & neurons, orange- GRPs, yellow – OPCs, red – astrocytes. Modified image from <https://www.abcam.com/neuroscience/neural-markers-guide>

1.2.3 In Vitro Characterization of Stem Cells

In order to discriminate particular cell types, specific markers have been identified to be exclusively expressed in different cell lineages and at specific developmental stages.

1.2.3.1 Sox2

Sox2 (Sex determining region of Y chromosome (Sry)-related high mobility group box2) is one of the earliest transcription factors expressed in the neural tube start at the earliest

stages of CNS development (neural plate) (Zappone et al., 2000). Sox2 forms a trimeric complex with OCT4 on DNA, controls the expression of several of genes involved in embryonic development and is critical for early embryogenesis and for embryonic stem cell pluripotency.

Sox2 is expressed mainly in the expanding cell population of the ventricular zone, in which the appropriate pool of mitotically active neocortical cell populations, including neural progenitors, is generated. An *in vitro* study therefore demonstrated that NRPs utilized a serine protease activity to eliminate Sox2 protein and neural progenitors could differentiate into neurons only when Sox2 was turned off and/or degraded and the Notch1 signaling was repressed. However, Sox2 did not interfere with gliogenesis, as glial precursors maintained Sox2 expression throughout differentiation and as long as they continued to divide, since Sox2 positive and GFAP-positive astrocytes were found in the culture (Bani-Yaghoob et al., 2006). Moreover, Sox2 is differentially expressed between radial glial, intermediate progenitor populations and differentiated neurons within the dorsal telencephalon, with RGCs from the SOX2^{EGFP} mouse line expressing higher intracellular levels of Sox2 (Hutton & Penvy, 2011).

1.2.3.2 Nestin

Nestin is a Class VI intermediate filament (IF) expressed in the developing central nervous system during the early embryonic neuroepithelial stem cells. Nestin is considered as a marker of neural stem/progenitor cells (NSPCs), since it is present in several cell types at the early stages of embryonic development: NECs, RGCs. The transition from proliferation to the post-mitotic state and differentiation is accompanied by the downregulation of Nestin and often with the concomitant upregulation of other tissue-specific IF proteins such as glial fibrillary acidic protein (GFAP) in astrocytes (Gilyarov, 2008). Partial and transient co-expression of Nestin with lineage-specific marker proteins has been observed, however this was observed at time points that define the onset of cell lineage specification before terminal differentiation (Wiese et al., 2004). Furthermore, the emergence of Nestin expression correlates with cell biological alterations before specific “glial” features are yet detectable. Therefore, given Nestin immunoreactivity yet lack of glial features, cells should be referred to as NECs while cells in the previous stage (lacking Nestin expression) can be considered as being more similar to epithelial cells (Götz & Barde, 2005).

Nestin expression is not initiated until the time of neural tube closure (Lendahl et al., 1990). Also, it has been found that Sox proteins bind to a site immediately upstream of the POU site in Nestin gene that is essential for activation of the Nestin enhancer (Tanaka et al., 2004). So, it cannot be ruled out that the fraction of cells that are Nestin-Sox2+ represent NECs, at

the early stage of development and before the onset of Nestin expression (Barraud et al., 2005)

1.2.3.3 GLAST

Glutamate-aspartate transporter (GLAST; EAAT1) is responsible for the transport of L-glutamate and also L- and D-aspartate. GLAST is essential for terminating the postsynaptic action of glutamate by rapidly removing released glutamate from the synaptic cleft. GLAST also acts as a symport by co-transporting sodium. GLAST expression appears around the onset of neurogenesis on cells with long radial processes and glial characteristics and is not expressed by earlier neuroepithelial cells (Malatesta et al., 2000). However, GLAST+ RGCs continue to express Nestin until their morphological transformation into astrocytes, where GLAST expression is maintained, but Nestin is downregulated. GLAST is also specific for astrocytes at later stages (Hartfuss et al., 2001).

1.2.3.4 GFAP

Anti-Glial Fibrillary Acidic Protein (GFAP), a class-III intermediate filament, is the main constituent of intermediate filaments in astrocytes. Also, given that astrocytes and neurons derive from the same pool of progenitor cells, RGCs, could be also referred that GFAP is also expressed by NPCs (Guttenplan & Liddelow, 2019).

1.2.3.5 Tubulin beta 3

Tubulin is the main component of microtubules. Tubulin beta 3 (TUBB3) is primarily expressed in neurons and is commonly used as a neuronal marker. It plays an important role in neuronal cell proliferation and differentiation. It is expressed not only in mature neurons, but also in early stages of neuronal differentiation by mitotic neuronal precursors (Memberg & Hall, 1995; Fitzgerald et al., 2006).

1.2.3.6 Tbr2

Tbr2 is a T-domain transcription factor (TF) in the developing brain, which highly expressed in neuronal progenitors in the SVZ and basal VZ of neocortex. Tbr2 is a key regulator of IPCs and is expressed when IPCs start to appear at E11.5 in mice (Englund et al., 2005; Mihalas et al., 2016).

1.2.3.7 PDGFRa

Platelet-derived Growth Factor Receptor alpha (PDGFRa) is a member of the class III subfamily of receptor tyrosine kinases (RTK). Ligand-induced receptor dimerization results in

trans-autophosphorylation, resulting in the activation of several intracellular signaling pathways that regulate proliferation, cell survival, cytoskeletal rearrangement, and cell migration. PDGFR α is specifically expressed in immature OPCs, which are both proliferative and capable of migration, but also in preoligodendrocytes, which are mitotically active. PDGFR α expression is rapidly extinguished as OPCs undergo terminal differentiation (Mokry et al., 2008).

1.2.4 Neurosphere assay

The neurosphere assay (NSA) is an *in vitro* culture system of free-floating clusters of neural stem cells (NSCs) (embryonic, fetal, or adult). After 2-3 days in serum-free medium supplemented with epidermal growth factor (EGF) and/or fibroblast growth factor 2 (FGF2) in the absence of an adhesion substrate, NSCs form into characteristic 3D clusters, called neurospheres.

The NSA was developed in 1992 by the laboratory of Reynolds and Weiss (B. Reynolds & Weiss, 1992) and was the first *in vitro* system to demonstrate the presence of cells in the adult brain with characteristics of true neural stem cells. NSA still remains an extremely useful tool to analyze proliferation, self-renewal capacity and multipotency of neural stem and progenitor cells (NSPCs) and consequently to study the biology of embryonic or adult CNS stem cells (Jensen & Parmar, 2006). The NSA is based on the concept that cells able to form neurospheres are likely to be NSCs, where a putative NSC, in culture, must demonstrate the ability to proliferate (self-renew) over an extended period of time, and generate a large number of progeny that can differentiate into the three major CNS lineages; astrocytes, oligodendrocytes and neurons (B. A. Reynolds & Rietze, 2005). Neurospheres, due to their 3D structure create a niche that is more physiologically relevant than 2D culture systems and allow the modeling of a dynamic changing environment such as varying growth factor or nutrient concentrations. Neurosphere culture thus allows the formation of rich extracellular matrix (ECM) cellular microenvironment, where cells are enriched for β 1 integrins, epidermal growth factor receptor and cadherins, since cells in neurospheres produce their own ECM molecules (laminins, fibronectin, chondroitin sulphate proteoglycans) and growth factors (Ahmed, 2009).

Several studies have focused on the limitations and peculiarities of the NSA. B. A. Reynolds & Rietze, 2005 demonstrated that after neurosphere dissociation only around 10% of re-plated cells survive, due to the culture conditions, which do not support the differentiation and long-term existence of the majority of the cells, but mainly support the survival and expansion of cells that are responsive to the cytokines EGF and/or bFGF. They

also pointed out that, in order to be assured that a stem cell population is finally isolated, cells should be cultured and demonstrate self-renewal over an extended period of time, such as more than five passages, which also should coincide with the generation of a large number of progeny (B. A. Reynolds & Rietze, 2005).

Studies have clarified that every neurosphere does not derive from a NSC and that the number of neurospheres does not provide an accurate readout of NSC frequency. Based on secondary sphere formation, after single-sphere dissociation and bulk passage, plating cells at clonal density, NSC fraction was estimated to be 2.4% (theoretical stem cell frequency). On the other hand, when individual clonally-derived neurospheres into a single-cell suspension were plated into a single well (one sphere per well), then each sphere generated about 50 secondary spheres, which could be translated to a 50-fold increase in the number of stem cells at each passage. But comparing then the growth curves with that one of actually serially passaging cells over 10 passages, they found out that bulk cultures had much lower growth rates than would be predicted from the presence of 2.4% NSCs. This suggests that assuming an one-to-one relationship between neurospheres and NSCs overestimates NSC fraction. An improved estimation of NSC fraction was that only 0.16% of neurosphere-derived cells could be long-term proliferating cells, and thus correspond to NSCs. In other words, this study shows that the majority of spheres are in fact derived from non-stem cells (B. A. Reynolds & Rietze, 2005).

Another limitation of the NSA is its sensitivity in culture methods and conditions, such as variations in cell density, which can alter the cellular microenvironment and in turn affect both the proliferation capacity and the positional cues sensed by cells, or differences in factors concentration in the media. Also, the method and frequency of passaging, as well as the number of passages after isolation, not only lead to differences in the composition of cell types, but also in the properties of the cells within each neurosphere. Every single cell in a neurosphere has its own intrinsic properties, making the neurosphere a highly heterogeneous cell population. Only a small percentage of neurosphere cells holds neurosphere-forming capacity and even fewer fulfill the criteria of being NSCs. Each neurosphere contains cells at various stages of differentiation (Figure 8), including stem cells as well as proliferating neural progenitor cells and postmitotic neurons and glia. Therefore, it should be clearly mentioned that neurospheres should be considered as a mixed population of NSCs, NPs, and more differentiated cells and not of neural stem cells exclusively (Jensen & Parmar, 2006).

Several studies suggest that the *in vitro* proliferative capacity and differentiation potential of neurosphere-expanded NSPCs vary in a manner that is reflective of the developmental stage of the donor. Many developmental control genes maintain their regionally specific expression in neurosphere cultures after several passages. Furthermore, neurosphere-

derived cells maintain the potential to differentiate into the specific neuronal subtypes of their region of origin. At the same time, neurosphere-expanded cells show also susceptibility to environmental cues, which has been proved to affect their differentiation mode and thus to differ from the original cell source (Jensen & Parmar, 2006).

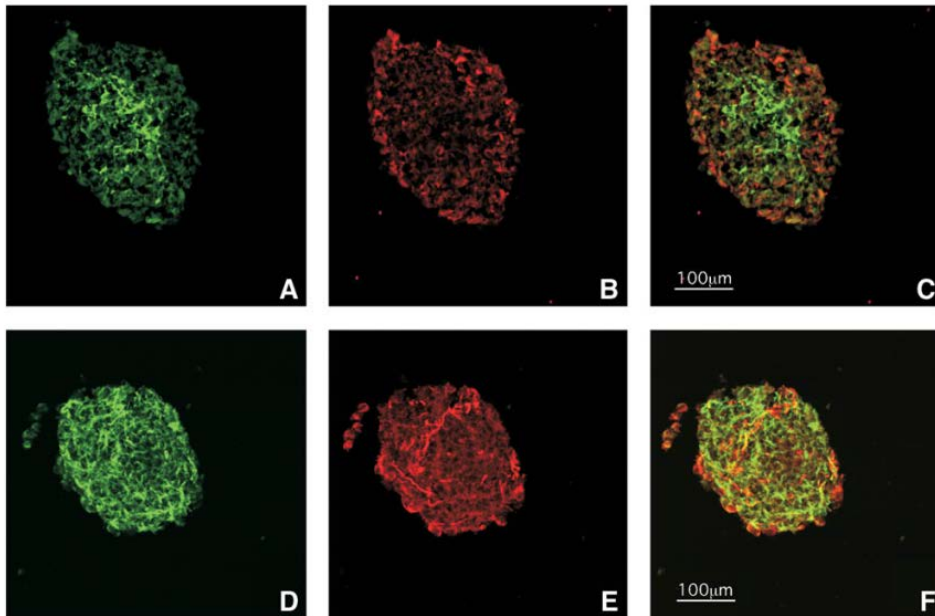


Figure 8 - Each neurosphere contains cells at various stages of differentiation. RC2 (B) and Nestin (D) that stain for progenitor cells show that NPCs are generally located toward the outside of the sphere. GFAP (A) positive cells are located in the center of the spheres, while few βIII-tubulin-positive neurons (E) can also be found evenly distributed within some spheres. (Jensen & Parmar, 2006)

1.3 NSPC-based Grafts in SCI

NSPCs are multipotent cells that can differentiate into all three types of neural lineage: neurons, oligodendrocytes and astrocytes. Various factors and environmental cues affect the differentiation capacity of NSPCs and finally the proportion of each potential phenotype and progeny population. These factors include the source of NSPCs (brain or spinal cord), the age of donor cells (adult, embryonic or fetal tissue), *in vitro* culture conditions and also the host transplant environment (normal versus injured spinal cord; interval time; and white matter versus gray matter) (Mothe & Tator, 2013).

Animal studies using NSPCs grafts have demonstrated that NSPCs rarely differentiate into neurons; rather NSPCs primarily differentiate into astrocytes at the injury site, which greatly

impairs their therapeutic efficacy for SCI repair (Zhao et al., 2017). Transplanted NSPCs into a compression lesion usually differentiate into oligodendrocytes, followed by astrocytes and neurons. In a hemisection or transected spinal cord model, grafted NSPCs mostly differentiated into astrocytes, few into oligodendroglial cells and rarely into neurons (Beyer et al., 2019). Astrocytic differentiation of grafted NSPCs has been associated with allodynia development in SCI animals (Hofstetter et al., 2005). On the other hand, promotion of oligodendrocyte differentiation, leading to remyelination, improved functional recovery (Sabelström et al., 2014).

As the environment in adult spinal cord restricted NSPC differentiation along a glial lineage, *in vitro* induction prior to transplantation and/or modification of the host environment have been suggested in order to increase the fraction of NSPCs that differentiate into neurons or oligodendrocytes (Q.-L. Cao et al., 2002; Q. L. Cao et al., 2001).

Several strategies have been used to promote NSPCs differentiation towards a specific lineage, such as pre-differentiation of NSPCs *in vitro* prior to transplantation, concomitant infusion of growth factors with NSPC transplants and transduction of NSPCs with lineage-specific determinants (Mothe & Tator, 2013). In these studies, biomaterials played crucial roles in cell protection, survival and differentiation, combining the advantages of the 3D culture and providing in parallel the substrate for further culture modifications.

In vitro studies, focusing on *in vitro* pre-differentiation of NSPCs, demonstrate that the intrinsic state of the engrafted NSPCs is important in determining their differentiating phenotype. Thus, the ability of donor NSPCs to respond to extracellular signals may depend critically on their level of maturation and state of differentiation, suggesting the possibility that manipulation of more restricted progenitors could result in increased efficiency of complex circuit reconstruction in the damaged CNS. NRPs and GRPs, whether grafted individually or together, have displayed great survival, migration and differentiation following transplantation into both the intact (A. C. Lepore & Fischer, 2005; Yang et al., 2000; Han et al., 2002; Angelo C. Lepore et al., 2004) and injured (Han et al., 2004; Lepore et al., 2004) CNS, while the differentiation of NRPs alone is inhibited in the injured spinal cord (Cao et al., 2002b). However, these studies focused on E13.5 rat spinal cord NSPCs, where NRPs and GRPs were specifically selected through immunopanning for ENCAM+ and A2B5+ cells, respectively. Also, *in vitro* differentiation of these cells toward neuronal fate was induced by removing FGF-2 and adding retinoic acid.

According to other strategies, acutely dissociated spinal cord NPCs (NRPs, GRPs) were immediately grafted, without further culture, so as not to lose the ability of grafted neurons to extend axons after grafting *in vivo*. Also, for severe injury models, NPCs were placed in the lesion site in a fibrin matrix with protein cocktail of growth factors, in order to support cell survival and vascular ingrowth (Lu et al., 2014).

Specific soluble factors have also been used for the directed differentiation of NSPCs. For example, platelet-derived growth factor (PDGF) has been shown to promote oligodendrocyte fate-specification, while bone morphogenetic protein-2 (BMP2) promotes astrocyte differentiation. Several factors have been reported for promoting neurogenesis from adult rat subventricular zone (SVZ)-derived NSPCs and specifically the dibutyl cyclic-AMP (dbcAMP), a membrane-permeable analogue of cyclic-AMP, and the cytokine interferon-gamma, which both enhanced neuronal differentiation after one-week exposure in culture (Kim et al., 2011).

Taking also into consideration the pathophysiology of SCI and the inhibitory environment of the lesion site, many studies have focused on myelin associated inhibitors. Xiaoran Li et al., 2013 developed a functionalized collagen scaffold functionalized with cetuximab an epidermal growth factor receptor (EGFR) neutralizing antibody, in order to inhibit the downstream signaling activated by myelin associated inhibitors and prevent NPC differentiation into glial lineage. Other modified collagen scaffolds combined the neuroprotective effect of neurotrophic factors (BDNF, NT3, FGF), in order to direct NSCs differentiation towards a desired lineage (neurons or oligodendrocytes) and induce axon extension into the lesion site, with two neutralizing proteins (EphA4LBD and PlexinB1LBD), in order to antagonize the myelin derived inhibitory molecules (Xing Li et al., 2016).

1.4 Thesis Objectives and Outline

NSPC-seeded scaffolds engrafted after SCI seem to have tremendous effects at the lesion site and can improve functional recovery. This study builds upon previous work of the IMBB Neural Tissue Engineering Lab on SCI grafts based on NSPCs-seeded porous collagen-based scaffolds (PCS). According to a recent study by Kouriantaki et al., NSPC-seeded PCS engrafted in a dorsal column crush SCI mouse model lead to significant improvement in locomotion recovery as assayed by the horizontal ladder walking assay. Specifically, the locomotion performance of injured animals treated with such grafts was not statistically different than uninjured animals, 12 weeks post injury.

The objective of this thesis is to further characterize these NSPCs-seeded grafts. Furthermore, to evaluate the ability to modulate NSPCs fate once seeded in PCSs. Accordingly, three main experiments were designed:

1. Characterization of NSPCs subpopulation. Primary E13.5 NSCs in 2D and 3D (NSCs-seeded PCS) cultures were studied and stained for markers that are expressed at specific cell developmental stages and can discriminate the different NSPCs subpopulations. In particular, Sox2 and Nestin were used as NSPCs markers, GLAST was used as RGCs marker, while for later developmental stages, Tuj1 -neuronal marker-, GFAP - astrocytes, but also RGCs marker- and PDGFRa - OPCs and preoligodendrocytes marker- were used.
2. Characterization of NSPCs-seeded PCSs. Grafts were cultured according to the protocol described in the recent Kouriantaki et al. study, fixed and stained at the day of implantation. Following the staining pattern revealed from the first experiment the identification of grafts cell population was able.
3. Neural fate manipulation of NSPCs in PCSs. Grafts were further cultured in differentiation medium and stained for specific markers as in the first experiment. Neuronal differentiation was induced using retinoic acid (RA).

2 Methods

2.1 Primary Neural Stem Cell Isolation

Primary NSCs were isolated from C57BL/6 embryos at gestational day 13.5 (E13.5 NSCs) as described previously (Kourgiantaki et al. 2020). Cortical hemispheres were dissected and mechanically dissociated into NSC growth medium.

2.2 Cell Culture

E13.5 primary NSCs were cultured following the NSA. 25×10^4 NSCs were cultured in T25 flasks (Nunc™ EasYFlask™ Cell Culture Flasks, 156367, Thermo-Fisher) into 5ml of NSC growth medium (DMEM-F12 - Dulbecco's Modified Eagle's Medium/Nutrient Mixture F-12 Ham, D6421, Sigma-Aldrich -, B27-VitaminA (1X) – B-27™ Supplement, minus vitamin A (Thermo 12587010), 0.6% D-glucose - D-(+)-Glucose solution, G8769, Sigma-Aldrich -, 100µg/ml primocin, Invivogen ant-pm-1) supplemented with 20ng/ml EGF (&D 236-EG-200) and 20ng/ml FGF-2 (R&D, 233-FB-025) growth factors (NSC full medium).

Cells were subcultured when neurosphere diameter reached approximately 100 µm while neurosphere center remained bright (4-5 days of culture). Neurospheres were dissociated into a single-cell suspension after a 6min incubation (37°C) with accutase (A6964, Sigma-Aldrich). Cells were ready for experiments at forth passage after isolation.

2.2.1 2D Culture

In 2D cultures, E13.5 NSCs were cultured on 48-well plates (Thermo Scientific 150687) coated with PDL (Poly-D-lysine hydrobromide, P6407-5MG, Sigma-Aldrich) and laminin (Laminin from Engelbreth-Holm-Swarm murine sarcoma basement membrane, L2020, Sigma-Aldrich). After an overnight incubation (37°C) of PDL coating and a two -hour incubation (37°C) of laminin (15 µg/ml) coating, neurospheres were subcultured and the single-cell NSPC suspension (after the accutase incubation) was seeded on the plate. 2.5×10^4 NSPC per well were seeded into 350 µl of NSC full medium.

2.2.2 3D Culture

In 3D cultures, E13.5 NSCs were seeded in porous collagen scaffolds (PCSs) as single-cell suspension. A drop of 3×10^4 cells in 2 μ l NSC full medium was placed at the bottom of a 48-well plate. Then, the scaffold was placed above the drop in order to adsorb the cell suspension due to capillary action. After 15min of incubation at 37°C, 350 μ l NSC full medium were added per well.

2.2.3 Neural Differentiation

Neural differentiation was induced using Retinoic Acid (RA) (10mM stock). Two different concentrations were tested: 0.1 μ M and 1 μ M.

After cell seeding in NSC full medium, cells were cultured in order to proliferate and grow for three days *in vitro* (3DIV). At 3DIV, the medium was switched into differentiation medium (NSC growth medium without growth factors) supplemented with RA (diluted into DMEM-F12). Cells were cultured in differentiation medium for five more days (until 8DIV).

Except from the condition of NSCs cultured into NSC full medium, another 'control' condition was tested. NSCs differentiation capacity was also studied in culture medium without growth factors – spontaneous differentiation.

2.3 Image Acquisition

2.3.1 2D culture

All experiments were conducted on 48-well plates. Imaging was done using a Zeiss epifluorescence microscope (Gravanis Lab, Medical School, University of Crete), using a 32x Plan-Apochromat lens. In every experiment a common exposure time (optimally selected) was used for each channel. The best image quality was achieved by focusing using the Hoechst staining, since it was the brightest and the most homogenous staining among all the cells.

2.3.2 3D culture

Cell-seeded scaffolds were placed on a glass-bottom plastic plate with in a drop of PBS. Images were acquired using a Leica TCS SP8 inverted confocal microscope using a 40x water-immersion objective lens. After confirming that the scaffold is at the right side, by visualizing Hoechst33342-stained cell nuclei using the microscope eyepiece, z-stacks were acquired in three positions per scaffold (almost the whole scaffold was covered by these three positions). Each position was selected based on Hoechst staining, preferring scaffold

sites that contain many cells. Big cell clusters were avoided, since in such clusters cells were poorly stained. The “Mark and Find” tool of LASx microscope software was used to optimize the stack at each position in order to image as many cells as possible. Usually, each z-stack was 80µm thick and was sampled at 1.5µm z-step.

2.4 Image Processing

2.4.1 Processing images from 2D cell culture

All acquired images were processed using the ImageJ software. Every image (.tif file), one for each channel, was opened by ImageJ and then presented as one stack (“Images to Stack” command) (Figure 9.1). The color of each channel was defined using the “Channels Tool” and the Color Display tool (Figure 9.2). A specific color-rule was utilized for each staining, same in all experiments. Hoechst33342 nucleic acid stain was visualized in the blue channel. Sox2, GLAST, Tuj1 and PDGFRA staining was visualized in the green channel. Nestin, GFAP, Tbr2 staining was visualized in the red channel. Then, all channels are presented in one image using the “Composite Display mode”.

The brightness and contrast of images were adjusted interactively using the “Color Balance” tool, so as the staining to be clear, in order to remove (if possible) most of the background noise and increasing the signal-to-noise ratio of the specific signal (Figure 9.3). The choice of “min” and “max” values (which define the contrast and brightness) depended every time on staining quality. In order to estimate accurately the specific signal, many imaging tests were conducted so as the staining pattern of each antibody to be identified. Brightness and contrast values were selected for every image individually, so as to achieve, the best image quality with a discrete pattern for each staining. Imaging-related difficulties (poor focus, overlap of 488 and 546 channels) or imperfect antibody staining did not allow to use common settings for images acquired different days. Instead, optimal imaging parameters were identified for each imaging session.

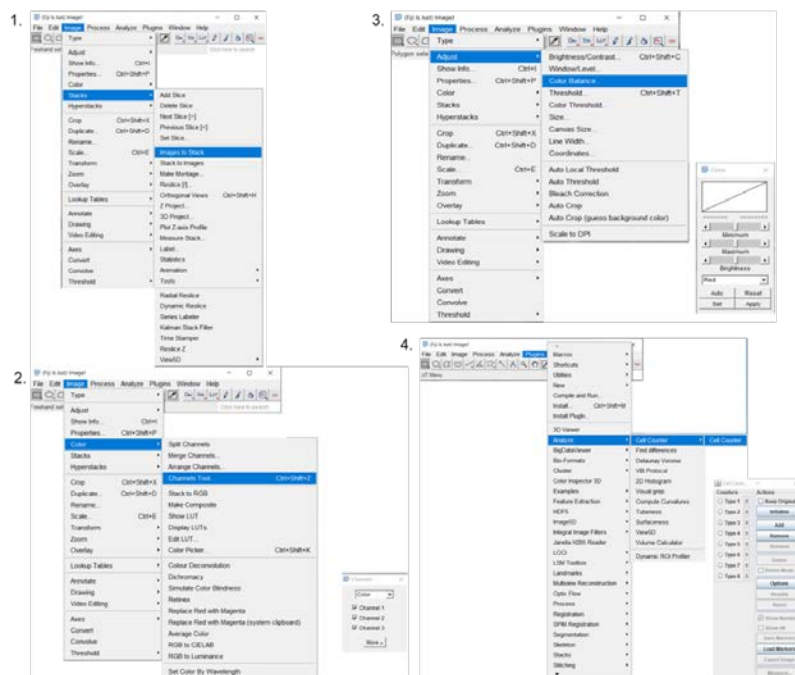


Figure 9 - Image processing using the ImageJ software. 1. "Images to Stack" command used for presentation of .tif files as one stack. 2. "Channels Tool" used for channels color definition in Color Display mode. 3. "Color Balance" tool used for brightness and contrast adjustment. 4. "Cell Counter" Plugin used for cell counting.

2.4.2 Processing images from 3D cell culture

Processing 3D images from 3D samples utilized the same pipeline as the one from 2D cultures. Having confirmed the specificity and staining pattern of each marker used in 2D experiments, the same markers were used to study cells grown inside scaffolds. However, inside scaffolds cells create clusters, attach to each other, therefore distinguishing the cytoplasm morphology of individual cells is challenging. The staining pattern of cytoplasmic markers was mostly localized around the nucleus, creating a ring around it, where the signal is brighter (Figure 21). However, long axons or processes are still detectable, when cells are more mature. The nuclear staining of Sox2 was processed in the same way as in 2D experiments due to the faint non-specific cytoplasmic signal.

2.5 Antibody Staining and Image Processing Optimization

For cell culture characterization the technique of immunocytochemistry (ICC) was used. Cells were fixed with paraformaldehyde (4% PFA) at every desirable stage of culture and then stained using primary antibodies for markers that are expressed in specific cell developmental stages.

2.5.1 Sox2

In this study, Sox2 was used as a marker of NSPCs using an anti-Sox2 antibody (1:100, ab15830, Abcam). The secondary antibody was the anti-rabbit Alexa 647 (1:1000, A21244, Invitrogen).

Sox2 staining is nuclear (Figure 10). However, images revealed also some faint cytoplasmic non-specific signal (Figure 11.1) that was removed by increasing the minimum value, till only the nucleus is well shaped (having also open the channel for nucleus staining) (Figure 11.2). Specific nuclear Sox2 signal was weak, but after increasing the contrast, specific signal was brighter and could be utilized for quantification of Sox2+ nuclei (Figure 11.3). Only for Sox2 staining, brightness and contrast values were kept the same for every image of the same experiment, since its signal is nuclear and not cytoplasmic and does not give any information about the cell morphology, which would help in discriminating more mature cells (non-specific signal). Then Sox2+ cells were counted based on nuclear signal in the green channel.

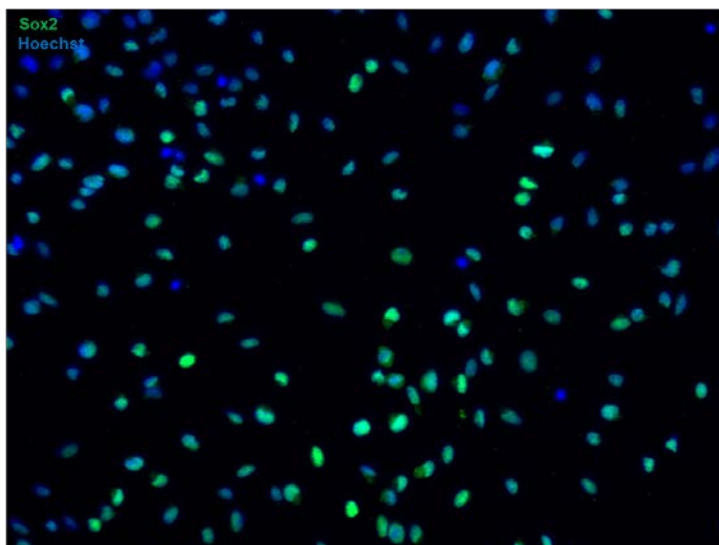


Figure 10 - Sox2 staining. Nuclear staining of NSPCs

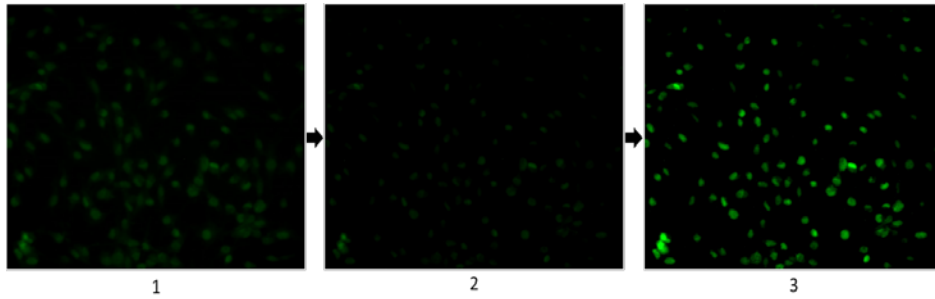


Figure 11 – Sox2 visualization optimization. Faint Sox2 staining with non-specific cytoplasmic signal (1). Brightness and contrast values were adjusted in order to remove the non-specific cytoplasmic signal (increasing the minimum value) (2) and keep the specific nuclear signal which can be used for counting Sox2+ nuclei (3).

2.5.2 Nestin

In this study, Nestin was used as a marker of NSPCs using an anti-Nestin antibody (1:1000, Novus NB100-1604). The secondary antibody was the anti-chicken Alexa 546 (1:1000, A11040, Life Technologies).

Nestin staining was specific and bright. Visualization of Nestin images usually did not require image correction other than removing background noise. Nestin staining is cytoplasmic (Figure 12).

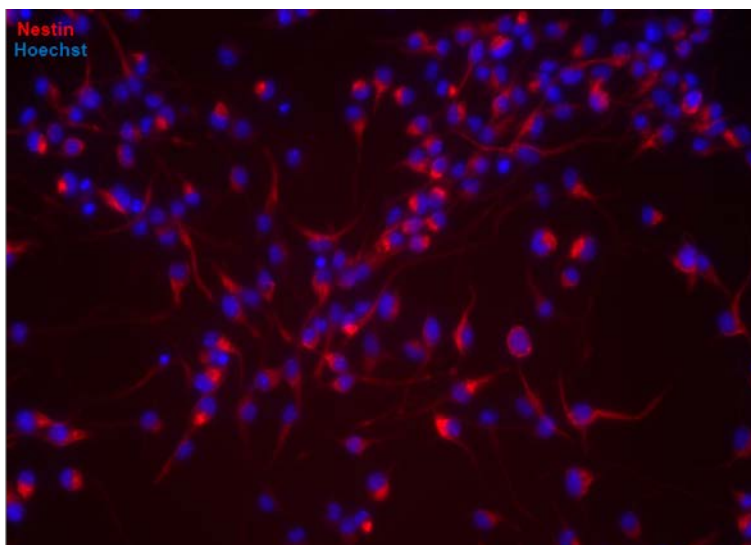


Figure 12 – Nestin staining. Cytoplasmic staining of NSPCs branches.

2.5.3 GLAST

GLAST was used as a marker of radial glial cells (RGCs), but is also expressed in astrocytes. GLAST was visualized using an anti-GLAST antibody (1:200, Abcam ab416). The secondary antibody was the anti-rabbit Alexa 647 (1:1000, A21244, Invitrogen).

GLAST staining is cytoplasmic (Figure13).

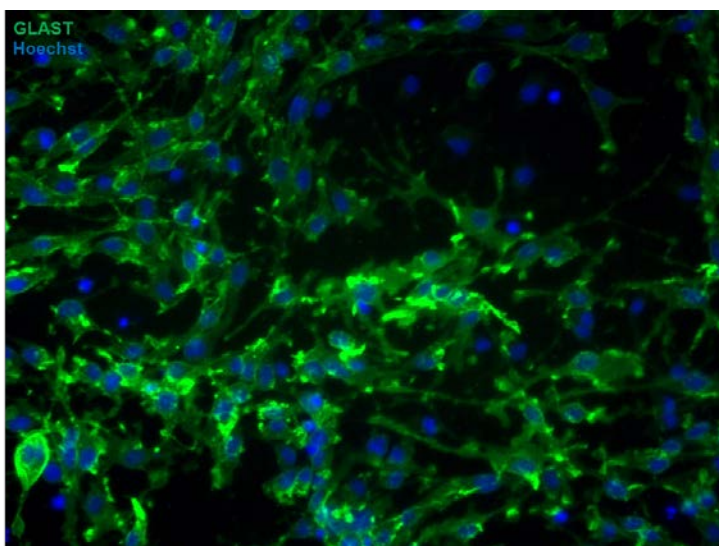


Figure 13 – GLAST staining. Cytoplasmic staining of RGCs processes.

2.5.4 GFAP

GFAP was used as the marker of astrocytes, but also RGCs, using an anti-GFAP antibody (1:1000, Millipore ab5541). The secondary antibody was the anti-chicken Alexa 546 (1:1000, A11040, Life Technologies).

GFAP staining is cytoplasmic (Figure 14).

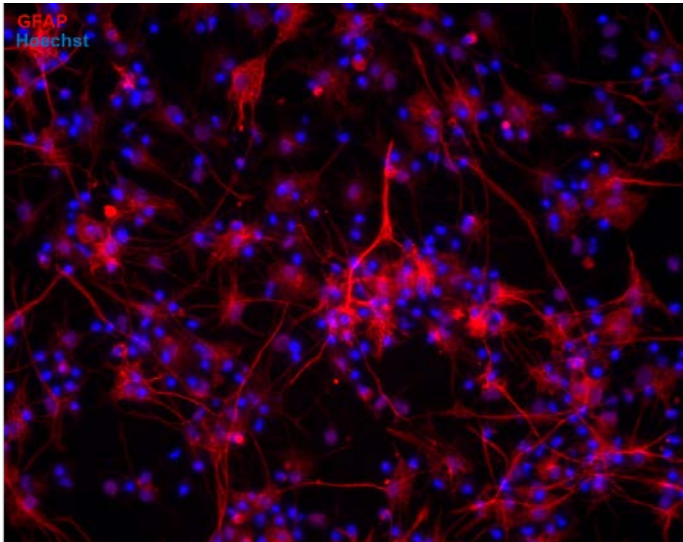


Figure 14 – GFAP staining. Cytoplasmic staining of GFAP.

2.5.5 Tubulin β 3

Tubulin beta 3 (TUBB3) was used as a marker of neurons, but also of mitotic neuronal precursors, using an anti-tubb3 antibody (1:500, Biolegend 801201, tuj1 clone). The secondary antibody was the anti-mouse Alexa 488 (1:1000, sc-2064, santa cruz).

Tuj1 staining is cytoplasmic (Figure 15). Tuj1 staining of immature neurons usually was faint, therefore imaging required long exposure time. On the other hand, mature neurons with wider cytoplasm (and higher Tuj1 expression levels) were brighter. Through image processing the background noise was removed (increasing the minimum) and increasing the contrast (lowering the maximum) of the specific signal, neurons were discrete and could be easily quantified. Tuj1 staining of immature neurons usually was faint, therefore imaging required long exposure time. On the other hand, mature neurons with wider cytoplasm (and higher Tuj1 expression levels) were brighter. Through image processing the background noise

was removed (increasing the minimum) and increasing the contrast (lowering the maximum) of the specific signal, neurons were discrete and could be easily quantified.

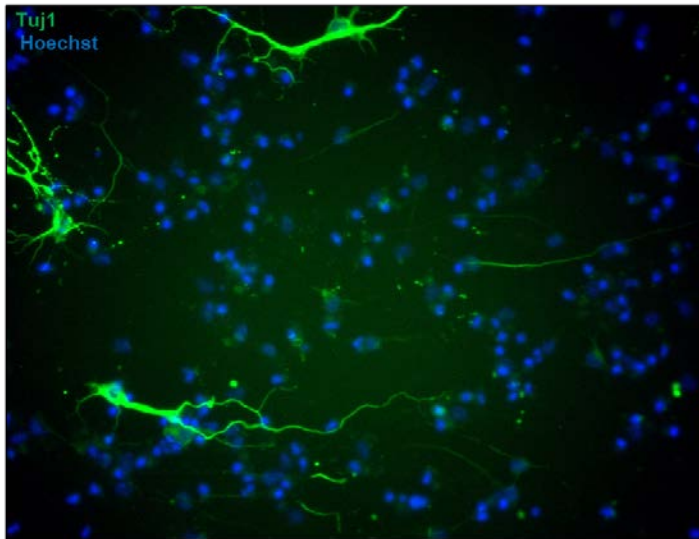


Figure 15 – Tuj1 staining. Cytoplasmic staining of neurons.

When acquiring images of IHC/ICC samples double immunostained for Tuj1 (488 sec antibody) and GFAP (546 sec antibody) another challenge was the partial overlap of 488 and 546 channels. When the 546 GFAP signal was significantly brighter than the 488 Tuj1 signal, some 546 emission leaked in the 488 channel. This leaked GFAP (red) signal complicated the identification of cells that stain weakly (yet specifically) for Tuj1 (Figure 16).

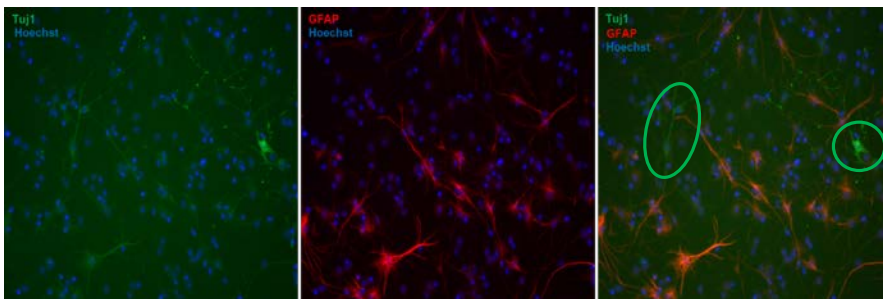


Figure 16 – Tuj1-GFAP double staining. Partial overlap of 488 and 546 channels. Some 546-emission (GFAP) leaked at the 488 channel (Tuj1), when GFAP signal was significantly brighter than the Tuj1 signal. Quantification of Tuj1 positive cells in the composite image (third image in line, green circles).

2.5.6 Tbr2

Tbr2 was evaluated as a marker for IPCs using an anti-Tbr2 antibody (1:100/1:200/1:500, Abcam, ab23345). The secondary antibody was the anti-rabbit Alexa 546 (1:1000, A10040, Invitrogen).

Tbr2 specific staining is nuclear. However, in the protocol followed, the signal was not specific and Tbr2 images did not differ from negative control used (no primary antibody was used; Figure 17). In only one test experiment, on PDL-laminin coated coverslip in 1 μ M RA and after image processing, some Tbr2 positive cells, with nuclear signal could be detected (Figure 18).

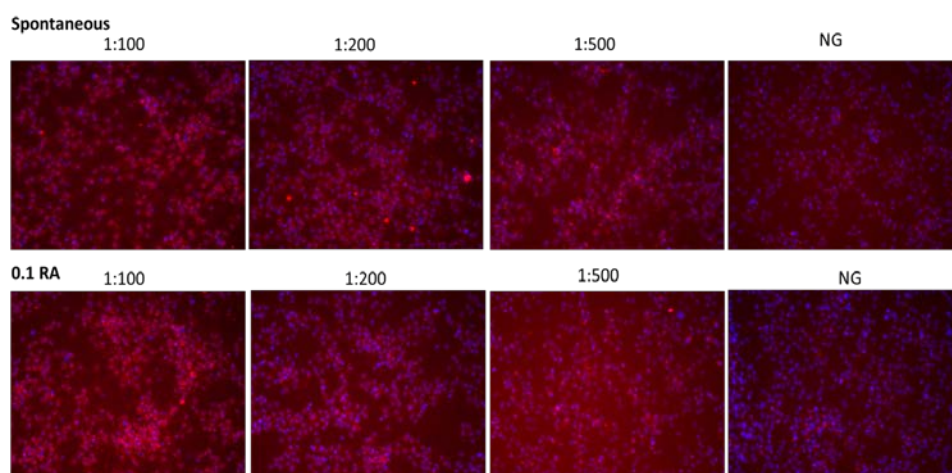


Figure 17 – Tbr2 staining protocol optimization. Different dilutions were tested in the two different differentiation conditions. There is no difference among all conditions. NG: no 1yAb.

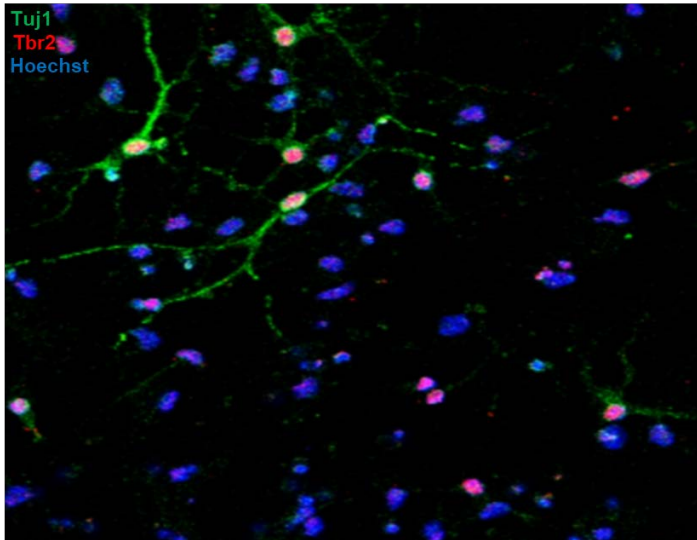


Figure 18 – Tbr2 staining. Double staining with Tuj1. Nuclear staining of IPCs in colocalization with Tuj1. 1 μ M RA after 5DIV. Confocal imaging.

2.5.7 PDGFRa

PDGFRa was used as a marker of OPCs, but also of more mature preoligodendrocytes, using an anti-PDGFRa antibody (1:200, R&D AF1062). The secondary antibody was the anti-goat Alexa 488 (1:1000).

PDGFRa staining is cytoplasmic (Figure 19).

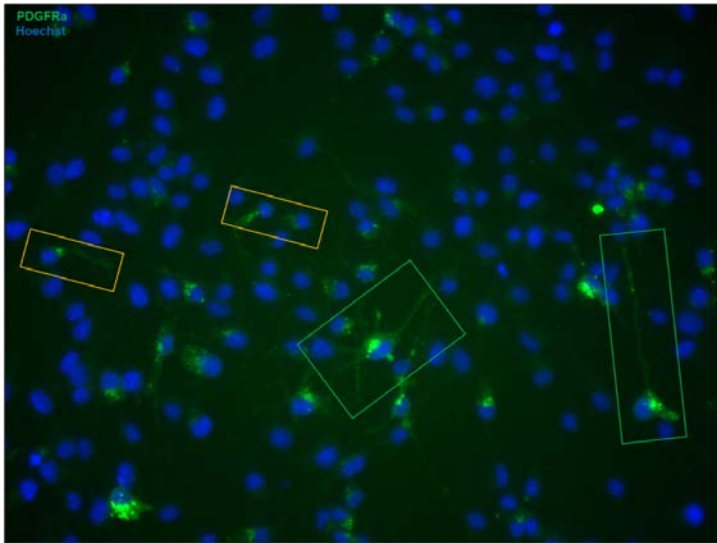


Figure 19 – PDGFR α staining. Cytoplasmic staining of OPCs. Immature OPCs have short processes (yellow frame). Preoligodendrocytes have brighter cytoplasm and longer, branched processes (green frame).

A technical problem with the anti-PDGFR α antibody was again the presence of significant non-specific signal when co-stained with another antibody (here, co-staining of Tuj1 and MBP was tested). In double staining with Tuj1, PDGFR α signal colocalized with Tuj1 signal suggesting antibody cross-talk (Figure 20). Consequently, anti-PDGFR α antibody was used only in single staining.

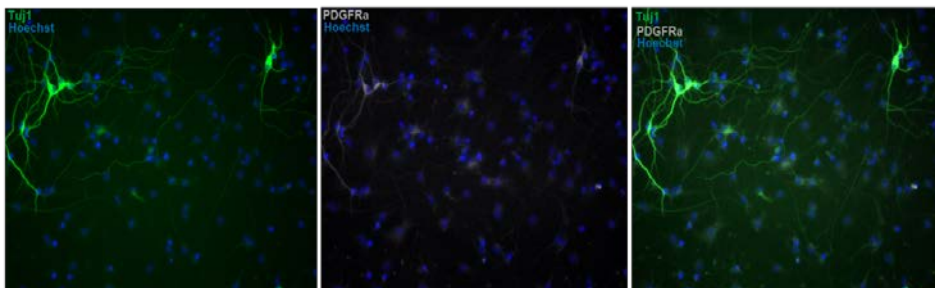


Figure 20 – PDGFR α -Tuj1 colocalization.

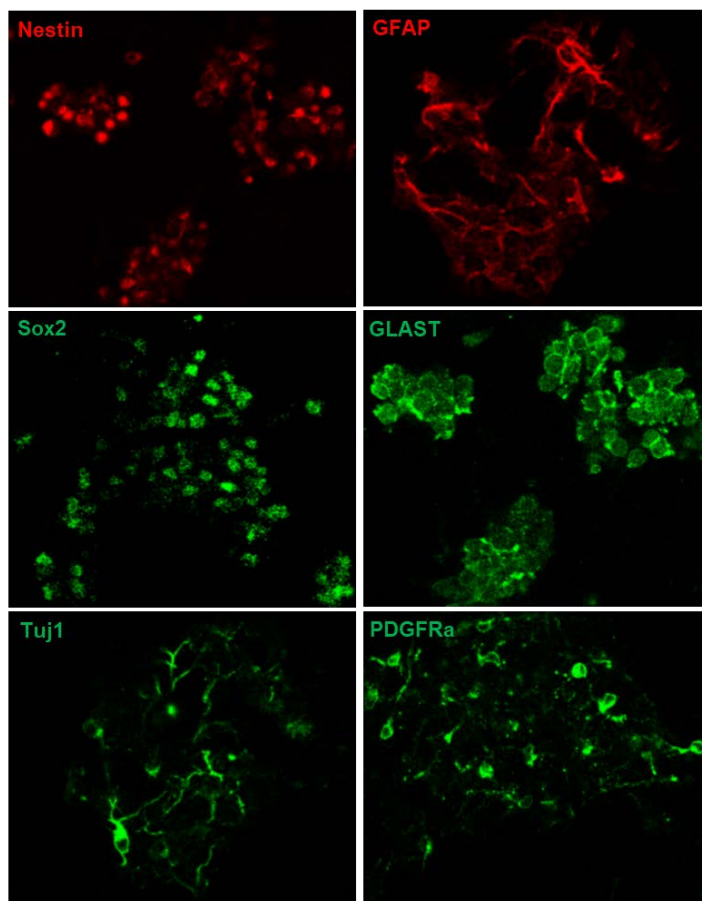


Figure 21 – Markers staining of cells in scaffolds. The staining pattern of cytoplasmic markers mostly localized around the nucleus. Long axons or processes of more mature cells are detectable (Tuj1, GFAP staining). One stack is presented.

2.6 Quantification

2.6.1 Cell Counting

2.6.1.1 2D culture

Cell counting was implemented using the “Cell Counter” Plug-in of ImageJ (Figure 9.4). One type of Counter was selected for every staining-channel. All counters could be presented at the same time in the same image. This way the colocalization of two stainings

could also be measured by counting the number of cells that were labeled by both different count types.

2.6.1.2 3D culture

“Cell Counter” was used for quantification (Figure 9.4). Selecting “Show All”, all counters were visible in all stacks. Firstly, all nuclei were marked in all stacks in order to define the total number of the cells (based on Hoechst33342 staining) and then, in composite display mode with the other channels, antibody staining was marked with a different type of cell counter.

2.6.2 Analysis

All experiments were conducted three times (three biological replicates). In 2D culture experiments, every biological replicate consisted of two technical replicates (two wells per condition). In 3D culture experiments, every biological replicate consisted of only one technical replicate (one scaffold), however images acquired in three different positions per scaffold were as technical replicates.

Results were organized and processed in Excel files. The mean value of each metric of interest (e.g. cell fraction) calculated was based on the technical replicates. Results (one value per biological replicate) were further analyzed in GraphPad Prism 8.0.2, organized in a column table.

In order to check if there is a statistically significant difference at the percentage of cells stained for each marker, an unpaired t-test was performed, comparing the two different conditions of culture (2D and 3D culture) (statistical significance: $P < 0.05$ with 95% confidence level). One table per marker was created with two columns (2D and 3D culture). The results of the test were annotated above the bars in graphs.

For 8DIV experiments on NSPC differentiation, one-way ANOVA test was utilized to compare the means of results from different conditions. No matching and pairing was selected. For multiple comparisons the comparison of the mean of each column (condition medium) with the mean of every other column (biological replicates in rows of each column) was checked. Tukey test was used.

Two-way ANOVA test was used to evaluate statistical significance on measured assays that depended on two factors (e.g. NSPC differentiation as a function of 3D / 2D culture and differentiation medium, NSPC differentiation as a function of 3D / 2D culture and 3DIV / 8DIV). For multiple comparisons Sidak test was used.

3 Results

3.1 Immunocytochemical Characterization of NSPCs and NSPC-Derived Progeny

Primary cortical E13.5 NSCs were cultured following the NSA. Every neurosphere contains a highly heterogeneous cell population, which consists of cells at various stages of differentiation. Therefore, the single-cell suspension derived from the neurosphere culture and used for the 2D and 3D (NSCs-seeded PCS) cultures consists also of various cell types in different developmental stages that also retain their differentiation capacity and follow distinct cell lineage pathways.

In order to identify the different cell types, cells were fixed after specific days in culture in specific growth or differentiation mediums and finally stained for markers expressed at specific developmental stages that can discriminate different NSPCs subpopulations.

Sox2 and Nestin were used as markers of NSPCs, GLAST was used as a marker of RGCs, while staining for later developmental stages utilized Tuj1 (neurons), GFAP (astrocytes, but also RGCs) and PDGFRa (OPCs and preoligodendrocytes). Cell morphology was also studied in 2D cultures since it can be utilized to discriminate different cell types.

3.1.1 NSPCs

NSPCs were optimally studied in NSC cultures in full medium for 3DIV. In this study, Sox2 is used as the earliest marker for NSPCs. Sox2 staining pattern is nuclear. After image processing, Sox2+ cells were counted based on the green channel (Figure 22).

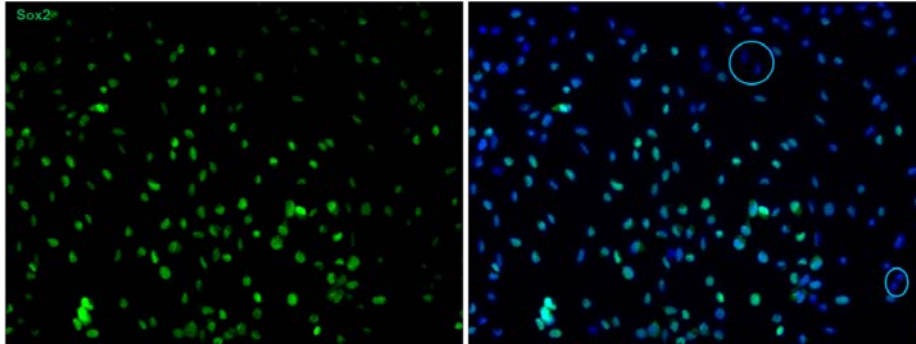


Figure 22 – Sox2 staining. Nuclear staining of NSPCs (green). NSPCs were counted at the green channel (all green cells are Sox2+) and the percentage of positive cells was calculated over the total number of cells (Hoechst). Blue circles contain Sox2- cells.

Another marker used for NSPCs was Nestin. Nestin staining was specific and bright. Visualization of Nestin images usually did not require image processing other than removing background noise. Nestin staining is cytoplasmic and in most of the cases it stains brighter one branch of the bipolar NSPCs (Figure 23).

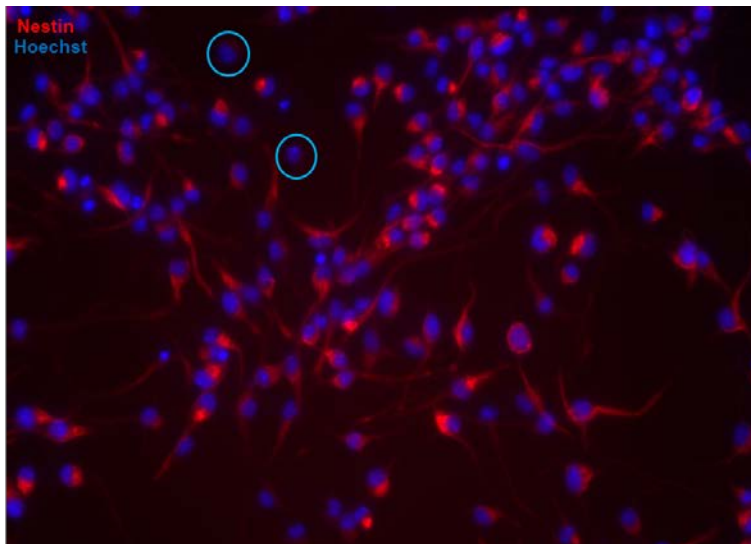


Figure 23 – Nestin staining. Cytoplasmic staining of NSPCs branches. Blue circles contain Nestin- cells.

3.1.2 RGCs

RGCs are characterized by the expression of above mentioned NSPCs markers (Sox2, Nestin), and in addition GLAST, a specific RGCs marker. However, image interpretation should consider that GLAST is also expressed in mature astrocytes. GLAST staining is cytoplasmic and has a characteristic 'spiky' pattern that stains the long processes of RGCs, with bright spots in the cytoplasm (Figure 24).

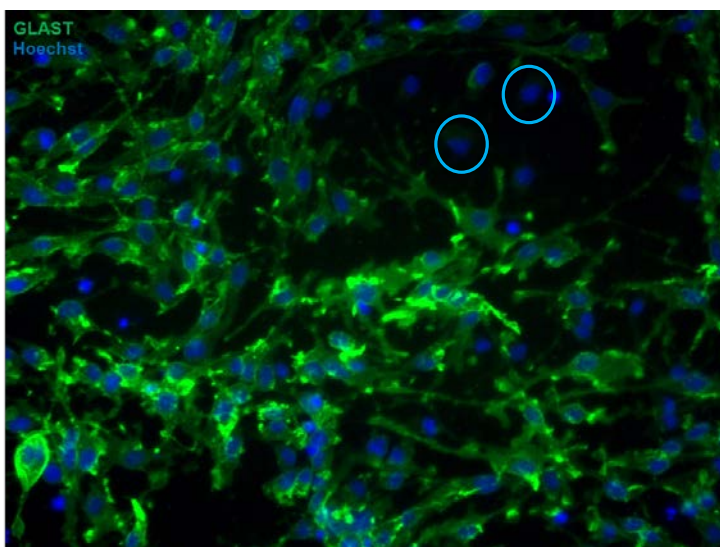


Figure 24 – GLAST staining. Cytoplasmic staining of RGCs processes. Blue circles contain GLAST+ cells.

Furthermore, RGCs are also GFAP+ at later stages (GFAP expression at later developmental stage, after GLAST expression) (see below, 3.1.5 Astrocytes for GFAP staining).

3.1.3 IPCs

IPCs could possibly be studied in cultures with differentiation medium (spontaneous and/or RA differentiation medium). Tbr2 was proposed as the IPCs marker. Thus, the anti-Tbr2 antibody that was used had only non-specific cytoplasmic signal. Although it was tested in three different (recommended) dilutions (1:100, 1:200, 1:500), in both spontaneous and 0.1 μ M RA differentiation medium, the staining was the same in all conditions and the protocol needed to be further optimized (Figure 25). Decreasing Triton-X concentration (from 0.1% to 0.05%) and increasing blocking buffer incubation (from 1h to 2h) were two

modifications of staining protocol that were checked, but no improvement was achieved in the single experiment conducted (Figure 26).

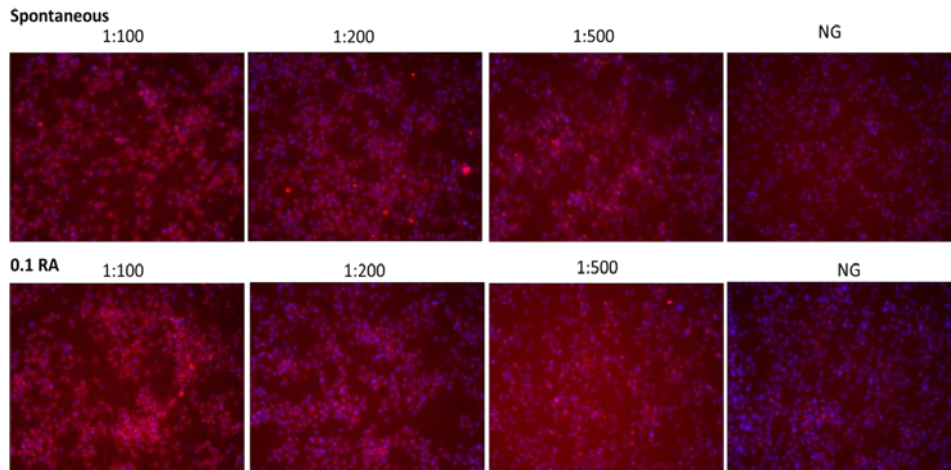


Figure 25 – Tbr2 staining optimization. Different dilutions were tested in the two different differentiation conditions. There was no difference among all conditions. NG: no 1yAb.

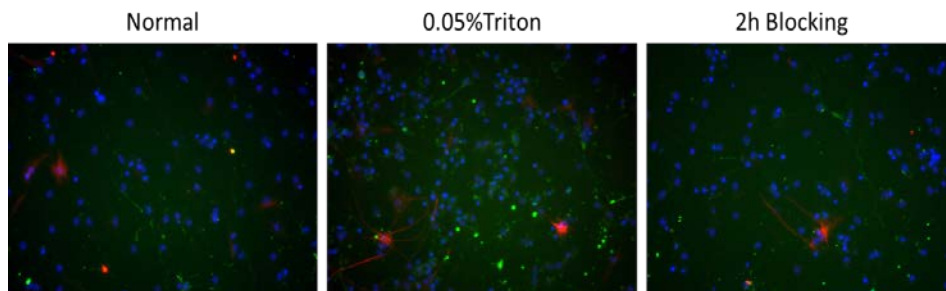


Figure 26 – Staining protocol optimization. Tbr2 at the median dilution, 1:200, was tested in 1 μ M RA, changing the Triton-X concentration or blocking incubation time. There was not any nuclear Tbr2 signal. There were only some cells with cytoplasmic (non-specific for IPCs) signal.

However, in one experiment that was conducted on glass coverslip and could be imaged with confocal microscope, some Tbr2 positive nuclei could be detected. Image processing in order to reduce background noise (cytoplasmic non-specific signal) was necessary, though. Tuj1 colocalization confirms the specificity of the signal in immature neurons (Figure 27).

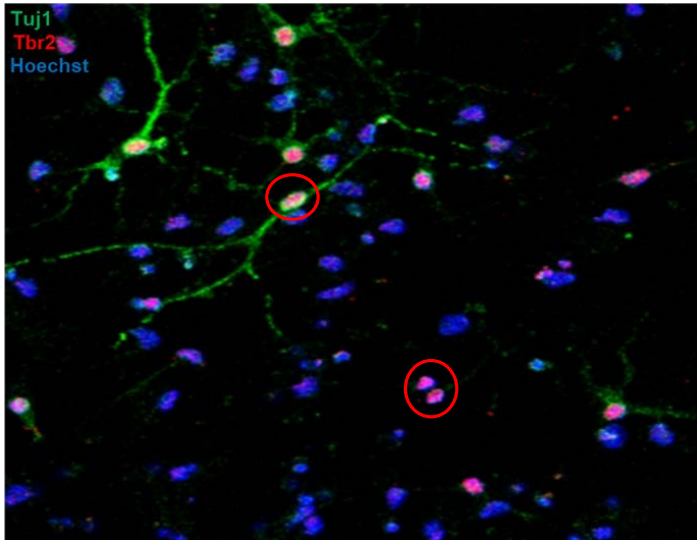


Figure 27 - Tbr2 staining. Double staining with TuJ1. Nuclear staining of IPCs in colocalization with TuJ1. Red circles contain Tbr2+ cells. 1 μ M RA after 5DIV. Confocal imaging

3.1.4 Neurons

Neurons could be better detected in cultures where NSPCs were grown in differentiation medium (spontaneous and/or RA differentiation medium). Tubulin beta 3 (TUBB3) was used as the marker of mature neurons, but also of mitotic neuronal precursors. TuJ1 staining is cytoplasmic. Immature neurons or mitotic neuronal precursors have thinner and shorter axons, while more mature neurons have brighter cytoplasm with elongated and branched axons (Figure 28).

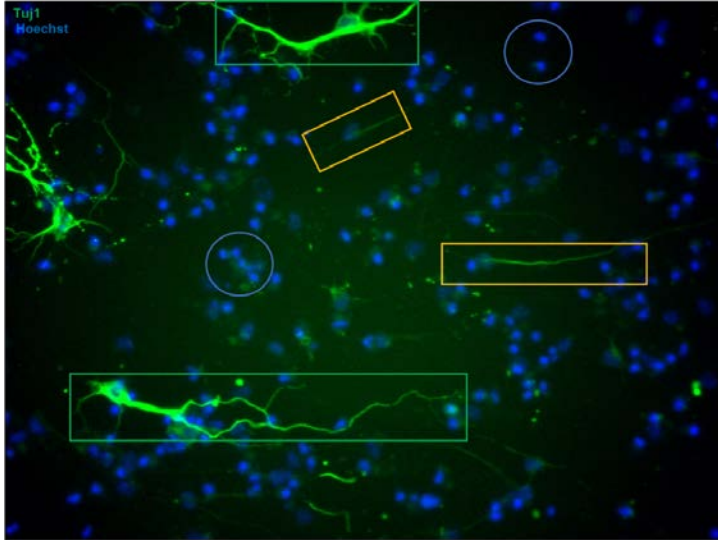


Figure 28– Tuj1 staining. Cytoplasmic staining of neurons. Neural precursors have thinner and shorter axons (yellow frame). Mature neurons have brighter cytoplasm with elongated and branched axons (green frame). Spontaneous differentiation medium for 5DIV. Blue circles contain Tuj1- cells.

3.1.5 Astrocytes

Abundant and mature astrocytes were found in cultures after 5DIV in spontaneous differentiation medium. GFAP was used as the marker of astrocytes, but also RGCs. GFAP staining is cytoplasmic. GFAP stains the two long processes of the bipolar RGCs with a thin linear pattern. On the other hand, GFAP pattern in mature astrocytes is brighter-thicker around the nucleus. Protoplasmic astrocytes stain for short and branched GFAP processes, while fibrous astrocytes have long and thin GFAP processes radiating from the central cell body (Figure 29).

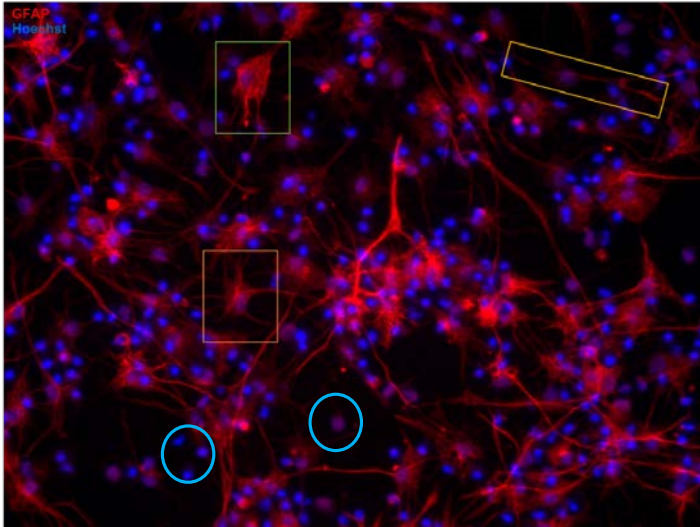


Figure 29 – GFAP staining. Cytoplasmic staining of astrocytes. Bipolar RGCs also stain for GFAP (yellow frame). Astrocytes have brighter-thicker GFAP pattern around the nucleus. Protoplasmic astrocytes stain for short and branched GFAP processes (green frame). Fibrous astrocytes have long GFAP processes radiating from the central cell body (orange frame). Blue circles contain GFAP+ cells. Spontaneous differentiation medium for 5DIV.

3.1.6 OPCs and Preoligodendrocytes

OPCs and preoligodendrocytes were studied in cultures after 5DIV in spontaneous or RA differentiation medium, but they were also observed in NSC full medium after 3DIV. PDGFRA was used as the marker for OPCs, but also of more mature preoligodendrocytes. PDGFRA staining is cytoplasmic. OPCs have short processes. Preoligodendrocytes have brighter cytoplasm and longer, branched processes (Figure 30).

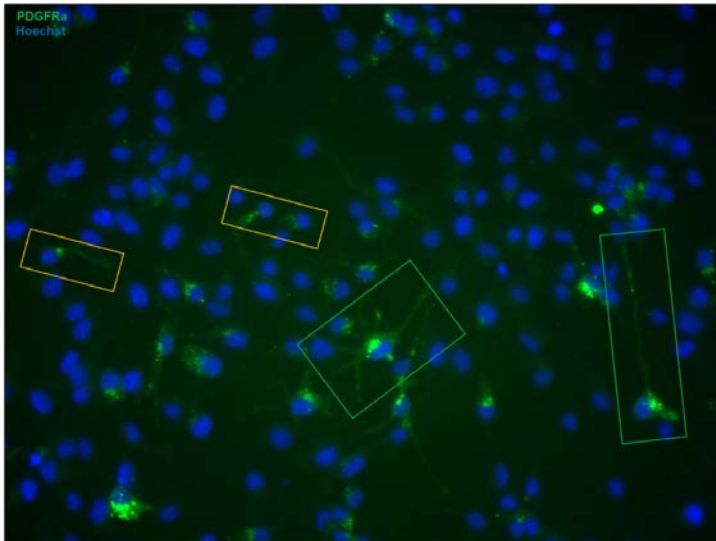


Figure 30 – PDGFR α staining. Cytoplasmic staining of OPCs. Immature OPCs have short processes (yellow frame). Preoligodendrocytes have brighter cytoplasm and longer, branched processes (green frame). NSC full medium for 3DIV.

3.1.7 Nestin-Sox2, Nestin-GLAST double stainings

NECs, the earliest type of NSCs, are characterized by the expression of both Sox2 and Nestin (Nestin⁺Sox2⁺). GLAST is a specific RGC marker, therefore RGCs are characterized by the expression all NSPCs markers (Sox2, Nestin, GLAST) (Figure 31, 32).

Nestin⁻Sox2⁺ cells could correspond to NECs, since Sox2 expression precedes Nestin expression, or even to GRPs, since Sox2 has been found to be co-expressed with GFAP (Bani-Yaghoub et al., 2006). Sox2⁻ cells could be more differentiated progenitors, probably IPCs, which could also be Nestin^{+/-}, with Nestin⁺ to be an earlier intermediate progenitor before the maintenance of Tbr2 expression (Englund et al., 2005). Sox2⁻Nestin⁻ cells could also contain cells that are in a more differentiated state (Tuj1⁺, GFAP⁺).

Nestin⁺GLAST⁻ cells correspond to progenitor cells that could be characterized as NECs or IPCs, since they lack the glial factor GLAST that is maintained only in GRPs. Nestin⁻GLAST⁺ cells probably are present in later developmental stages at the lineage of glial cells, so they could be characterized as GRPs or astrocytes. Moreover, Nestin⁻GLAST⁻ cells could be either more similar to NECs or more mature-differentiated cells.

It should be also noticed that negative (and double negative) cells could also be dead or stressed cells that are contained in the total number of Hoechst positive cells.

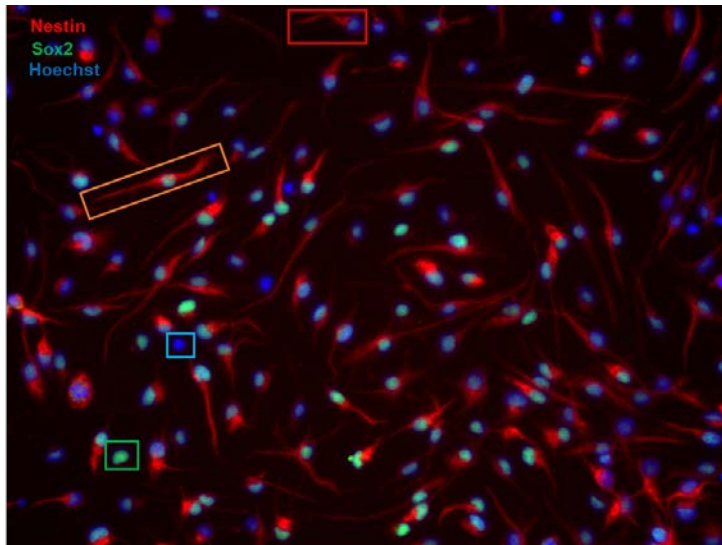


Figure 31 – Representative morphologies of cells in Nestin - Sox2 double staining. Nestin⁺Sox2⁺ (orange frame), Nestin⁺Sox2⁻ (red frame), Nestin⁻Sox2⁺ (green frame), Nestin⁻Sox2⁻ (blue frame).

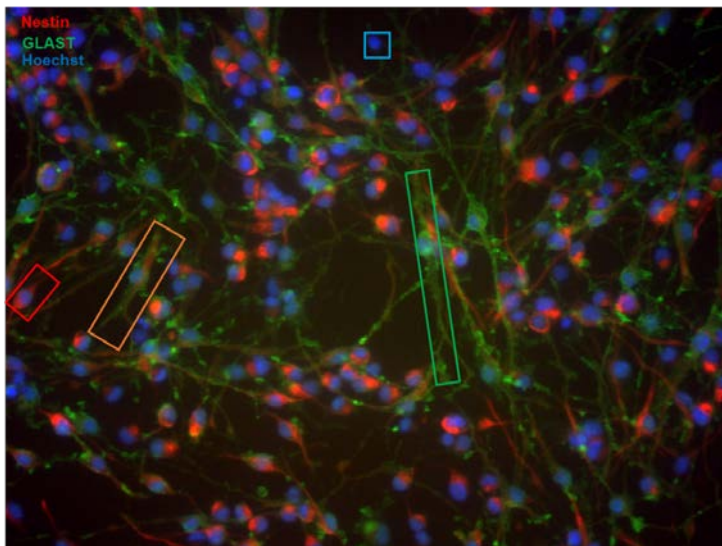


Figure 32 – Representative morphologies of cells in Nestin - GLAST double staining. Nestin⁺GLAST⁺ (orange frame), Nestin⁺GLAST⁻ (red frame), Nestin⁻GLAST⁺ (green frame), Nestin⁻GLAST⁻ (blue frame).

3.2 Characterization of NSPC-seeded Porous Collagen Scaffolds

3.2.1 3D Culture







Cortical embryonic neural stem cells (E13.5 NSCs) isolated from C57BL/6 mice were cultured in NSC full medium, supplemented with EGF and FGF-2 as free-floating neurospheres. Once neurospheres had been formed (after 4-5 days), cells were subcultured and seeded in porous collagen scaffolds (PCSs) as single-cell suspension and cultured in NSC full medium for 3DIV. Such NSPCs-seeded PCS were used as grafts in a mouse dorsal column crush model in a recent study (Kourgiantaki et al., 2020) that demonstrated significantly improved locomotion recovery in 'treated' groups compared with the control group (laminectomy only; no spinal cord injury) 12-weeks post-injury (Kourgiantaki et al., 2020).

Since the results of Kourgiantaki et al. show significant improvement in locomotion recovery of SCI mice treated with NSPC-seeded PCS, it is of interest to characterize in detail the utilized graft, including describing the type and developmental stage of cells present in the graft just before implantation.

Grafts were cultured in NSC full medium for 3DIV before implantation. The characterization was based on the methods of immunocytochemistry described above (3.1 Characterization of NSPCs subpopulation). The evaluation took place by quantifying the percentage of cells that stain positive for each marker. In order to study the effect of 3D culture in PCSs, 2D cultures of NSCs grown on PDL-laminin coated 48-well plates were used as control.

Scaffolds, after 3DIV culture in NSC full medium, were fixed and stained for markers of early developmental stages: Sox2 and Nestin (NSPCs markers), GLAST (RGCs marker), and for later developmental stages: Tuj1 (neuronal marker), GFAP (astrocytes, but also RGCs marker), PDGFR α (OPCs and preoligodendrocytes marker) (Figure 33, 34). Sox2 was utilized in double staining with Nestin, and so as GLAST. Tuj1 was used in double staining with GFAP (merge images are not shown).

Markers of early developmental stages

- **Sox2**
 - NSPCs marker  
- **Nestin:**
 - NSPCs marker  
- **GLAST:**
 - RGCs marker 
 - also expressed in astrocytes 

Markers of later developmental stages







- **GFAP**
 - Astrocytes marker 
 - RGCs 
- **Tuj1**
 - neuronal marker 
 - mitotic neuronal precursors (immature neurons) 
- **PDGFRa:**
 - OPCs 
 - Preoligodendrocytes 

Figure 33 – Markers evaluated for characterization of NSPC subpopulations. Colour code for different cell types. Colour code: light blue – NECs, blue – NSPCs & RGCs, green – NRPs & neurons, yellow – OPCs & preoligodendrocytes, red – astrocytes.

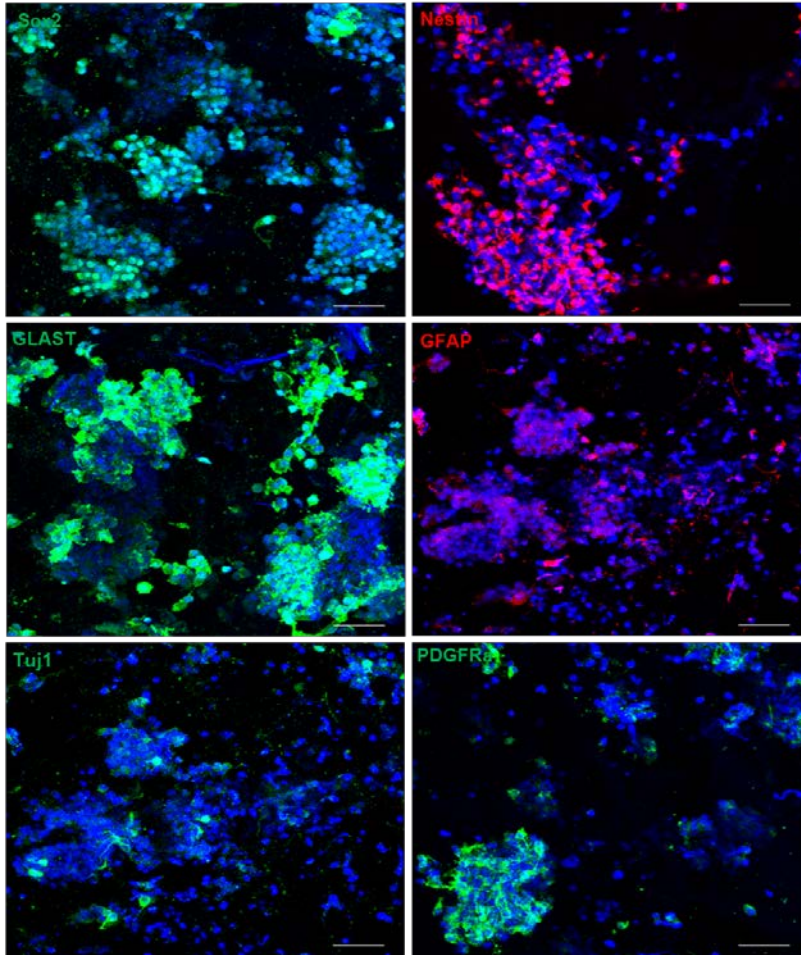


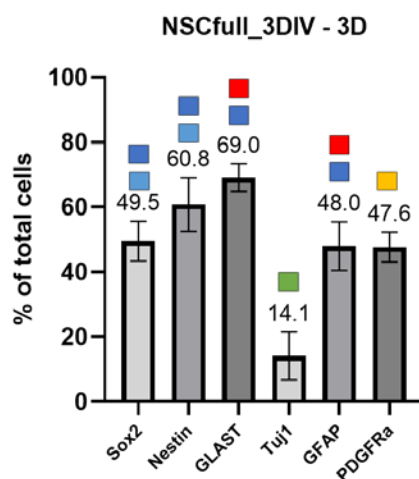
Figure 34 – Growth of NSC inside porous collagen scaffolds cultured in NSC full medium for 3DIV. Immunofluorescence staining for markers of early developmental stages: Sox2 and Nestin (NSPCs), GLAST (RGCs), and markers for later developmental stages: Tuj1 (neurons), GFAP (astrocytes, but also RGCs), PDGFRa (OPCs and preoligodendrocytes). Maximum projection of all stacks. Scale bar 50µm.

After 3 days of growth inside a PCS, cells were grown in clusters and stained for all markers utilized (Sox2, Nestin, GLAST, Tuj1, GFAP, PDGFRa). Cell clusters formation does not allow studying cell morphology inside PCSs.

The fraction of cells that stain for every marker was quantified manually. Results show that the largest percentage of cells grown in NSC full medium in the PCSs for 3DIV are NSPCs, characterized by the expression of Sox2 (49.5 ± 6.1 %), Nestin (60.8 ± 8.3 %) and GLAST (69 ± 4.3 %). Results demonstrate that the cell population consisted also of GRPs, containing RGCs and/or astrocytes (based on GFAP expression) and OPCs (based on

PDGFRa expression). The percentage of GFAP⁺ (48±3.3 %) and PDGFRa⁺ (47.6±4.6 %) cells is significantly higher than the neural marker Tuj1 (14.1±7.4 %), indicating a preference of cell differentiation towards glial cells instead of neurons (Graph 1).

It should be noted that total Nestin percentage was calculated from the mean of all biological replicates, where the mean of every biological replicate corresponded to the mean of the two different values that were calculated for each staining (Sox2-Nestin, Nestin-GLAST) only if it was conducted from the same batch of cells.



Graph 1 – Differentiation markers in NSPCs grown inside porous collagen scaffolds for 3 days. Fraction of cells expressing various markers of NSPCs and NSPC-derived differentiated cells. Results are expressed as mean ± s.e.m. n=3.

3.2.2 2D Culture

2D culture of E13.5 NSCs on flat surfaces was used as the control condition. Cells seeded as single-cell suspension on PDL-laminin coated 48-well plate were cultured in NSC full medium for 3DIV. Then cells were fixed and stained for the same markers as section 3.2.1 (Figure 35). Nestin⁺ cells demonstrated a characteristic bipolar morphology, with one branch being brighter stained. GLAST⁺ cells have also bipolar morphology and long processes. Most Tuj1⁺ cells have the morphology of neuronal precursors with short axons. GFAP⁺ cells have only the morphology of bipolar RGCs. PDGFRa⁺ cells are met with both morphologies of OPCs and preoligodendrocytes.

Again, Sox2 was utilized in double staining with Nestin, and so as GLAST. So, total Nestin percentage was calculated from the mean of all biological replicates, where the mean of every biological replicate corresponded to the mean of the two different values that were

calculated for each staining (Sox2-Nestin, Nestin-GLAST) only if it was conducted from the same batch of cells.

Quantification results show that the highest percentage of cells grown in NSC full medium on PDL-laminin coated 48-well plate for 3DIV are NSPCs, characterized by the expression of Sox2 (68.5 ± 5.3 %) and GLAST (72.6 ± 2.9 %) and with higher levels of the more intermediate marker Nestin (89.2 ± 0.7 %). GRPs are also present, with the percentage of GFAP (30.4 ± 5.3 %) and PDGFR α (24 ± 4.4 %) being significantly higher than the neuronal marker Tuj1 (7 ± 2.5 %) (Graph 2).

At first Tuj1 co-stained with GFAP in several cells. But due to the technical problem of emission leakage of 546 channel (GFAP) at the 488 channel (Tuj1), Tuj1 staining was repeated as single staining. Both results are shown. Tuj1 quantification in double-stained sections (Tuj1(GFAP)) was achieved in the composite image of the three channels (Hoechst, Tuj1, GFAP) where the real green cells were discrete from the GFAP (red) positive cells (Figure 16). Finally, there is a difference in the percentage of Tuj1 positive cells between the two methods (Graph 2), indicating that in double staining the real Tuj1 signal is covered from GFAP.

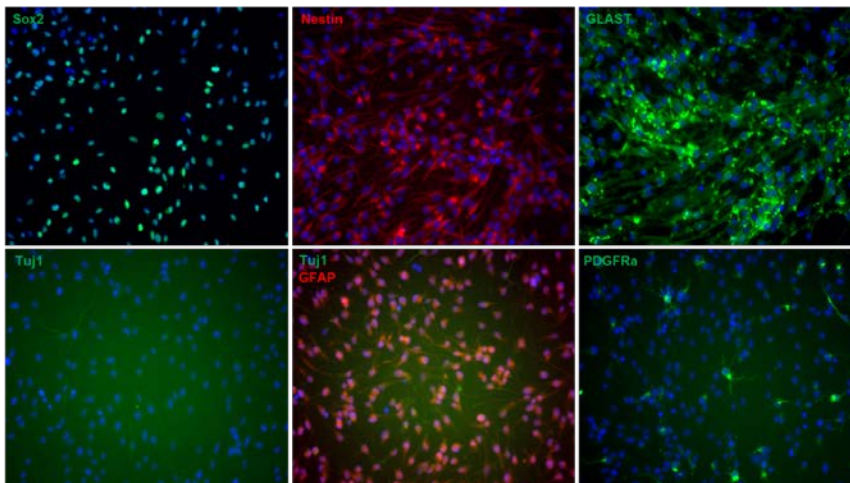
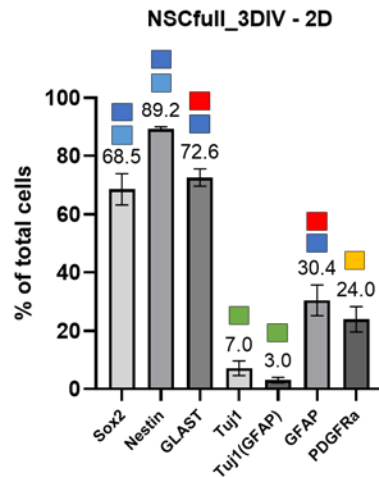


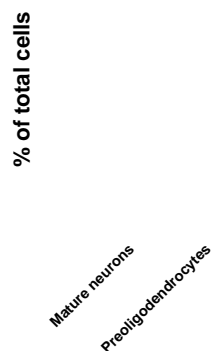
Figure 35 – NSCs seeded on PDL-laminin coated 48-well plate cultured in NSC full medium for 3DIV. Immunofluorescence staining for markers of early developmental stages: Sox2 and Nestin (NSPCs), GLAST (RGCs), and for later developmental stages: Tuj1 (neuronal marker), GFAP (RGCs), PDGFR α (OPCs and preoligodendrocytes). Spatial distribution of cells is more homogeneous in 2D culture.



Graph 2 - Differentiation markers in NSPCs grown on flat surfaces for 3 days. Fraction of cells expressing various markers of NSPCs and NSPC-derived differentiated cells. Results are expressed as mean \pm s.e.m. n=3.

It should be noted that, since 2D culture permits the study of cell morphology, it permits the discrimination between immature and more mature cells. Specifically, Tuj1 staining can distinguish immature mitotic neuronal precursors, which have thinner and shorter axons from the more mature neurons that have brighter cytoplasm with elongated and branched axons (Figure 28, 35). PDGFRa staining can also discriminate between OPCs, with short processes, and preoligodendrocytes that have brighter cytoplasm and longer, branched processes (Figure 30, 35). GFAP staining reveals that all GFAP⁺ cells, in NSC full medium for 3DIV, are RGCs, since they have the characteristic bipolar morphology (Figure 35).

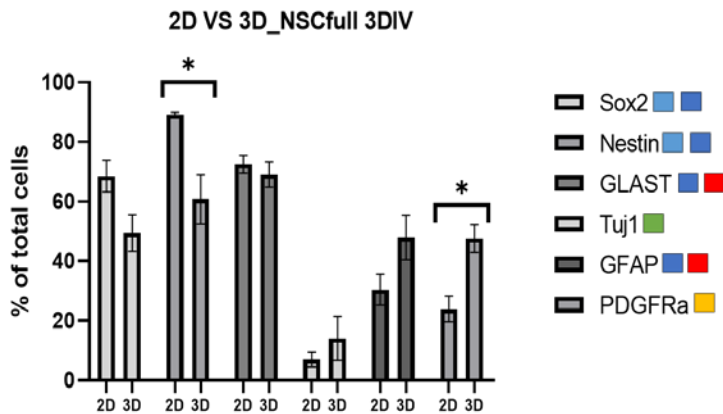
Quantification revealed that the percentage of more mature neurons is 0.7 ± 0.1 % (based on cells stained only for Tuj1), while the percentage of preoligodendrocytes is higher at 6.6 ± 2.5 % (Graph 3). This difference agrees with the difference between the total number of Tuj1⁺ and PDGFRa⁺ cells (Graph 2). These results indicate that despite the fact that cells are grown in NSC full medium, there is also a subpopulation of cells in a more differentiated state (neurons and GRPs).



Graph 3 – Differentiation capacity in 2D culture for 3DIV in NSC full medium. Even in NSC full medium, cultured for 3DIV, there are cells in a more differentiated state. There are more mature neurons (0.7%) and preoligodendrocytes at higher percentage (6.6%). n=3, results are expressed as mean \pm s.e.m.

3.2.3 Comparison of NSPC Differentiation in 3D & 2D Culture

Comparison of the above results and performing t-test for each marker, comparing the two different ways of culture (48-well plate (2D) and porous collagen scaffolds (3D)), shows that there is a statistically significant difference only in the fraction of Nestin⁺ cells and PDGFRa⁺ cells (Graph 4). Nestin levels are lower in 3D culture, while in contrast PDGFRa levels are higher in 3D culture. Results also show 3D culture results in less Sox2⁺ cells, however this difference is marginally not significant (P =0.0784). On the other hand, there are more Tuj1⁺ cells (results from single Tuj1 staining ICC in 2D culture) and GFAP⁺ cells in 3D culture. These results indicate that PCSs seem to favour NSPCs differentiation, mainly into glial cells, since the percentage of glial markers (GFAP, PDGFRa) is higher than the neuronal marker Tuj1. Also, OPCs growth seems to be better supported in 3D culture. More biological replicates are needed in order to reach statistically significant results.

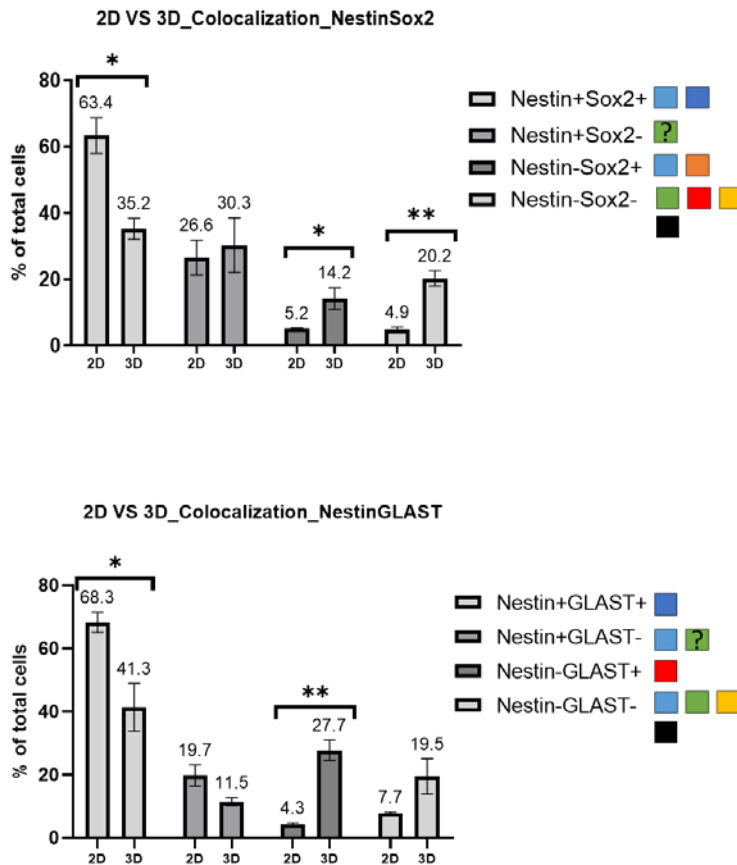


Graph 4 – Comparison of the percentage of positive cells for every developmental marker between 2D and 3D culture. Statistically significant difference in Nestin and PDGFRa levels. There is also a slight difference in Sox2 levels, being lower, and Tuj1, GFAP levels being a little higher in 3D culture. n=3, results are expressed as mean ± s.e.m. *P<0.05.

3.2.3.1 Detailed characterization of NSPCs

The markers Sox2 and GLAST were used in double staining with Nestin. Double positive cells (Nestin⁺Sox2⁺, Nestin⁺GLAST⁺), single positive (Nestin⁺Sox2⁻/ Nestin⁺Sox2⁺, Nestin⁺GLAST⁻ / Nestin⁺GLAST⁺) and double negative (Nestin⁻Sox2⁻, Nestin⁻GLAST⁻) cells were counted manually (Figure 31, 32).

Analysing above results and performing t-test for each combination, comparing the two different ways of culture (48-well plate (2D) and PCSs (3D)) shows that there is a statistically significant difference in the percentage of double positive cells (Nestin⁺Sox2⁺, Nestin⁺GLAST⁺) with the percentage of NSPCs (NECs and RGCs) being higher in 2D culture (Graph 5). On the other hand, the percentage of Nestin⁻Sox2⁺ and Nestin⁻GLAST⁺ cells is significantly higher in 3D culture, so as the percentage of double negative, Nestin⁻Sox2⁻, cells (Graph 5). These results indicate that in 2D culture, cells remain in the median stage of NSPCs, which agrees with above results about Nestin⁺ cells (Graph 4). Cells in 3D culture seem to follow a stricter pattern, being either at the stage of NECs or even GRPs (Nestin⁻Sox2⁺) or at the stage of astrocytes (Nestin⁻GLAST⁺), which agrees with above results about GFAP and PDGFRa levels (Graph 4). Also, Nestin⁻Sox2⁻ higher percentage in 3D culture, which again confirms that in PCSs cells are in more differentiated state and probably Tuj1⁺, GFAP⁺. It should be also noted that negative cells could also be dead or stressed cells that are contained in the total number of Hoechst positive cells.



Graph 5 – Comparison of the percentage of positive cells from Nestin and Sox2 or GLAST double staining. Statistically significant higher the percentage of double positive cells in 2D culture. In 3D culture the percentage of Nestin-Sox2+ and Nestin-GLAST+ cells is significantly higher, so as the percentage of double negative, Nestin-Sox2-, cells. n=3, results are expressed as mean ± s.e.m. *P<0.05, **P<0.01.

3.2.4 NSPC Differentiation Capacity as a Function of NSPC Passage

Previous studies suggested that NSPC passage before transplantation affects NSPC differentiation capacity (Eriksson et al., 2003). So, it would be interesting to compare the percentage of positive cells for each marker when NSPCs of different passage were grown for 3 days inside PCSs. In this study all experiments consisted of only three biological replicates, which usually corresponded to different passages. So, data from each technical replicate could be used for the comparison test. However, no statistical test was conducted and no clear conclusion could be made.

3.2.4.1 3D Culture

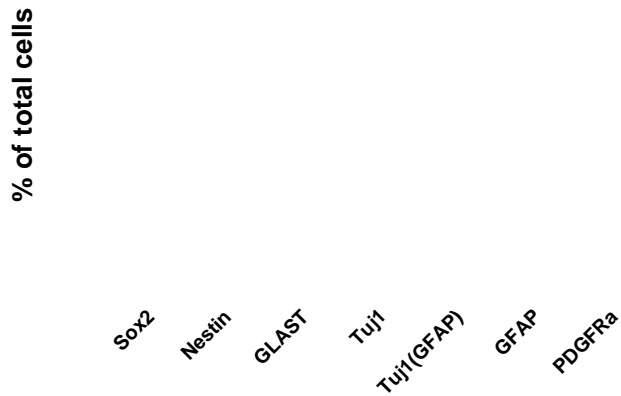
According to the results (Graph 6), in 3D culture and along the passages, an upward trend is observed in GLAST, GFAP, but also Sox2, while a downward trend is observed in PDGFRa. So, this upward trend seems to lead to astroglial lineage and to inhibition to oligodendrocytes lineage. On the other hand, although, from p7 to p10, the percentage of Nestin positive cells seems to be increased, the earlier p6 is even higher than p10. Similarly, as far as Tuj1 is concerned, the percentage of positive cells is very high only at the median p6. Of course, these variances could be random and due to technical problems, or even due to the way of quantification for 3D cultures.

% of total cells

Graph 6 – NSPC differentiation as a function of passage number in 3D culture. Upward trend is observed in GLAST, GFAP, but also Sox2, while a downward trend is observed in PDGFRa. n=3, results are expressed as mean \pm s.e.m.

3.2.4.2 2D Culture

In contrast, in 2D culture, results do not show big variances in NSPC differentiation as a function of cell passage. A downward trend is observed in all markers, except from Nestin which remains almost the same along the passages. In comparison with the 3D culture (Graph 6), there is an opposite trend in differentiation markers of later developmental stages, as far as GLAST and GFAP is concerned, which seem to be increased in 3D culture. PDGFRa has the same downward trend.



Graph 7 – NSPC differentiation as a function of passage number in 2D culture. Downward trend is observed in all markers, except from Nestin which remains almost the same along the passages. n=3, results are expressed as mean \pm s.e.m.

Furthermore, since NSPC passage has been implicated in cell differentiation capacity, it would be interesting to study the percentage of mature neurons and preoligodendrocytes at 3DIV, as a function of NSPC passage. Results (Graph 8) show that there is no trend in the fraction of mature neurons, but there is a downward trend in the number of preoligodendrocytes. This result is compatible with the graph of total PDGFRa positive cells (Graph 7) and also confirms the hypothesis that cells do not retain great differentiation capacity in higher passages.

% of total cells

Graph 8 – Comparison of the number of mature neurons and preoligodendrocytes among passages in 2D culture. No trend is observed in the number of mature neurons, but there is a downward trend in the number of preoligodendrocytes. n=3, results are expressed as mean \pm s.e.m.

3.3 Neural fate manipulation of NSPCs in PCSs

In order to induce neural differentiation of NSPCs, grafts (NSPC-seeded PCS grown for 3DIV in NSC full medium) were further cultured in neural differentiation medium and stained for ICC. Neural differentiation medium contained the same supplements with NSC growth medium, except from growth factors, and was supplemented with RA (0.1 or 1 μ M). Cells were cultured in neural differentiation medium for five more days (until 8DIV).

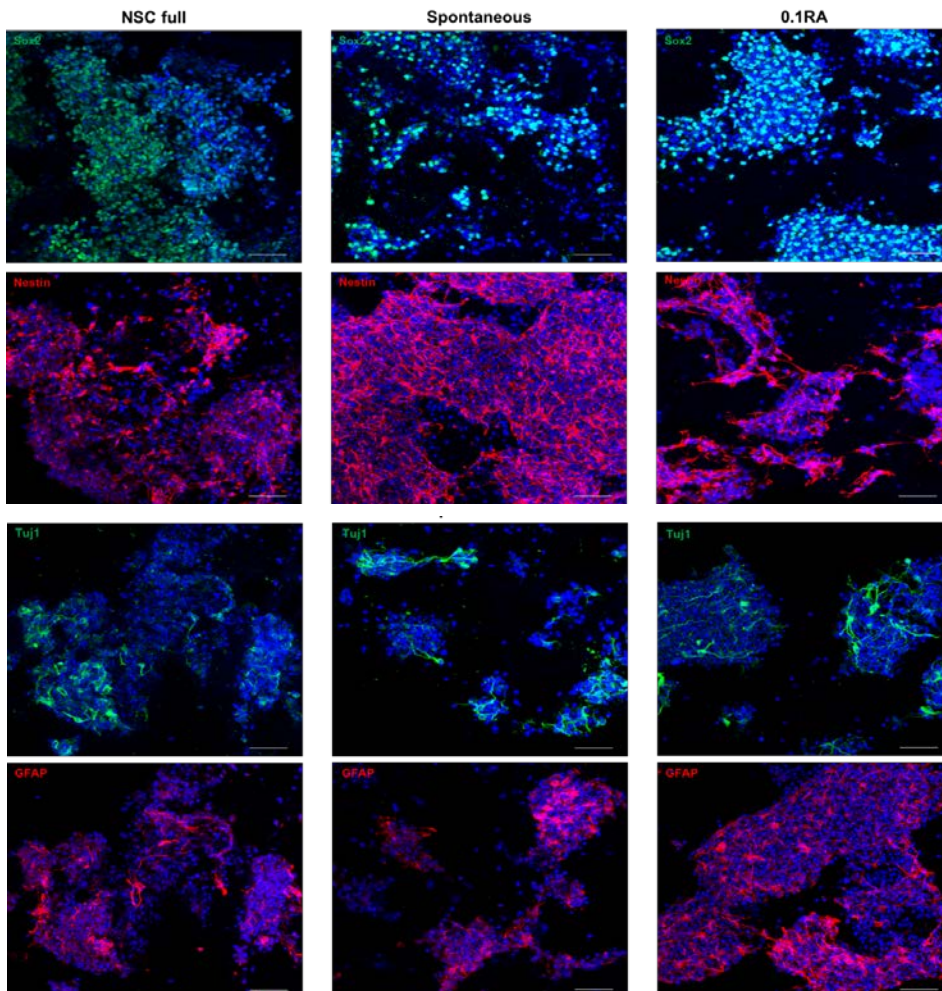
Except from the condition of NSPCs cultured into NSC full medium for 8DIV in total, another 'control' condition was tested. NSPCs differentiation capacity was also studied in NSC growth medium without growth factors – spontaneous differentiation, for five more days (until 8DIV). Again 'control' cultures were first grown for 3DIV in NSC full medium before the switch into differentiation medium.

2D cultures of NSCs grown on PDL-laminin coated 48-well plates were also used as control. The same manipulations and differentiation protocols with 3D culture were used.

3.3.1 3D culture

Scaffolds, after 3DIV culture in NSC full medium and 5DIV in differentiation medium, were fixed and stained for markers of early developmental stages: Sox2 and Nestin (NSPCs markers) and for later developmental stages: Tuj1 (neuronal marker), GFAP (astrocytes, but also RGCs marker), PDGFR α (OPCs and preoligodendrocytes marker) (Figure 36). Sox2

was utilized in double staining with Nestin and Tuj1 in double staining with GFAP (merge images are not shown). GLAST was not used since it was supposed that would have great overlap with GFAP in differentiation state. Also, the differentiation medium supplemented with 1 μ M RA was not tested in 3D cultures.



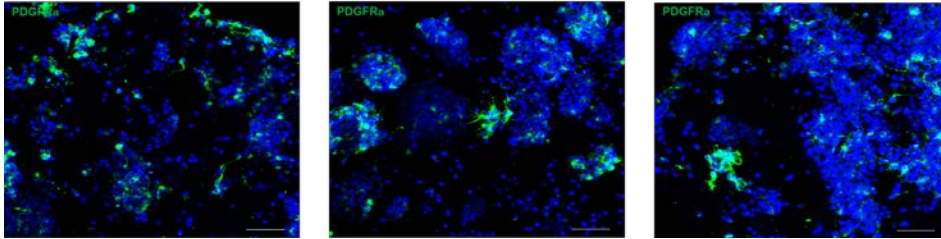
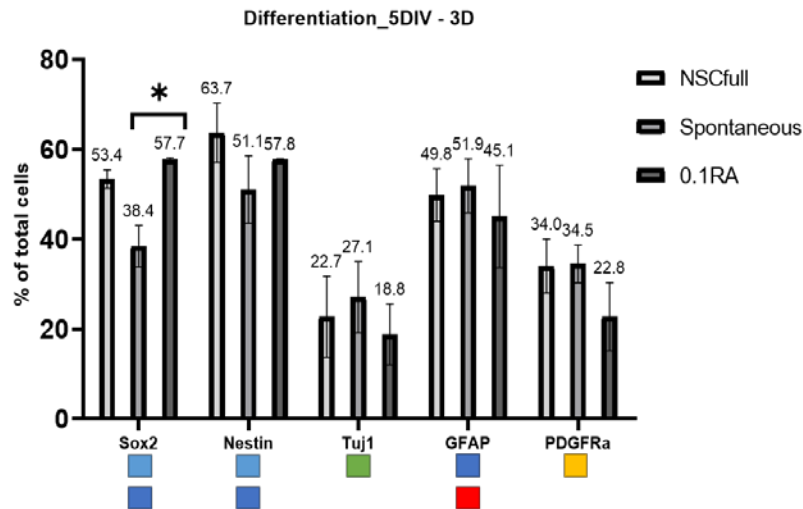


Figure 36 - Visualizing the fate of NSCs seeded in porous collagen scaffolds and cultured in three differentiation conditions for 5DIV. Immunofluorescence staining for markers of early developmental stages: Sox2 and Nestin (NSPCs), GLAST (RGCs), and for later developmental stages: Tuj1 (neurons), GFAP (astrocytes, but also RGCs), PDGFRa (OPCs and preoligodendrocytes). Maximum projection of all stacks. Scale bar 50µm.

In 3D culture, after 8DIV in culture, bigger cell clusters are formed (than in 3DIV) that stained for all different types of markers. Cell morphology corresponds to more mature cells (than in 3DIV), with longer processes or axons.

After quantifying the percentage of cells that stain for every marker, results show that in NSC full medium for 8DIV the largest fraction of cells are NSPCs, characterized by the expression of Sox2 (53.4 ± 1.7 %) and Nestin (63.7 ± 5.4 %). The cell population consists also of GRPs, containing RGCs and/or astrocytes (based on their GFAP expression (49.8 ± 5.8 %) and a lower percentage of OPCs (based on their PDGFRa expression (34 ± 6 %). Again, the fraction of Tuj1⁺ cells (22.7 ± 9 %) is lower than the fraction of cells that express other differentiation markers, indicating a preference of cell differentiation towards glial cells, also observed in 3DIV (Graph 9). The same trend is also observed both in the spontaneous medium and in 0.1µM RA medium, with the only difference in the percentage of Sox2⁺ cells that is significantly lower in spontaneous than in 0.1µM RA.

Except from Sox2⁺ cells in spontaneous medium, results show no difference among the different conditions. Cells grown in PCSs, after 5DIV in 0.1RA differentiation medium do not show any neural differentiation trend. Therefore, it appears the differentiation medium (0.1µM RA) chosen was not efficient for neuronal differentiation.



Graph 9 - Fraction of cells that express assayed markers in 3D culture when grown in various medium conditions. E13.5 NSCs were cultured in the PCSs for more 5DIV in different differentiation mediums. n=3, results are expressed as mean \pm s.e.m., one-way ANOVA, *P<0.05

3.3.2 2D Culture

In 2D culture, after 8DIV, cells morphology corresponds to more differentiated cells, especially based on Tuj1 and GFAP staining (Figure 37). Cells have longer processes and axons.

Quantification reveals that the fraction of cells that express the measured marker do not differ among the four different conditions. The highest percentage of cells grown in all conditions are Sox⁺. Nestin⁺ cells are in lower percentage. The fraction of GFAP⁺ cells is similar to the one of Sox²⁺ cells. These results indicate that most cells probably are GRPs or astrocytes. Furthermore, Tuj1⁺ and PDGFRa⁺ cells are at the same percentage, which is lower than all the rest markers (Graph 10).

On the other hand, studying the cell morphology and after discrimination of immature and more mature cells, there is a difference between NSC full medium and spontaneous differentiation medium, as far as neuron maturity is concerned. Despite the low total percentage of Tuj1⁺ cells, the percentage of mature neurons is significantly higher in spontaneous medium in comparison with NSC full medium, indicating that cells retain their differentiation capacity. However, this is not observed in differentiation medium supplemented with RA, confirming that the differentiation medium did not have any effect. In contrast, preoligodendrocyte percentage did not have any difference among differentiation conditions, but there seems to be an upward trend in comparison with NSC full medium, but this difference is not statistically significant (Graph 11). Moreover, in 8DIV cultures, although

the morphology of mature astrocytes was obvious, the discrimination between fibrous and protoplasmic astrocytes and quantification were not feasible, since cells were in close proximity and attached with each other.

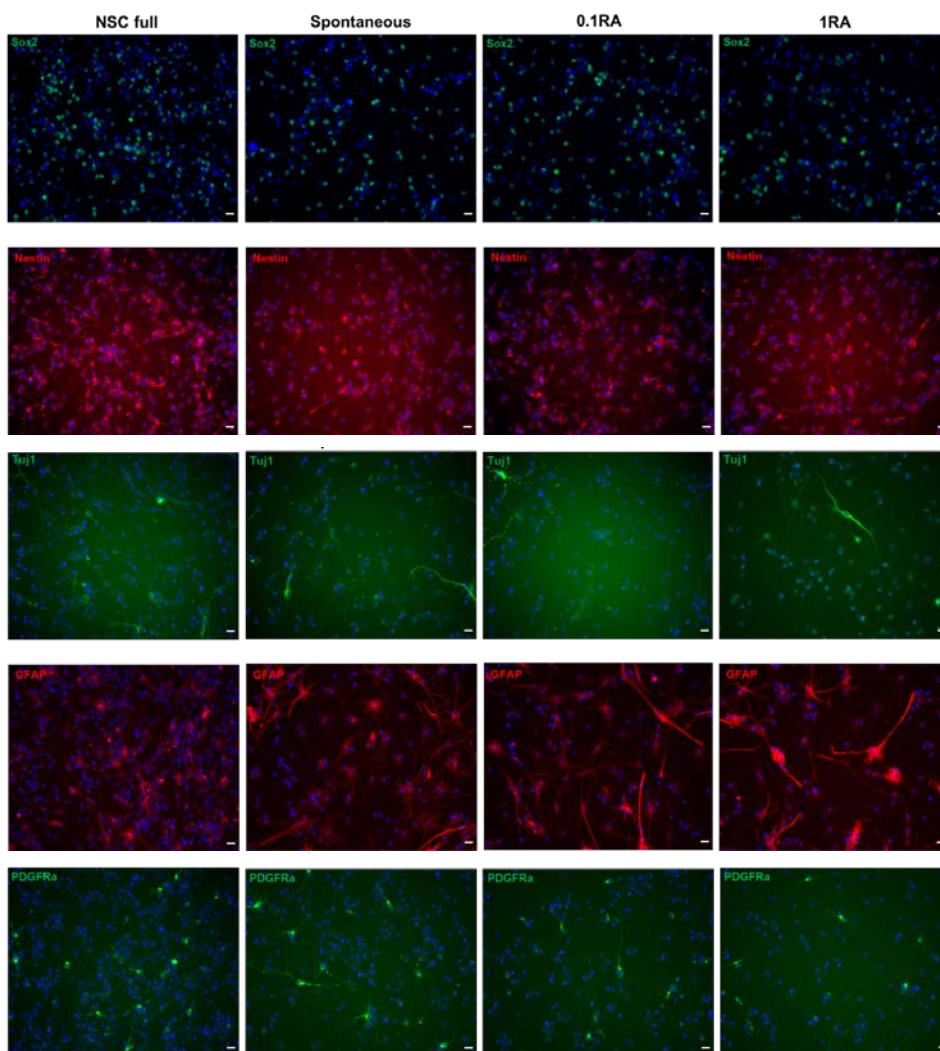
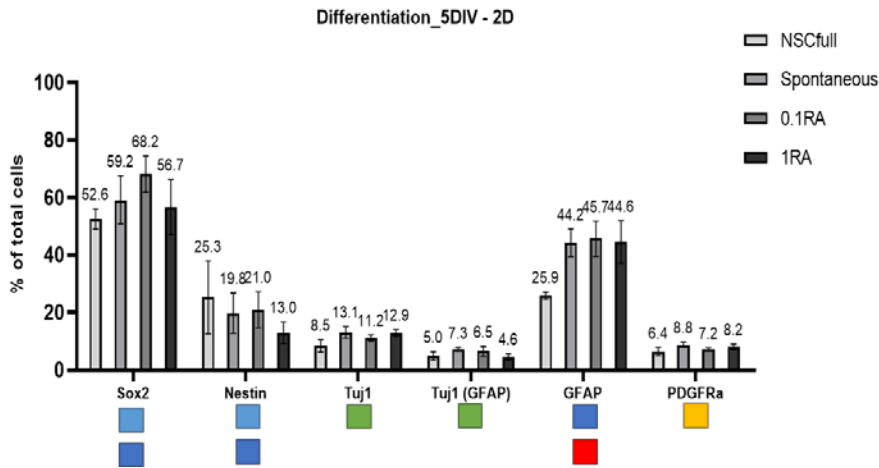
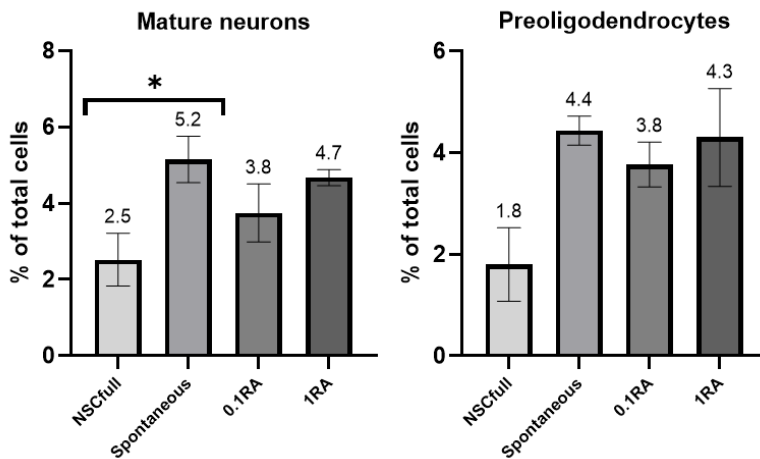


Figure 37 – NSCs seeded on PDL-laminin coated 48-well plate cultured in in differentiation medium for more 5DIV. Immunofluorescence staining for markers of early developmental stages: Sox2 and Nestin (NSPCs), GLAST (RGCs), and for later developmental stages: Tuj1 (neuronal marker), GFAP (astrocytes and RGCs), PDGFR α (OPCs and preoligodendrocytes). Scale bar 50 μ m.



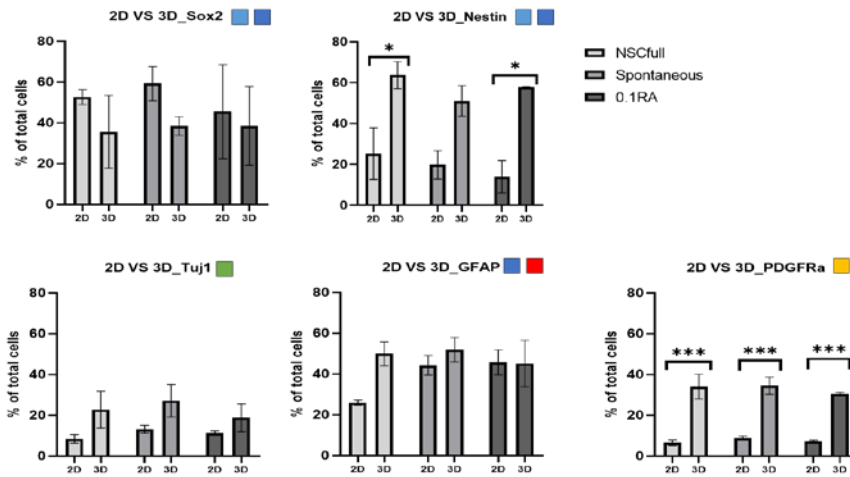
Graph 10 - Fraction of cells that express assayed markers in 2D culture when grown in various medium conditions. E13.5 NSCs were cultured for 8DIV in differentiation mediums. n=3 (n=4 for Tuj1), results are expressed as mean \pm s.e.m, one-way ANOVA.



Graph 11 – Differentiation capacity in 2D culture for 5DIV in differentiation mediums. Statistically significant difference in the percentage of mature neurons in NSC full medium and in spontaneous differentiation medium. There is no statistically significant difference among the different conditions, as far as the preoligodendrocytes is concerned, but there is an upward trend in differentiation mediums in comparison with the NSC full medium. n=3 (n=4 for mature neurons), results are expressed as mean \pm s.e.m, one-way ANOVA, *P<0.05.

3.3.3 Comparison of NSPC Differentiation between 3D & 2D Culture

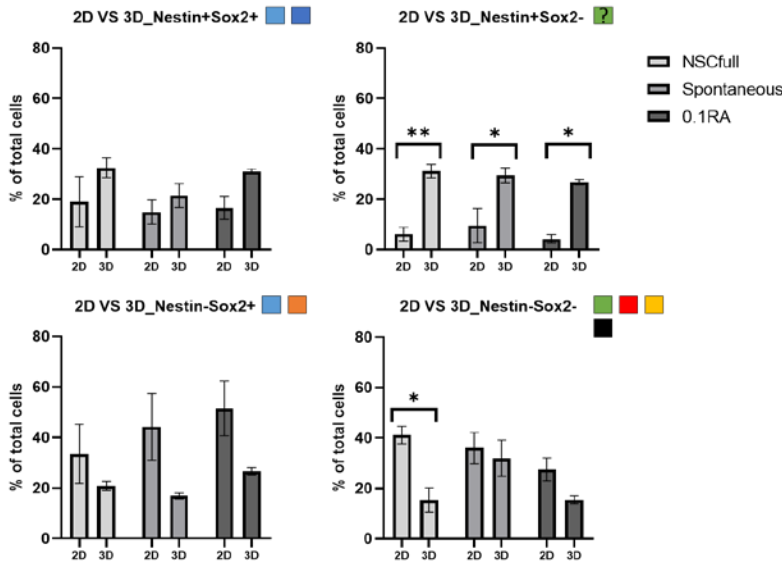
Comparison of the above results and performing two-way ANOVA for each marker in the three different conditions (1 μ M RA was not tested in 3D cultures), comparing the two different ways of culture (48-well plate (2D) and porous collagen scaffolds (3D)), shows that there is a statistically significant difference only in the fraction of Nestin⁺ cells and PDGFRa⁺ cells (Graph 12), so as in 3DIV-NSC full medium cultures (Graph 4). Specifically, there is great difference in all different conditions in the percentage of PDGFRa⁺ cells, which is higher in 3D culture. This result confirms that even after 8DIV culture and despite the culture medium, PCSs favor the growth of OPCs. Also, there is a significant difference in Nestin+ cells, but in that case the percentage is now higher in 3D culture, in comparison with the 2D culture. This result shows that NSPCs growth is supported for longer time in the PCSs. Furthermore, a slight difference in Tuj1 levels is observed, with higher percentage of Tuj1⁺ cells in 3D culture, indicating that neurons growth is also better supported in PCSs.



Graph 12 – Comparison of cell fraction that express assayed markers 2D and 3D culture at 8DIV. Statistically significant difference in Nestin and PDGFRa levels. There is also a slight difference in Tuj1 levels, being higher in 3D culture. n=3 (n=4 for 2D Tuj1), results are expressed as mean \pm s.e.m, two-way ANOVA *P<0.05, ***P<0.0001.

3.3.3.1 Detailed characterization of NSPC fates

Results from the analysis of Sox2 - Nestin double staining, after two-way ANOVA for each marker in the three different conditions (1 μ M RA was not tested in 3D cultures), comparing the two different ways of culture, show that there is a statistically significant difference in the percentage of Nestin⁺Sox2⁻ cells. Due to the lack of Sox2, these cells probably are a fraction of cells that tend to follow the neuronal lineage (probably OPCs), since Sox2 expression is maintained in only in GRPs and is downregulated in IPCs, Nestin has been found in co-localization with Tbr2 (Englund et al., 2005). The percentage of Nestin⁺Sox2⁻ cells is higher in 3D culture, in all different conditions, confirming the support of progenitor cells growth in PCs (Graph 13). On the other hand, the percentage of Nestin⁻Sox2⁻ cells is higher in 2D culture in NSC full medium. This staining corresponds to either more differentiated cells that have lost the expression of NSPCs markers or to dead or stressed cells. But, since the percentage of differentiation markers in NSC full medium are lower in 2D culture (Graph 12), probably Nestin⁻Sox2⁻ are dead or stressed cells.

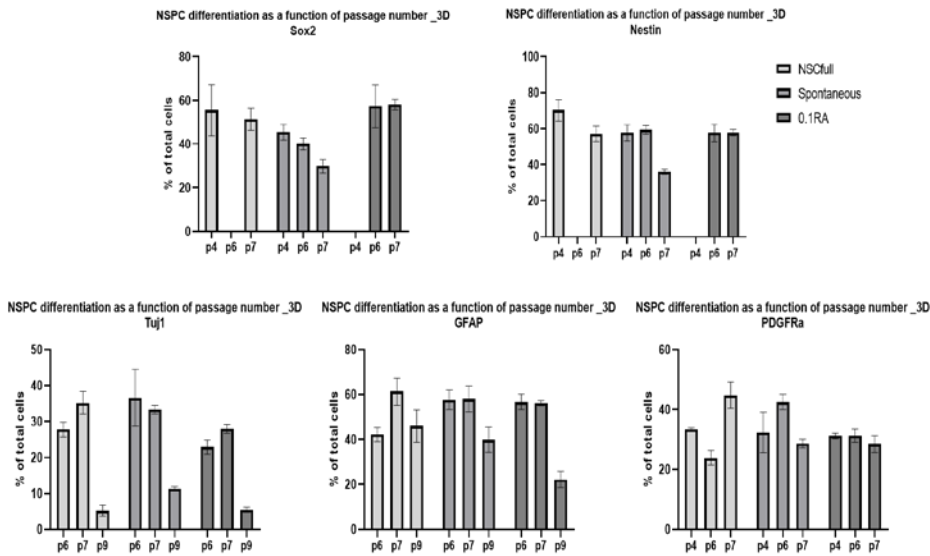


Graph 13 – Comparison of the percentage of positive cells from Nestin and Sox2 double staining in 8DIV. Statistically significant higher the percentage of Nestin⁺Sox2⁻ in 3D culture. In 2D culture the percentage of Nestin⁻Sox2⁻ is significantly higher. n=3, results are expressed as mean \pm s.e.m, two-way ANOVA, *P<0.05, **P<0.01.

3.3.4 NSPC Differentiation Capacity as a Function of NSPC Passage

3.3.4.1 3D Culture

The percentage of positive cells for each marker was studied among the different cell passages in all different culture conditions (Graph 14). In PCSs, after 8DIV, NSPCs markers (Sox2, Nestin) do not show any difference, except from the later passage 7, in spontaneous differentiation medium, where the percentage of both Sox2⁺ cells and Nestin⁺ cells is lower. The same trend also demonstrates the neural differentiation marker Tuj1 in very late passage 9, but passages 6 and 7 seem not to differ. The fraction of GFAP⁺ cells is significantly lower in passage 9 only in 0.1RA condition. The fraction of PDGFRa⁺ cells does not depend on NSPC passage. Therefore, late passages (passage above 9) should not be utilized. Results seem consistent when NSPCs are used until passage 7.

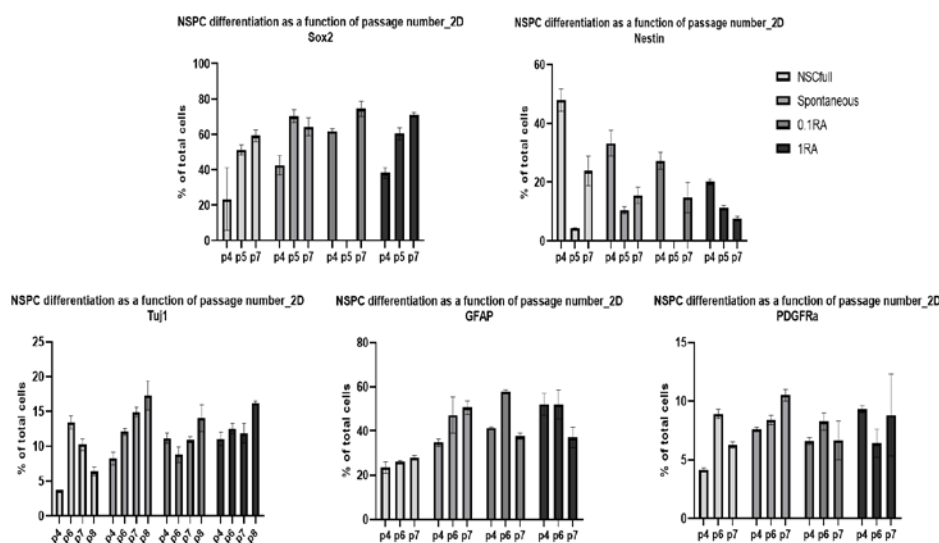


Graph 14 – NSPC differentiation as a function of passage number in 3D culture after 8DIV. No significant downward trend in passages 4-7, but passage 9 should be avoided for differentiation experiments in PCSs. n=3, results are expressed as mean ± s.e.m.

3.3.4.2 2D Culture

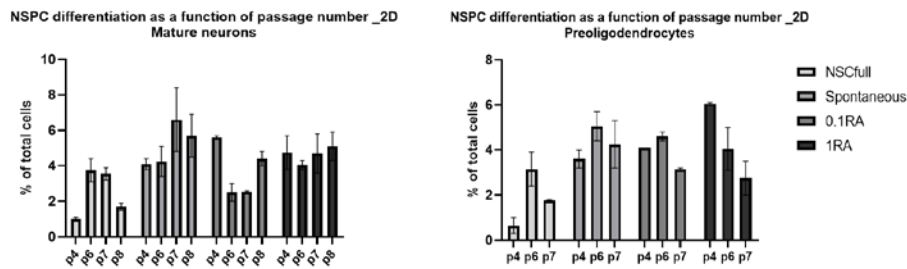
In 2D culture, a more complicate pattern is observed compared to 3D culture. The fraction of Sox2⁺ cells seems to increase as higher NSPC passage in all differentiation conditions

(Graph 15). In contrast, the fraction of Nestin⁺ cells follows the opposite trend. An unexpected outcome is also the upward trend of Tuj1, considering that in higher passages NSPCs are expected to lose their differentiation capacity. GFAP demonstrates a different pattern in the different condition mediums, where in NSC full medium seems to be stable, with an upward trend in spontaneous and downward in RA supplemented medium. The fraction of PDGFRa⁺ cells seems not to depend on NSPC passage among the different mediums. The results do not provide a specific conclusion regarding the effect of NSPC passage in NSPC differentiation.



Graph 15 – NSPC differentiation as a function of passage number in 2D culture after 8DIV. n=3, results are expressed as mean ± s.e.m.

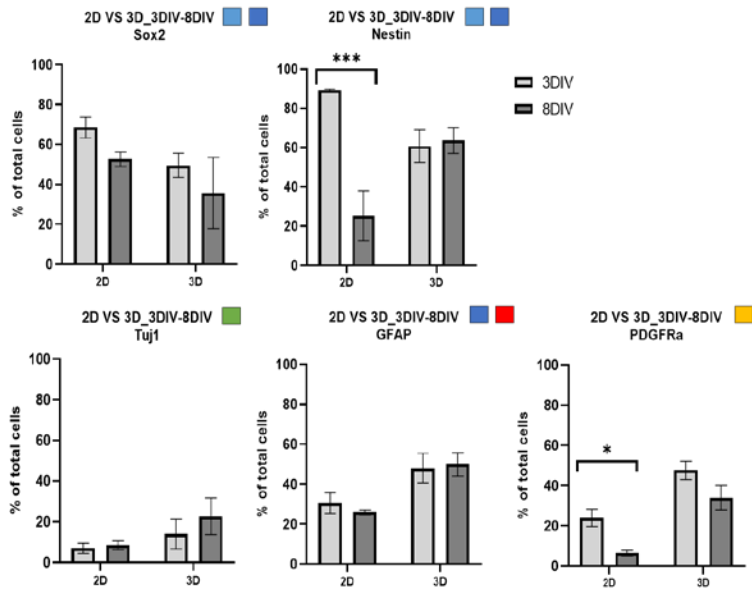
Graph 16 shows the fraction of mature differentiated cells in 2D culture. The percentage of mature neurons is not affected by NSPC passage in 1RA condition, and spontaneous differentiation, where only a slight upward trend is observed in higher passages. On the other hand, a difference is observed in median passages (p6, p7) in NSC full medium and in 0.1RA, where an upward and downward trend is observed, respectively. The percentage of preoligodendrocytes is higher in later passages in NSC full medium, but lower in 1RA. In spontaneous and 0.1RA differentiation medium the percentage looks more stable. However, no clear conclusion could be made and more biological replicates are needed



Graph 15 – NSPC differentiation as a function of passage number in 2D culture after 8DIV. n=3, results are expressed as mean ± s.e.m.

3.3.5 Comparison between 3DIV and 8DIV in NSC full medium

Comparing the results from the 3DIV and 8DIV in NSC full medium, the effect of PCSs on cells growth and differentiation could be also studied (Graph 16). After performing a two-way ANOVA test, results demonstrate a statistically significant difference in Nestin⁺ cells. While in 3DIV culture NSPCs are more in 2D culture, their percentage decreases till 8DIV. In PCSs Nestin⁺ cells seem to remain for longer time (till 8DIV) at around the same percentage. Also, the percentage of PDGFRa⁺ cells decreases after 8DIV, while in 3D culture there is only a slight decrease in 8DIV. This result does not agree with the case that PCSs support OPCs growth, but probably it relates with the fact that for the 5DIV in NSC full medium the growth factors are not renewed (two additional days where probably growth factors have been consumed). As far as Tuj1 is concerned, an upward trend is observed in 3D culture after 8DIV, a result which indicates that in PCSs cells retain in greater level their capacity to differentiate into neurons. Sox2 also demonstrates a downward trend in both 2D and 3D culture, while GFAP presents a more stable pattern.



Graph 16 – Comparison between 3DIV and 8DIV in NSC full medium in both 2D and 3D culture. n=3, results are expressed as mean ± s.e.m., two-way ANOVA, *P<0.05, ***P<0.0001.

4 Discussion

Spinal cord injury (SCI) refers to damage in the spinal cord or specific nerves located at the spinal canal's end. SCI causes transient or permanent neurological dysfunctions to the motor/sensory systems and has tremendous impacts on patient quality of life. The complex pathophysiology of SCI combined with the failure of CNS axon regeneration make SCI treatments challenging, while their clinical translation still remains questionable and controversial.

One of the most promising therapeutic strategies for SCI is cell transplantation, where treatments based on NSPCs have demonstrated the most promising results. NSPCs are multipotent cells that can differentiate into neurons, astrocytes and oligodendrocytes. In SCI, NSPCs restrict secondary enlargement of lesion, modulate the formation of glial scar by astrocytes, secrete growth factors and provide a neuronal substrate for rehabilitation of disrupted tracts. NSPCs neuroimplants, consisting of NSPC seeded inside biomaterials, can be directly at the lesion site, where they can differentiate and, working as substrates for regenerating axons, can bridge the neural tracts.

Recently, NSPC-seeded porous collagen scaffold (PCS) grafts ("neuroimplants") were used in a dorsal column crush SCI mouse model, which led to neuronal differentiation and significant improvement in locomotion recovery 10-12 weeks post injury (Kourgiantaki et al., 2020). Building upon the results of Kourgiantaki et al. 2020, this thesis aims to characterize in more detail the utilized NSPC-seeded grafts and evaluate the ability to modulate NSPCs fate once seeded in PCSs.

Firstly, specific ICC markers were evaluated for their ability to identify specific NSPCs subpopulations (NECs, RGCs) and their progeny (IPCs, neurons, astrocytes, OPCs, preoligodendrocytes). According to literature and previous studies conducted in the IMBB Neural Tissue Engineering Lab, the following markers were validated: Sox2 and Nestin for NECs and RGCs, GLAST for RGCs and astrocytes, GFAP for astrocytes and RGCs, Tuj1 for neurons, and PDGFRA for OPCs and preoligodendrocytes. However, a good assay for neural precursors is still needed, with Tbr2 or Pax6 as potential markers, or even an earlier marker for NECs, such as Sox1.

Three days after seeding NSPCs in PCS and growing in NSC complete medium (the grafts utilized in the Kouriantaki et al. study) NSPC markers (Sox2 (49.5 ± 6.1 %), Nestin (60.8 ± 8.3 %) and GLAST (69 ± 4.3 %)) were observed in the largest fraction of cells. Markers of GRPs and astrocytes were also present in a significant fraction of cells (GFAP: 48 ± 3.3 %, PDGFRA: 47.6 ± 4.6 %), while a small fraction of cells stained for the neuronal Tuj1 marker (14.1 ± 7.4 %). This result does not agree with the Kourgiantaki et al. study, which reports that

after culture in NSC full medium for 3DIV > 99% of cells stained positive for Nestin. This difference could be due to utilizing different NSPC quantification and analysis, due to small changes in NSC culture medium utilized (DMEM-F12 from different vendors, use of N2 supplement instead of B27 supplement), or even due to different manipulations from the different users since primary NSCs seem to be very sensitive to alterations in their microenvironment.

NSC sensitivity to different manipulations and culture microenvironments make the comparison of relative studies very difficult. The source of NSCs (brain or spinal cord), the age of donor cells (adult, embryonic or fetal tissue), the *in vitro* culture conditions (study of acutely dissociated cells, neurosphere culture, 2D culture), so as the time of culture and the specific culture media and supplements that are used, play crucial role in cellular growth and differentiation capacity.

A comparison of the fraction of cells that stained for various markers (for NSPCs and their progeny) in 3D culture against the control 2D culture condition (cells grown in NSC full medium) for 3DIV shows that 3D culture seems to favor NSPC differentiation and support of OPCs. More detailed characterization of NSPCs via Nestin - Sox2 and Nestin - GLAST double stainings, revealed that NSPCs grown in PCSs probably remain either at the stage of NECs or progress at more differentiated GRPs (Nestin⁻GLAST⁺, Nestin⁺GLAST⁻), while 2D culture resulted in more Nestin⁺Sox2⁺ and Nestin⁺GLAST⁺ cells (Graph 5). Such NSPCs subpopulation characterization (Nestin - Sox2 and Nestin - GLAST double stainings) has not been reported in previous studies.

Then, taking into consideration previous reports about the effectiveness of spinal cord NRPs and GRPs grafts in SCI, and the *in vitro* pre-differentiation of NSPCs before transplantation (Cao et al., 2001, 2002), this study focused on manipulating NSPCs grown in PCSs towards the neural fate. E13 NSPCs were cultured in spontaneous medium, in absence of growth factors, or in neuronal differentiation medium supplemented with RA (0.1µM and/or 1µM) and without growth factors, for additional 5DIV (after 3DIV in NSC full medium, with growth factors) either inside PCS (3D culture) and on PDL-laminin coated surfaces (2D culture). Results show that in both cultures there was no difference in the fraction of cells that stained for each marker among the different conditions. Spontaneous medium did not affect NSPC differentiation compared to full NSC medium. Furthermore, supplementing the spontaneous medium with RA did not increase neuronal differentiation compared to full NSC medium. Probably, a different RA concentration should be used (in median concentration of 0.5 µM) or NSPCs need to be cultured for more days in order to be able to reliably detect neuronal markers (7-10DIV). However, results show that 3D culture in PCS retained Nestin expression compared to 2D. In particular, 3D culture resulted in significantly more Nestin⁺Sox2⁻ cells, which could correspond to IPCs. Of course, staining for

specific IPC markers is required in order to validate this speculation. Also, at 8DIV growth in all medium conditions in PCS favored NSPC differentiation towards OPCs compared to 2D culture.

Comparison of NSPC differentiation after 3DIV and 8DIV culture in NSC full medium showed that in 2D culture the percentage of Nestin⁺ and PDGFRA⁺ cells decreased from 3DIV to 8DIV. On the other hand, when grown in PCS the fraction of cells that stained for NSPC markers remained constant over the same period. Finally, in 3D culture a slight decrease in PDGFRA⁺ OPCs was observed between 3DIV and 8 DIV, which could be due to the consumption of growth factors after 5 days in culture without medium replacement.

Future experiments based on the findings of this study could focus on PSCs preference towards the OPC fate, and possibly correlate this result with the ability of neuroimplants to enhance locomotion recovery *in vivo*, for example by testing possible effects on OPC-related phenotypes, such as axon growth and myelination. More combinatorial ICC stainings for markers of early developmental stages combined with markers of later developmental stages could provide information about the percentage of each cell type that are at the same time grown in the cell culture.

Finally, some improvements in experimental procedure are needed. More biological replicates are necessary for further confirmation of the results with stronger statistical significance. A protocol for cell morphology observation in 3D cultures would also help for characterization of different cell types but also of their state of differentiation. Cell quantification procedures probably still needs optimization, in order to efficiently count all kinds of cells even in clusters, in combination with optimized cell staining for 3D cultures. Also, the formation of big cell clusters could be avoided, if cells were optimally seeded in PCSs, so as to have a homogenous conformation inside the scaffold.

References

- Ahmed, S. (2009). The culture of neural stem cells. *Journal of Cellular Biochemistry*, 106(1), 1–6. <https://doi.org/10.1002/jcb.21972>
- Ahuja, C. S., Wilson, J. R., Nori, S., Kotter, M. R. N., Druschel, C., Curt, A., & Fehlings, M. G. (2017). Traumatic spinal cord injury. *Nature Reviews. Disease Primers*, 3, 17018. <https://doi.org/10.1038/nrdp.2017.18>
- Arai, Y., & Taverna, E. (2017). Neural Progenitor Cell Polarity and Cortical Development. In *Frontiers in Cellular Neuroscience* (Vol. 11). <https://doi.org/10.3389/fncel.2017.00384>
- Assinck, P., Duncan, G. J., Hilton, B. J., Plemel, J. R., & Tetzlaff, W. (2017). Cell transplantation therapy for spinal cord injury. In *Nature Neuroscience* (Vol. 20, Issue 5, pp. 637–647). <https://doi.org/10.1038/nn.4541>
- Bani-Yaghoub, M., Tremblay, R. G., Lei, J. X., Zhang, D., Zurakowski, B., Sandhu, J. K., Smith, B., Ribocco-Lutkiewicz, M., Kennedy, J., Walker, P. R., & Sikorska, M. (2006). Role of Sox2 in the development of the mouse neocortex. *Developmental Biology*, 295(1), 52–66. <https://doi.org/10.1016/j.ydbio.2006.03.007>
- Barraud, P., Thompson, L., Kirik, D., Björklund, A., & Parmar, M. (2005). Isolation and characterization of neural precursor cells from the Sox1-GFP reporter mouse. *The European Journal of Neuroscience*, 22(7), 1555–1569. <https://doi.org/10.1111/j.1460-9568.2005.04352.x>
- Barry, D. S., Pakan, J. M. P., & McDermott, K. W. (2014). Radial glial cells: Key organisers in CNS development. In *The International Journal of Biochemistry & Cell Biology* (Vol. 46, pp. 76–79). <https://doi.org/10.1016/j.biocel.2013.11.013>
- Bartholdi, D., & Schwab, M. E. (1995). Methylprednisolone inhibits early inflammatory processes but not ischemic cell death after experimental spinal cord lesion in the rat. In *Brain Research* (Vol. 672, Issues 1-2, pp. 177–186). [https://doi.org/10.1016/0006-8993\(94\)01410-j](https://doi.org/10.1016/0006-8993(94)01410-j)

- Beyer, F., Samper Agrelo, I., & Küry, P. (2019). Do Neural Stem Cells Have a Choice? Heterogenic Outcome of Cell Fate Acquisition in Different Injury Models. *International Journal of Molecular Sciences*, 20(2). <https://doi.org/10.3390/ijms20020455>
- Bonner, J. F., Haas, C. J., & Fischer, I. (2013). Preparation of neural stem cells and progenitors: neuronal production and grafting applications. *Methods in Molecular Biology*, 1078, 65–88. https://doi.org/10.1007/978-1-62703-640-5_7
- Cao, Q.-L., Howard, R. M., Dennison, J. B., & Whittemore, S. R. (2002). Differentiation of engrafted neuronal-restricted precursor cells is inhibited in the traumatically injured spinal cord. *Experimental Neurology*, 177(2), 349–359. <https://doi.org/10.1006/exnr.2002.7981>
- Cao, Q. L., Zhang, Y. P., Howard, R. M., Walters, W. M., Tsoulfas, P., & Whittemore, S. R. (2001). Pluripotent stem cells engrafted into the normal or lesioned adult rat spinal cord are restricted to a glial lineage. *Experimental Neurology*, 167(1), 48–58. <https://doi.org/10.1006/exnr.2000.7536>
- Caruso, M. C., Daugherty, M. C., Moody, S. M., Falcone, R. A., Bierbrauer, K. S., & Geis, G. L. (2017). Lessons learned from administration of high-dose methylprednisolone sodium succinate for acute pediatric spinal cord injuries. *Journal of Neurosurgery. Pediatrics*, 20(6), 567–574. <https://doi.org/10.3171/2017.7.PEDS1756>
- Dimou, L., & Gallo, V. (2015). NG2-glia and their functions in the central nervous system. In *Glia* (Vol. 63, Issue 8, pp. 1429–1451). <https://doi.org/10.1002/glia.22859>
- Dimou, L., & Götz, M. (2014). Glial cells as progenitors and stem cells: new roles in the healthy and diseased brain. *Physiological Reviews*, 94(3), 709–737. <https://doi.org/10.1152/physrev.00036.2013>
- Englund, C., Fink, A., Lau, C., Pham, D., Daza, R. A. M., Bulfone, A., Kowalczyk, T., & Hevner, R. F. (2005). Pax6, Tbr2, and Tbr1 are expressed sequentially by radial glia, intermediate progenitor cells, and postmitotic neurons in developing neocortex. *The Journal of Neuroscience: The Official Journal of the Society for Neuroscience*, 25(1), 247–251. <https://doi.org/10.1523/JNEUROSCI.2899-04.2005>

- Eriksson, C., Björklund, A., & Wictorin, K. (2003). Neuronal differentiation following transplantation of expanded mouse neurosphere cultures derived from different embryonic forebrain regions. *Experimental Neurology*, *184*(2), 615–635. [https://doi.org/10.1016/S0014-4886\(03\)00271-1](https://doi.org/10.1016/S0014-4886(03)00271-1)
- Fitzgerald, D. P., Cole, S. J., Hammond, A., Seaman, C., & Cooper, H. M. (2006). Characterization of neogenin-expressing neural progenitor populations and migrating neuroblasts in the embryonic mouse forebrain. *Neuroscience*, *142*(3), 703–716. <https://doi.org/10.1016/j.neuroscience.2006.06.041>
- Franco, S. J., & Müller, U. (2013). Shaping Our Minds: Stem and Progenitor Cell Diversity in the Mammalian Neocortex. In *Neuron* (Vol. 77, Issue 1, pp. 19–34). <https://doi.org/10.1016/j.neuron.2012.12.022>
- Franco-Quijorna, I., Amo-Aparicio, J., Martínez-Muriana, A., & López-Vales, R. (2016). IL-4 drives microglia and macrophages toward a phenotype conducive for tissue repair and functional recovery after spinal cord injury. In *Glia* (Vol. 64, Issue 12, pp. 2079–2092). <https://doi.org/10.1002/glia.23041>
- Gilyarov, A. V. (2008). Nestin in central nervous system cells. In *Neuroscience and Behavioral Physiology* (Vol. 38, Issue 2, pp. 165–169). <https://doi.org/10.1007/s11055-008-0025-z>
- Götz, M., & Barde, Y.-A. (2005). Radial glial cells defined and major intermediates between embryonic stem cells and CNS neurons. *Neuron*, *46*(3), 369–372. <https://doi.org/10.1016/j.neuron.2005.04.012>
- Guérout, N., Li, X., & Barnabé-Heider, F. (2014). Cell fate control in the developing central nervous system. In *Experimental Cell Research* (Vol. 321, Issue 1, pp. 77–83). <https://doi.org/10.1016/j.yexcr.2013.10.003>
- Guillemot, F. (2005). Cellular and molecular control of neurogenesis in the mammalian telencephalon. In *Current Opinion in Cell Biology* (Vol. 17, Issue 6, pp. 639–647). <https://doi.org/10.1016/j.ceb.2005.09.006>

- Guttenplan, K. A., & Liddelov, S. A. (2019). Astrocytes and microglia: Models and tools. *The Journal of Experimental Medicine*, 216(1), 71–83. <https://doi.org/10.1084/jem.20180200>
- Han, S. S. W., Kang, D. Y., Mujtaba, T., Rao, M. S., & Fischer, I. (2002). Grafted lineage-restricted precursors differentiate exclusively into neurons in the adult spinal cord. *Experimental Neurology*, 177(2), 360–375. <https://doi.org/10.1006/exnr.2002.7995>
- Hartfuss, E., Galli, R., Heins, N., & Götz, M. (2001). Characterization of CNS precursor subtypes and radial glia. *Developmental Biology*, 229(1), 15–30. <https://doi.org/10.1006/dbio.2000.9962>
- Hofstetter, C. P., Holmström, N. A. V., Lilja, J. A., Schweinhardt, P., Hao, J., Spenger, C., Wiesenfeld-Hallin, Z., Kurpad, S. N., Frisén, J., & Olson, L. (2005). Allodynia limits the usefulness of intraspinal neural stem cell grafts; directed differentiation improves outcome. *Nature Neuroscience*, 8(3), 346–353. <https://doi.org/10.1038/nn1405>
- Hutton, S. R., & Pevny, L. H. (2011). SOX2 expression levels distinguish between neural progenitor populations of the developing dorsal telencephalon. *Developmental Biology*, 352(1), 40–47. <https://doi.org/10.1016/j.ydbio.2011.01.015>
- Jensen, J. B., & Parmar, M. (2006). Strengths and Limitations of the Neurosphere Culture System. In *Molecular Neurobiology* (Vol. 34, Issue 3, pp. 153–162). <https://doi.org/10.1385/mn:34:3:153>
- Kamiya, K., Koda, M., Furuya, T., Kato, K., Takahashi, H., Sakuma, T., Inada, T., Ota, M., Maki, S., Okawa, A., Ito, Y., Takahashi, K., & Yamazaki, M. (2015). Neuroprotective therapy with granulocyte colony-stimulating factor in acute spinal cord injury: a comparison with high-dose methylprednisolone as a historical control. *European Spine Journal: Official Publication of the European Spine Society, the European Spinal Deformity Society, and the European Section of the Cervical Spine Research Society*, 24(5), 963–967. <https://doi.org/10.1007/s00586-014-3373-0>

- Katoh, H., Yokota, K., & Fehlings, M. G. (2019). Regeneration of Spinal Cord Connectivity Through Stem Cell Transplantation and Biomaterial Scaffolds. *Frontiers in Cellular Neuroscience*, 13, 248. <https://doi.org/10.3389/fncel.2019.00248>
- Kim, H., Zahir, T., Tator, C. H., & Shoichet, M. S. (2011). Effects of dibutyl cyclic-AMP on survival and neuronal differentiation of neural stem/progenitor cells transplanted into spinal cord injured rats. *PloS One*, 6(6), e21744. <https://doi.org/10.1371/journal.pone.0021744>
- Kintner, C. (2002). Neurogenesis in embryos and in adult neural stem cells. *The Journal of Neuroscience: The Official Journal of the Society for Neuroscience*, 22(3), 639–643. <https://www.ncbi.nlm.nih.gov/pubmed/11826093>
- Kourgiantaki, A., Tzeranis, D. S., Karali, K., Georgelou, K., Bampoula, E., Psilodimitrakopoulos, S., Yannas, I. V., Stratakis, E., Sidiropoulou, K., Charalampopoulos, I., & Gravanis, A. (2020). Neural stem cell delivery via porous collagen scaffolds promotes neuronal differentiation and locomotion recovery in spinal cord injury. *Npj Regenerative Medicine*, 5(1), 1–14. <https://doi.org/10.1038/s41536-020-0097-0>
- Lai, H. C., Seal, R. P., & Johnson, J. E. (2016). Making sense out of spinal cord somatosensory development. In *Development* (Vol. 143, Issue 19, pp. 3434–3448). <https://doi.org/10.1242/dev.139592>
- Lendahl, U., Zimmerman, L. B., & McKay, R. D. (1990). CNS stem cells express a new class of intermediate filament protein. *Cell*, 60(4), 585–595. [https://doi.org/10.1016/0092-8674\(90\)90662-x](https://doi.org/10.1016/0092-8674(90)90662-x)
- Lepore, A. C., & Fischer, I. (2005). Lineage-restricted neural precursors survive, migrate, and differentiate following transplantation into the injured adult spinal cord. *Experimental Neurology*, 194(1), 230–242. <https://doi.org/10.1016/j.expneurol.2005.02.020>
- Lepore, A. C., Han, S. S. W., Tyler-Polsz, C. J., Cai, J., Rao, M. S., & Fischer, I. (2004). Differential fate of multipotent and lineage-restricted neural precursors following

- transplantation into the adult CNS. *Neuron Glia Biology*, 1(2), 113–126.
<https://doi.org/10.1017/s1740925x04000213>
- Li, X., Liu, D., Xiao, Z., Zhao, Y., Han, S., Chen, B., & Dai, J. (2019). Scaffold-facilitated locomotor improvement post complete spinal cord injury: Motor axon regeneration versus endogenous neuronal relay formation. *Biomaterials*, 197, 20–31.
<https://doi.org/10.1016/j.biomaterials.2019.01.012>
- Li, X., Liu, S., Zhao, Y., Li, J., Ding, W., Han, S., Chen, B., Xiao, Z., & Dai, J. (2016). Training Neural Stem Cells on Functional Collagen Scaffolds for Severe Spinal Cord Injury Repair. In *Advanced Functional Materials* (Vol. 26, Issue 32, pp. 5835–5847).
<https://doi.org/10.1002/adfm.201601521>
- Li, X., Xiao, Z., Han, J., Chen, L., Xiao, H., Ma, F., Hou, X., Li, X., Sun, J., Ding, W., Zhao, Y., Chen, B., & Dai, J. (2013). Promotion of neuronal differentiation of neural progenitor cells by using EGFR antibody functionalized collagen scaffolds for spinal cord injury repair. *Biomaterials*, 34(21), 5107–5116.
<https://doi.org/10.1016/j.biomaterials.2013.03.062>
- Lu, P., Kadoya, K., & Tuszynski, M. H. (2014). Axonal growth and connectivity from neural stem cell grafts in models of spinal cord injury. In *Current Opinion in Neurobiology* (Vol. 27, pp. 103–109). <https://doi.org/10.1016/j.conb.2014.03.010>
- Malatesta, P., Hartfuss, E., & Götz, M. (2000). Isolation of radial glial cells by fluorescent-activated cell sorting reveals a neuronal lineage. *Development*, 127(24), 5253–5263.
<https://www.ncbi.nlm.nih.gov/pubmed/11076748>
- Martynoga, B., Drechsel, D., & Guillemot, F. (2012). Molecular Control of Neurogenesis: A View from the Mammalian Cerebral Cortex. In *Cold Spring Harbor Perspectives in Biology* (Vol. 4, Issue 10, pp. a008359–a008359).
<https://doi.org/10.1101/cshperspect.a008359>
- Memberg, S. P., & Hall, A. K. (1995). Dividing neuron precursors express neuron-specific tubulin. *Journal of Neurobiology*, 27(1), 26–43.
<https://doi.org/10.1002/neu.480270104>

- Mihalas, A. B., Elsen, G. E., Bedogni, F., Daza, R. A. M., Ramos-Laguna, K. A., Arnold, S. J., & Hevner, R. F. (2016). Intermediate Progenitor Cohorts Differentially Generate Cortical Layers and Require Tbr2 for Timely Acquisition of Neuronal Subtype Identity. *Cell Reports*, *16*(1), 92–105. <https://doi.org/10.1016/j.celrep.2016.05.072>
- Mokrý, J., Karbanová, J., Filip, S., Čížková, D., Pazour, J., & English, D. (2008). Phenotypic and Morphological Characterization of In Vitro Oligodendroglialogenesis. In *Stem Cells and Development* (Vol. 17, Issue 2, pp. 333–342). <https://doi.org/10.1089/scd.2007.0091>
- Molofsky, A. V., Krencik, R., Ullian, E. M., Tsai, H.-H., Deneen, B., Richardson, W. D., Barres, B. A., & Rowitch, D. H. (2012). Astrocytes and disease: a neurodevelopmental perspective. *Genes & Development*, *26*(9), 891–907. <https://doi.org/10.1101/gad.188326.112>
- Mothe, A. J., & Tator, C. H. (2013). Review of transplantation of neural stem/progenitor cells for spinal cord injury. *International Journal of Developmental Neuroscience: The Official Journal of the International Society for Developmental Neuroscience*, *31*(7), 701–713. <https://doi.org/10.1016/j.ijdevneu.2013.07.004>
- Nagoshi, N., Nakashima, H., & Fehlings, M. G. (2015). Riluzole as a neuroprotective drug for spinal cord injury: from bench to bedside. *Molecules*, *20*(5), 7775–7789. <https://doi.org/10.3390/molecules20057775>
- Naruse, M., Ishizaki, Y., Ikenaka, K., Tanaka, A., & Hitoshi, S. (2017). Origin of oligodendrocytes in mammalian forebrains: a revised perspective. In *The Journal of Physiological Sciences* (Vol. 67, Issue 1, pp. 63–70). <https://doi.org/10.1007/s12576-016-0479-7>
- Ono, K., Takebayashi, H., Ikeda, K., Furusho, M., Nishizawa, T., Watanabe, K., & Ikenaka, K. (2008). Regional- and temporal-dependent changes in the differentiation of Olig2 progenitors in the forebrain, and the impact on astrocyte development in the dorsal pallium. In *Developmental Biology* (Vol. 320, Issue 2, pp. 456–468). <https://doi.org/10.1016/j.ydbio.2008.06.001>

- Paridaen, J. T., & Huttner, W. B. (2014). Neurogenesis during development of the vertebrate central nervous system. In *EMBO reports* (Vol. 15, Issue 4, pp. 351–364). <https://doi.org/10.1002/embr.201438447>
- Pereira, I. M., Marote, A., Salgado, A. J., & Silva, N. A. (2019). Filling the Gap: Neural Stem Cells as A Promising Therapy for Spinal Cord Injury. *Pharmaceuticals* , 12(2). <https://doi.org/10.3390/ph12020065>
- Ramasamy, S., Narayanan, G., Sankaran, S., Yu, Y. H., & Ahmed, S. (2013). Neural stem cell survival factors. In *Archives of Biochemistry and Biophysics* (Vol. 534, Issues 1-2, pp. 71–87). <https://doi.org/10.1016/j.abb.2013.02.004>
- Ravi, M., Paramesh, V., Kaviya, S. R., Anuradha, E., & Paul Solomon, F. D. (2015). 3D Cell Culture Systems: Advantages and Applications. In *Journal of Cellular Physiology* (Vol. 230, Issue 1, pp. 16–26). <https://doi.org/10.1002/jcp.24683>
- Reynolds, B. A., & Rietze, R. L. (2005). Neural stem cells and neurospheres--re-evaluating the relationship. *Nature Methods*, 2(5), 333–336. <https://doi.org/10.1038/nmeth758>
- Reynolds, B., & Weiss, S. (1992). Generation of neurons and astrocytes from isolated cells of the adult mammalian central nervous system. In *Science* (Vol. 255, Issue 5052, pp. 1707–1710). <https://doi.org/10.1126/science.1553558>
- Rietze, R. L., & Reynolds, B. A. (2006). Neural stem cell isolation and characterization. *Methods in Enzymology*, 419, 3–23. [https://doi.org/10.1016/S0076-6879\(06\)19001-1](https://doi.org/10.1016/S0076-6879(06)19001-1)
- Sabelström, H., Stenudd, M., & Frisé, J. (2014). Neural stem cells in the adult spinal cord. *Experimental Neurology*, 260, 44–49. <https://doi.org/10.1016/j.expneurol.2013.01.026>
- Shao, A., Tu, S., Lu, J., & Zhang, J. (2019). Crosstalk between stem cell and spinal cord injury: pathophysiology and treatment strategies. In *Stem Cell Research & Therapy* (Vol. 10, Issue 1). <https://doi.org/10.1186/s13287-019-1357-z>
- Soares, S., von Boxberg, Y., & Nothias, F. (2020). Repair strategies for traumatic spinal cord injury, with special emphasis on novel biomaterial-based approaches. In *Revue Neurologique* (Vol. 176, Issue 4, pp. 252–260). <https://doi.org/10.1016/j.neurol.2019.07.029>

- Spassky, N., Goujet-Zalc, C., Parmantier, E., Olivier, C., Martinez, S., Ikenaka, K., Macklin, W., Zalc, B., & -L. Thomas, J. (1998). Multiple restricted origin of oligodendrocytes. In *Journal of Neuroimmunology* (Vol. 90, Issue 1, p. 10). [https://doi.org/10.1016/s0165-5728\(98\)91253-x](https://doi.org/10.1016/s0165-5728(98)91253-x)
- Tanaka, S., Kamachi, Y., Tanouchi, A., Hamada, H., Jing, N., & Kondoh, H. (2004). Interplay of SOX and POU factors in regulation of the Nestin gene in neural primordial cells. *Molecular and Cellular Biology*, 24(20), 8834–8846. <https://doi.org/10.1128/MCB.24.20.8834-8846.2004>
- van Niekerk, E. A., Tuszyński, M. H., Lu, P., & Dulin, J. N. (2016). Molecular and Cellular Mechanisms of Axonal Regeneration After Spinal Cord Injury. In *Molecular & Cellular Proteomics* (Vol. 15, Issue 2, pp. 394–408). <https://doi.org/10.1074/mcp.r115.053751>
- Wiese, C., Rolletschek, A., Kania, G., Blyszczuk, P., Tarasov, K. V., Tarasova, Y., Wersto, R. P., Boheler, K. R., & Wobus, A. M. (2004). Nestin expression ? a property of multi-lineage progenitor cells? In *Cellular and Molecular Life Sciences* (Vol. 61, Issues 19-20, pp. 2510–2522). <https://doi.org/10.1007/s00018-004-4144-6>
- Wu, Y., Liu, Y., Chesnut, J. D., & Rao, M. S. (2008). Isolation of neural stem and precursor cells from rodent tissue. *Methods in Molecular Biology*, 438, 39–53. https://doi.org/10.1007/978-1-59745-133-8_5
- Yang, H., Mujtaba, T., Venkatraman, G., Wu, Y. Y., Rao, M. S., & Luskin, M. B. (2000). Region-specific differentiation of neural tube-derived neuronal restricted progenitor cells after heterotopic transplantation. *Proceedings of the National Academy of Sciences of the United States of America*, 97(24), 13366–13371. <https://doi.org/10.1073/pnas.97.24.13366>
- Zappone, M. V., Galli, R., Catena, R., Meani, N., De Biasi, S., Mattei, E., Tiveron, C., Vescovi, A. L., Lovell-Badge, R., Ottolenghi, S., & Nicolis, S. K. (2000). Sox2 regulatory sequences direct expression of a (beta)-geo transgene to telencephalic neural stem cells and precursors of the mouse embryo, revealing regionalization of

gene expression in CNS stem cells. *Development* , 127(11), 2367–2382.

<https://www.ncbi.nlm.nih.gov/pubmed/10804179>

Zhao, Y., Xiao, Z., Chen, B., & Dai, J. (2017). The neuronal differentiation microenvironment is essential for spinal cord injury repair. *Organogenesis*, 13(3), 63–70.

<https://doi.org/10.1080/15476278.2017.1329789>

Zhong, Y., & Shultz, R. (2017). Minocycline targets multiple secondary injury mechanisms in traumatic spinal cord injury. In *Neural Regeneration Research* (Vol. 12, Issue 5, p.

702). <https://doi.org/10.4103/1673-5374.206633>

Zhou, Y., Wang, Z., Li, J., Li, X., & Xiao, J. (2018). Fibroblast growth factors in the management of spinal cord injury. In *Journal of Cellular and Molecular Medicine* (Vol.

22, Issue 1, pp. 25–37). <https://doi.org/10.1111/jcmm.13353>

Protocols

Cortical E13.5 Neural Stem Cell Culture

(K.Karali, F.Bampoula)

Tissue Dissection

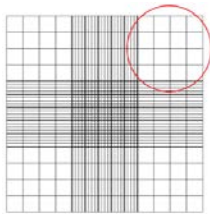
Before starting, sterilize all dissecting instruments and spray working surfaces with 70% ethanol.

1. Sacrifice mother using cervical dislocation and wait till the hind/paw reflex is absent
2. Spray the belly with 70% ethanol and carefully cut it open to remove the embryos, place the embryos in a petri dish with cold HBSS/5% P/S medium
3. Carefully remove the embryos from the amniotic sac and place them in new petri dish with clean HBSS/5% P/S medium
4. In order to remove the cortex from an embryo, place it in a petri dish with cold HBSS/5% P/S medium under the stereoscope
5. Immobilize the embryo with a forceps (place the forceps in the ear and eye)
6. Carefully in order not to damage the brain, starting from the back of the head and moving forward peel the two membranes covering the brain
7. After having exposed the brain dissected from the skull
8. Remove the midbrain and isolate the forebrain and then isolate the two hemispheres
9. Remove parts of the midbrain from the inner side
10. Carefully remove the meninges and dissect the cortex from the ganglionic eminences and place it in a 15mL tube with cold HBSS/5% P/S medium on ice
11. Repeat the procedures for all embryos

Tissue processing for NSC

1. Remove excess HBSS/5% P/S medium from the tube and leave the dissected cortices at the bottom.
2. Add 1mL of warm (37°C) NSC full medium (see recipe below, can be substituted with just DMEM/F12 medium) for every 4-8 brains (500µL for 1-3 brains)
3. Dissociate cells with the use of a 1mL tip, do approximately 10 up-downs until cloudy. At this stage avoid to produce bubbles.
4. Add an extra 5mL warm NSC full medium (can be substituted with just DMEM/F12 medium) for every 1mL.
5. Spin for 5 min at 100g.

6. Carefully throw away the supernatant and keep the pellet
 7. Reconstitute the pellet in warm NSC full medium (1-2 mL per 4-8 brains) using a 1 mL tip
 8. Count the concentration of cells with a hemocytometer
 9. Plate in a T25 flask 5x10⁴ cells/mL or 25x10⁴ cells in total
- Hemocytometer cell concentration calculation



Dilute 10 μ L cell suspension in 10 μ L trypan Blue dye
 Load 10 μ L of the resulting suspension on the hemocytometer
 Count the number cells in 4 squares (circled) and calculate the average K of these 4 measurements.
 Cell concentration C in the initial cell suspension (in cells/mL) can be calculated as: $C = K \times 2 \times 10^4$

Cell Culture Media

NSC full medium (recipe for 50 mL)

- 1000 μ L B-27TM Supplement (50X), minus vitamin A (Gibco #12587010)
- 660 μ L D-glucose (45% stock SIGMA G8769)
- 100 μ L Primocin (50 mg/mL stock)
- 50 μ L FGF (20 μ g/mL stock)
- 50 μ L EGF (20 μ g/mL stock)
- 48300 μ L of DMEM/F12 (THERMO #11330-032)

1x HBSS/5% P/S medium (recipe for 50mL)

- 5mL 10x HBSS medium (gibco #14185-045)
- 2.5 mL Penicillin-Streptomycin (10,000 U/mL)
- 42.5 mL sterile filtered dH₂O

Spontaneous differentiation Medium

NSC full medium without EGF, FGF growth factors.

RA differentiation medium

- NSC full medium without EGF, FGF and supplemented with RA (0.1 μ M or 1 μ M final concentration)
- Dilute RA (10mM stock) in DMEM/F12 medium after two successive dilutions (10mM \rightarrow 10 μ M \rightarrow 0.1 μ M or 1 μ M final concentration) ! **protect RA from light**

Feed primary cortical NSC culture after 2 days by adding 1 mL of warm NSC full medium.
Check for neurosphere formation and their morphology every day

Passage

The following protocol describes passage of NSCs grown in one T25 flask. Multiply volumes if more than one flask is passaged.

1. When relatively large but bright in the center neurospheres have formed a passage of the cells is necessary
2. Put the contents of one T25 flask in a 50 mL tube
3. Centrifuge for 5 min at 10g (repeat if no pellet is formed)
4. Discard supernatant
5. Add 500 μ L of accutase (when the pellet covers the ring at the bottom of the tube), make sure that the pellet is not stuck at the bottom of the tube
6. Incubate at 37°C for 3min
7. Dissociate the cells with pipetting up/down several times using a 1000 μ L tip until cloudy (be careful not to produce bubbles)
8. Incubate at 37°C for 3min
9. Dissociate the cells with pipetting up/down several times using a 200 μ L tip until cloudy (be careful not to produce bubbles)
10. Add 5 mL of warm DMEM/F12 medium in the tube and centrifuge for 5 min at 100g (or until a pellet is formed)
11. Add 2ml of warm complete embryonic NSC full medium and dissociate the pellet
12. Count the concentration of cells with a hemacytometer
13. Plate the cell in the appropriate number of T25 flask 5x10⁴ cells/mL or 25x10⁴ cells in total OR plate the cells for experiments

Cell seeding

2D culture

1. Coat 48-well plates with PDL poly-D-lysine (SIGMA, P6407) at 100 μ g/ml (in dH₂O sterile filtered)
2. Incubate o/n in a humidified 37°C, 5% CO₂ incubator
3. Remove PDL and save (can be reused 1-2 times)
4. Wash 3 times with dH₂O sterile filtered
5. Coat with Laminin 15 μ g/ml (Laminin stock 1mg/mL. L2020 SIGMA)

6. Incubate for 2 hours or more in a humidified 37°C, 5% CO₂ incubator
7. Remove Laminin and save (can be reused 1 time)
8. Wash 3 times with dH₂O sterile filtered
9. Remove excess water
10. Add 350µl NSC full medium and allow it to temper for 10 min or more in in a humidified 37°C, 5% CO₂ incubator before adding the cells
11. Add the appropriate volume of cell suspension with 2.5×10^4 cells

3D culture

1. Condense cells so as the concentration of cell suspension to be 15×10^3 cells/µl (centrifuge the 2ml of cell suspension and substitute cell pellet into the appropriate volume of NSC full medium)
2. Place 2µl of cell suspension at the bottom of a 48-well plate
3. Place the scaffold above the drop of cell suspension
4. Incubate for 15min in a humidified 37°C, 5% CO₂ incubator
5. Add 350µl NSC full medium and incubate in a humidified 37°C, 5% CO₂ incubator

Differentiation

After 3DIV in NSC full medium, cells were incubated in differentiation medium for additional 5DIV.

1. Discard NSC full medium
2. Wash once with warm DMEM-F12 medium in order to remove dead cells
3. Add 350µl differentiation medium (NSC full medium or Spontaneous differentiation medium or RA differentiation medium)
4. Incubate in a humidified 37°C, 5% CO₂ incubator for 5DIV

Check every day cell culture and cell morphology

Discard medium from NSCs seeded in scaffolds carefully: use a 200µL tip and aspirate medium carefully in order not to aspirate the scaffold.

NSC Freezing Protocol

1. Make sure Mr.Frosty is filled with isopropyl alcohol and its temperature has reached RT before proceeding.
2. Freeze NSCs when neurospheres are relatively small but remain bright in their center NSCs-(usually 2 days after seeding).
3. Pour the contents (neurospheres) of a T25 flask into a 15 mL conical tube.

4. Centrifuge for 5 min at 100xg (repeat if no pellet is formed)
5. Discard supernatant
6. Add 1 mL Freezing Medium (90% NSC full medium with 10% DMSO)
7. Gently pipet NSCs up and down to resuspend neurospheres in the medium (this step DOES NOT aim to break neurospheres into a single-cell suspension)
8. Transfer the neurospheres suspension (1 ml) into pre-labeled, cryovial (1 vial per 1 T25 flask).
9. Place vials inside a Mr. Frosty passive freezer. Place at -80 °C overnight.

Thawing Cells

1. Thaw cells when all required cell culture reagents are available.
2. Get a vial of frozen neurospheres from -80oC and incubate in a 37°C water bath until only a small sphere of ice is maintained. Closely monitor until the cells are completely thawed. Maximum cell viability is dependent on the rapid and complete thawing of frozen cells.

IMPORTANT: Do not vortex cells.

4. Disinfect the outside of the vial with 70% ethanol. Proceed immediately to the next step.
5. In a laminar flow hood, use a 1 mL pipette to transfer the cells to a sterile 15 mL conical tube. Be careful not to introduce any bubbles during the transfer process.
6. Using a 10 mL pipette, slowly add dropwise 10 mL of DMEM/F12 (Step 1 above) to the 15 mL conical tube.

IMPORTANT: Do not vortex cells.

7. Centrifuge the tube at 100xg for 5 minutes to pellet the cells.
8. Discard as much of the supernatant as possible. Steps 5-8 are necessary to remove residual DMSO.
9. Resuspend the cells in 1mL of NSC full Medium.
10. Transfer the cell mixture to a T25 cell culture flask (add 4ml expansion medium)
11. Incubate the cells at 37°C in a humidified incubator with 5% CO₂.

Immunocytochemistry (ICC) Fluorescence Staining

(K.Karali, F.Bampoula)

Preparation

- Make sure there are adequate amounts (prepare if necessary) of the following
- **10 mg/ml BSA in PBS**
 - This solution is NOT sterile so it MUST not be used in live cells.
- **10% TritonX100**
- **0.3% TritonX100 in PBS**
- **Fixation solution** (4% PFA in PBS).
 - CAUTION: PFA is toxic. DO NOT INHALE PFA FUMES
 - Ideally, PFA needs to be prepared fresh (See recipe). Alternatively, aliquote fresh 4% PFA and store PFA aliquotes in -20oC until use. Use PFA aliquotes once and discard extra amount (do NOT re-freeze).
- **Permeabilization buffer** (0.1% TritonX100 in PBS):
- **Blocking buffer** (10% normal serum, 1 mg/ml BSA, 0.3% TritonX100 in PBS).
 - Use the normal serum from the host species of secondary antibodies.
- **Antibody diluent solution** (1% normal serum, 0.1% TritonX100 in PBS)
 - Use the normal serum from the host species of secondary antibodies.

	48 – well plate	Scaffolds
Washes (V_{wash})/Fix	200 μ L	80 μ L
Block/2ary Abs/Counterstain	100 μ L	80 μ L
1ary Abs	80 μ L	80 μ L

Table 1: Volumes for dilutions

Procedure

Fixation, Permeabilization and Blocking

- Transfer samples inside a chemical hood.
- Gently aspirate medium and wash cells/scaffolds with V_{wash} PBS at RT for 1 min.
 - Several cell types may detach when the medium is removed. Be as gentle as possible.

- Transfer the scaffold with forceps into a PCR 200µL tube.
- Fix cells/scaffolds with V_{wash} fixation solution for 10 min (cells) or 15min (scaffolds) at RT (on a shaker only for scaffolds).
- Aspirate and discard fixation solution. Wash cells twice with V_{wash} PBS at RT 5min (cells) or 10min (scaffolds).
- Permeabilize cells by treating with V_{wash} permeabilization buffer at RT for 5min (cells) or 10min (scaffolds).
- Aspirate and discard permeabilization buffer.
- Block by treating sample with V_{wash} blocking buffer 1h (cells) or 2h (scaffolds) at RT. Incubate on a shaker (place scaffolds horizontally and shake at 120 rpm, shake cells at 70rpm).

Primary Antibody Incubation

- Prepare primary antibody solution by diluting each primary antibody in an appropriate ratio in antibody diluent solution.
- Aspirate and discard blocking buffer. Add V_{ab} µl primary antibody solution per sample.
- Incubate samples in primary antibody solution O/N at 4°C. Incubate on a shaker.

1y Abs	Dilutions
Sox2 (Abcam, ab15830)	1:100
Nestin (Novus, NB100-1604)	1:1000
GLAST (Abcam, ab416)	1:200
Tuj1 (Biolegend, 801201, tuj1 clone)	1:500
GFAP (Millipore, ab5541)	1:1000
PDGFRa (R&D, AF1062)	1:200

Table 2: Working dilutions of 1y Abs

Secondary Antibody Incubation

- Prepare secondary antibody solution by diluting each primary antibody according to an appropriate dilution factor d_i in antibody diluent solution.
 - Prepare solution in dark. Avoid its direct exposure to intense light.
 - Secondary antibodies are diluted 1:1000 ($d_i=1000$).
 - Use an Eppendorf centrifuge to spin samples 14000xg for 30sec at RT. Aspirate and use the supernatant. This step removes secondary antibody aggregates.
- Aspirate and discard primary antibody solution.

- Wash samples twice in V_{wash} permeabilization buffer for 5min (cells) or 10min (scaffolds) at RT on a shaker.
- Add V_{ab} μ l secondary antibody solution per sample.
- **ALL FOLLOWING STEPS MUST BE IMPLEMENTED IN THE DARK**
 - Prevent direct exposure of fluorophores to light to avoid photobleaching.
- Incubate samples in secondary antibody solution 1h (cells) or 3h (scaffolds) at RT IN THE DARK on a shaker.
 - Samples should not be exposed to direct light.

Counterstain

- Prepare counterstain solution.
 - Hoechst33342 (Invitrogen, H3570) is used, diluted in PBS (1:10000)
- Aspirate and discard secondary antibody solution.
- Wash samples twice in V_{wash} permeabilization buffer for 5min (cells) or 10min (scaffolds) at RT IN THE DARK on a shaker.
- Wash samples once in V_{wash} PBS for 5min (cells) or 10min (scaffolds) at RT IN THE DARK on a shaker.
- Add V_{wash} μ l counterstain solution per sample.
- Incubate samples in counterstain solution 30min (cells) or 1h (scaffolds) at RT IN THE DARK on a shaker.
 - Samples should not be exposed to direct light.
- Aspirate and discard counterstain solution.
- Wash samples twice in V_{wash} PBS for 5min (cells) or 10min (scaffolds) at RT IN THE DARK on a shaker.
- In the end, samples need to be submersed in PBS (with P/S 1:10) and are stored at 4°C in the dark (e.g. inside aluminum foil) until imaging.
 - During sample storage, samples should not dry as this induces huge background fluorescence.
- Image samples in a fluorescence microscope as soon as possible